THE UNIVERSITY OF ADELAIDE

A GEOCHEMICAL AND ISOTOPIC STUDY OF MAFIC AND INTERMEDIATE ROCKS IN THE OLARY PROVINCE, SOUTH AUSTRALIA - MAGMA SERIES DISCRIMINATION AND GEOCHRONOLOGICAL FRAMEWORK.

by HSR FREEMAN

November, 1995

A GEOCHEMICAL AND ISOTOPIC STUDY OF MAFIC AND INTERMEDIATE ROCKS IN THE OLARY PROVINCE, SOUTH AUSTRALIA- MAGMA SERIES DISCRIMINATION AND GEOCHRONOLOGICAL FRAMEWORK.

Hamish Stewart Rees Freeman B. Sc.

The University of Adelaide
The Department of Geology and Geophysics

This thesis is submitted as partial fulfilment for the
Honours Degree of Bachelor of Science.
November 1995

Australian National Grid Reference
(SI 54-2) 1:250 000

Abstract

Sampling and analysis of the mafic and intermediate igneous rocks from the Olary Block in South Australia has revealed eight geochemically distinct rock types. The Outalpa Amphibolite is characterised by low concentrations of Fe(total), Ti, P, LREE and HFSE relative to the Cathedral Rock samples of Pierini (1994). The Antro and Poodla granitoids have intermediate compositions and exhibit remarkable geochemical similarity except for alkali abundances. Three types of apparently later greenschist facies dolerites can be distinguished by geochemical means. The HPT (high phosphorous & titanium) dolerites have higher concentrations of LREE and HFSE than the LPT (low phosphorous & titanium) dolerites. The Rainy Day dolerite has low phosphorous and high titanium concentrations, and has HFSE and LREE concentrations intermediate between the HPT and LPT dolerites.

The Maldorky Lamprophyre that crops out south of the Olary township has lamproitic affinities, and is geochemically similar to the post-Delamerian Ordovician lamprophyres near Truro and Anabama Hill.

εNd(T) values are generally higher for the Outalpa amphibolite, LPT dolerites and Rainy Day dolerites, indicating derivation from a more depleted source or greater crustal interaction. The Poodla Granitoid has significantly lower εNd(T) than the Antro Granitoid: this is consistent with petrographic and geochemical evidence that suggests a greater level of crustal contamination of the former.

A Pb/Pb zircon date for the Antro Granitoid was obtained using the evaporation ('Kober') method. A magmatic age of 1679±13Ma is comparable to SHRIMP ages from the Broken Hill Block (e.g. Page and Laing, 1992). Significantly, this age may constrain the intrusion of the Outalpa Amphibolite to post ~1700Ma and pre- ~1680Ma.

Contents

Abstract	(ii)
List of Plates, Tables, Figures and Maps	(v)
Abbreviations	(vii)
Acknowledgements	(viii)
	Page
Chapter 1 Introduction	1
Preamble	1
1.1 Aims	1
1.2 Method	2
Chapter 2 Regional Geology	4
2.1 Introduction	4
2.2 Regional Geology	4
2.3 Stratigraphy	5
2.4 Structure and Metamorphism in the Olary Block	7
2.5 Geochronological Constraints	8
Chapter 3 Petrographic and Field Description of the Mafic and Intermediate Rocks	10
3.1 Outalpa Amphibolite	10
3.2 Antro Granitoid	13
3.3 Poodla Granitoid	13
3.4 Olary Block Dolerites and Gabbros	16
3.5 Maldorky Lamprophyre	17
Chapter 4 Geochemistry	20
4.1 Inroduction	20
4.2 Outalpa Amphibolite	20
4.2.1 General	20
4.2.2 Comparison of Outalpa and Cathederal Rock Samples	21
4.3 Antro and Poodla Granitoids	25
4.3.1 General	25
4.3.2 Trace Element Comparison	27
4.3.3 Tectonic Discrimination	27
4.4 Olary Block Dolerites	28
4.4.1 General	28

4.4.2 Incompatible Trace Elements 30
4.4.3 Source Characteristics and Crustal Contamination; Dolerites vs Amphibolites 33
4.4.4 Tectonic Discrimination 34
4.5 Maldorky Lamprophyre 35
4.6 Summary 37

Chapter 5 Isotopes 38
5.1 Introduction to Isotope Systematics 38
5.2 Isotopic Data 39
5.2.1 Comparison of the Mafic Suites 40
5.2.2 Interregional Comparison 42
5.2.3 Isochrons 42
5.3 Pb/Pb Zircon Evaporation 42
5.4 Conclusion 45

Chapter 6 Petro-Tectonic Models for Continental Tholeiite Generation 46
6.1 Possible Sources of Continental Tholeiites 46
6.2 Lithospheric Thickness and Mantle Temperature 46
6.3 Plume Impact versus Plume Incubation 47
6.4 Implications for the Olary Block Mafic Rocks 48

Chapter 7 Conclusion 49

References 52

Appendix A: Analytical Techniques

Appendix B: Thin Section Descriptions

Appendix C: Normalisation Factors and XRF Whole Rock Data

Appendix D: Normalised REE Data

Appendix E: Isotope Data and Isochron Plots

Appendix F: Results from Three Pb/Pb Zircon Evaporation Analyses on the Antro Granitoid at'Rainy Day'

Appendix G: Alteration of the Intermediate Granitoids: A Discussion

Appendix H: Tectonic Discrimination Diagrams

List of Figures, Tables, Plates and Maps

		Page
Figure 1.1	Olary district locality map	3
Figure 2.2.1	Stratigraphic correlation	5
Figure 2.4.1	Metamorphism in the Olary Block	8
Figure 4.2.1	Zr/TiO_2 v Nb/Y classification of volcanic rocks	22
Figure 4.2.3	Ce/Y v TiO_2 discrimination of Olary Block amphibolites	22
Figure 4.2.4	Nd v P discriminatin of Olary Block amphibolites	22
Figure 4.2.2	(a) & (b) Primitive mantle-normalised trace element diagrams; amphibolites.	23
Figure 4.2.5	Y/Nb v Zr/Nb for the Olary amphibolites	24
Figure 4.3.1	Major oxides v SiO_2 for the Antroo and Poodla Granites	25
Figure 4.3.2	(a) & (b) Primitive mantle-normalised trace element diagrams; Poodla and Antro Granites.	26
Figure 4.3.3	Nb v Y tectonic discrimination of granitoids	27
Figure 4.4.1	P_2O_5 v Fe_2O_3 discrimination between the three types of dolerites	28
Figure 4.4.2	Bivariate trace element and oxide plots for the Olary Block dolerites	29
Figure 4.4.4	(a) & (b) Primitive mantle-normalised trace element diagrams; HPT dolerites.	31
Figure 4.4.5	(a) Primitive mantle-normalised trace element diagram; LPT/Rainy Day dolerites.	32
	(b) REE patterns: Olary Block dolerites.	32
Figure 4.4.6	Source characteristics and crustal contamination of the Olary Block amphibolites and dolerites	33
Figure 4.4.7	OIT-normalised incompatible element diagram for the dolerites	34
Figure 4.5.1	(a) & (b) Bivariate plots for Maldorky Lamprophyre.	35/36
Figure 4.5.2	Incompatible trace element pattern for the Maldorky Lamprophyre	36
Figure 4.5.3	Tectonic discrimination of Maldorky Lamprophyre	36
Figure 5.1.1	Isotropic evolution of Nd in a chrondritic uniform reservior and depleted mantle	39
Figure 5.2.1	Epsilon Nd v time for the Olary Block mafic rocks	41
Figure 5.3.1	Histogram for zircon evaporation analyses	44
Figure 6.2.1	Relationship between lithospheric thickness, mantle potential temperature and magma volume	45

		Page
Table 1.1	Nominated outcrops	2
Table 2.4.1	Timing of events in the Olary Block	9
Table 4.2.1	Major element comparison of amphibolites	21

Plate 1 11 & 12
Plate 2 14 & 15
Plate 3 18 & 19

Map I: THE GEOLOGY OF THE AREA WEST OF AMEROO HILL, OLARY BLOCK (1:5000).

Map II: THE GEOLOGY OF THE AREA 2km NE OF ANTRO WOOLSHED, OLARY BLOCK *'Rainy Day* '(1:2500).

MapIII: THE GEOLOGY OF THE AREA 5km EAST OF ANTRO WOOLSHED, OLARY BLOCK (1:2500).

Abbreviations

B.E.	Bulk Earth
bt	biotite
CFB	continental flood basalt
CHUR	chondritic uniform reservoir
cpx	clinopyroxene
DM	depleted mantle
EMI	enriched mantle type I
EMII	enriched mantle type II
εNd(T)	epsilon neodymium value at time, T
E-type MORB	enriched mid ocean ridge basalt
feld	feldspar
Ga	Giga-anna (billions of years before present)
HFSE	high field strength element
HPT	Olary Block high phosphorous & titanium dolerite
HREE	heavy rare earth element
LIL	large ion lithophile (element)
LOI	Loss on ignition
LPT	Olary Block low phosphorous & titanium dolerite
LREE	light rare earth element
Ma	Mega-anna (millions of years before present)
Mg#	magnesium number (=$Mg^{2+}/Mg^{2+}+Fe^{2+}$)
MORB	mid-ocean ridge basalt
mu	muscovite
OIB	ocean island basalt
OIT	ocean island tholeiite
plag	plagioclase
P.M.	primordial mantle
P-T-t	pressure-temperature-time
qtz	quartz
REE	rare earth element
T_{DM}	depleted mantle model age
tour	tourmaline
XRF	X-ray fluorescence
zir	zircon

Acknowledgments

This has been a year of highs and lows, and I would not have survived without the help of many people. Many thanks firstly go to my supervisor John Foden, for invaluable discussion and help during a hectic year. And to Leigh Schmidt and Colin Rothnie from North Exploration, for organising the project, and for help with drafting, field supplies, and geological assistance. On the technical side, I would like to thank John Stanley (for running XRF samples), David Bruce (for help with the mass spec. and isotope lab), JDP and Bruce Schaefer (for zircon preparation, loading and running) and Geoff Trevelyn who was always in good humour. Others in the department that have made my life a lot easier include Annette, Jon, Martin, Jo, Soph and Gerald. Thankyou also to Ross Both, Fran Parker and JDP for organising and supervising the Kalgoorlie field trip; definitely a highlight of the year.

The biggest thanks go to my family, for all their love and support throughout the year. The Honours crowd, without whom I would have died in a corner quite some time ago, is a group of people I will miss immensely next year. Special thanks must go to Kelli, for many valuable discussions throughout the year; and to Justin and Dawn, for all the geological speculation in the field, and for subsequent discussion. Outside of Uni, thanks must go to James, Tim, Stefan and Matt.

Last of all, I must thank Dina, for putting up with me this year, and trying to understand those long hours at Uni. I promise I will make up to you.

CHAPTER 1: INTRODUCTION

Preamble

Integrated petrogenetic studies of mafic igneous rocks are crucial in determining the geochemical character of the Earth's interior. For example, extensive Nd, Sr and Pb isotopic and geochemical studies of oceanic basalts have revealed large scale mantle heterogeneities and have alluded to the nature of sub-lithospheric processes. Comparison of young and old basalts may enable the interpretation of ancient magmatic events. However the potential for preservation of oceanic basalts is low, as the oceanic lithosphere is continuously recycled via subduction processes. In contrast, continental basalts are, broadly speaking, more common in ancient settings and, therefore, can provide information on the processes involved in ancient magma generation.

1.1 Aims

This is a study of the Proterozoic mafic to intermediate igneous rocks that crop out in the vicinity of Bimbowrie and Outalpa Stations, and south of the Olary township. The main purpose of this study is to provide a geochemical and isotopic investigation into the selected mafic to intermediate intrusives with the primary aims encompassing:

(i) Establishment of stratigraphic field relationships of the igneous rocks with the surrounding rock types to try to obtain the relative ages of the intrusives.

(ii) Field description and distribution of each of the rock types (incorporating 1:5000 and 1:2500 outcrop scale maps).

(iii) Generation of new geochemical data and use of this data in conjunction with available data from previous studies to geochemically categorise the mafic and intermediate phases into a number of suites.

(iv) Isotopic characterisation and determination of dates through Sm-Nd and Rb-Sr radiogenic isotope techniques; and, to achieve further confinement intrusive ages via Pb-Pb zircon evaporation.

(v) Petrological and geochemical determination of the alteration products and precursors, to identify and characterise the alteration events that have influenced the intrusives. The variable magnetic susceptibility of the mafic rocks will also be addressed.

(vi) Correlation of the Olary Block mafic and intermediate rocks with other well constrained South Australian and Australian magmatic events.

1.2 Method

Eight locations in the vicinity of Bimbowrie Homestead and one area SE of Olary were chosen for detailed study on the mafic and intermediate rocks. Outcrop locations and rock types are listed on Table 1.1 and shown on Fig 1.1.

No.	Outcrop	Grid Reference	Rock type
#1	Baxter's Bore	0416920mE 6459620mN	Gabbro & dolerite
#2	'Rainy Day'	0413000mE 6456000mN	Qtz monzodiorite & gabbro
#3	Willow Well West	0413890mE 6454640mN	Mafic syenite & dolerite
#4	East Doughboy (Horse Paddock)		Dolerite & gabbro
#5	Ameroo North		Qtz diorite
#6	Ameroo West	0423200mE 6444630mN	Amphibolite & granodiorite
#7	Antro Feldspar Mine	0414910mE 6452910mN	Dolerite & gabbro (2types)
#8	Alconie Hill	0412400mE 6462660mN	Syenogranite
#9	Maldorky mafic dykes	0457760mE 6420450mN	Lamprophyre

Table 1.1 Outcrops nominated for this study. The outcrop numbers indicate the location of the outcrop on the Olary map, Fig 1.1.

Fresh and unweathered samples were collected where possible, and field relationships were mapped and noted. Petrographical an x-ray fluorescence (XRF) analyses were conducted on representative samples from the different outcrops. Discrimination based on whole rock geochemistry enabled some insight into the geochemical peculiarities of the different rock types as well as their original tectonic setting.

Rb-Sr and Sm-Nd were used to further refine the discrimination of the mafic and intermediate rocks first based on geochemical factors, and to investigate source characteristics and crustal assimilation processes. Pb/Pb zircon evaporation (the 'Kober' method) was performed on one sample enabling the acquisition of a crystallisation age.

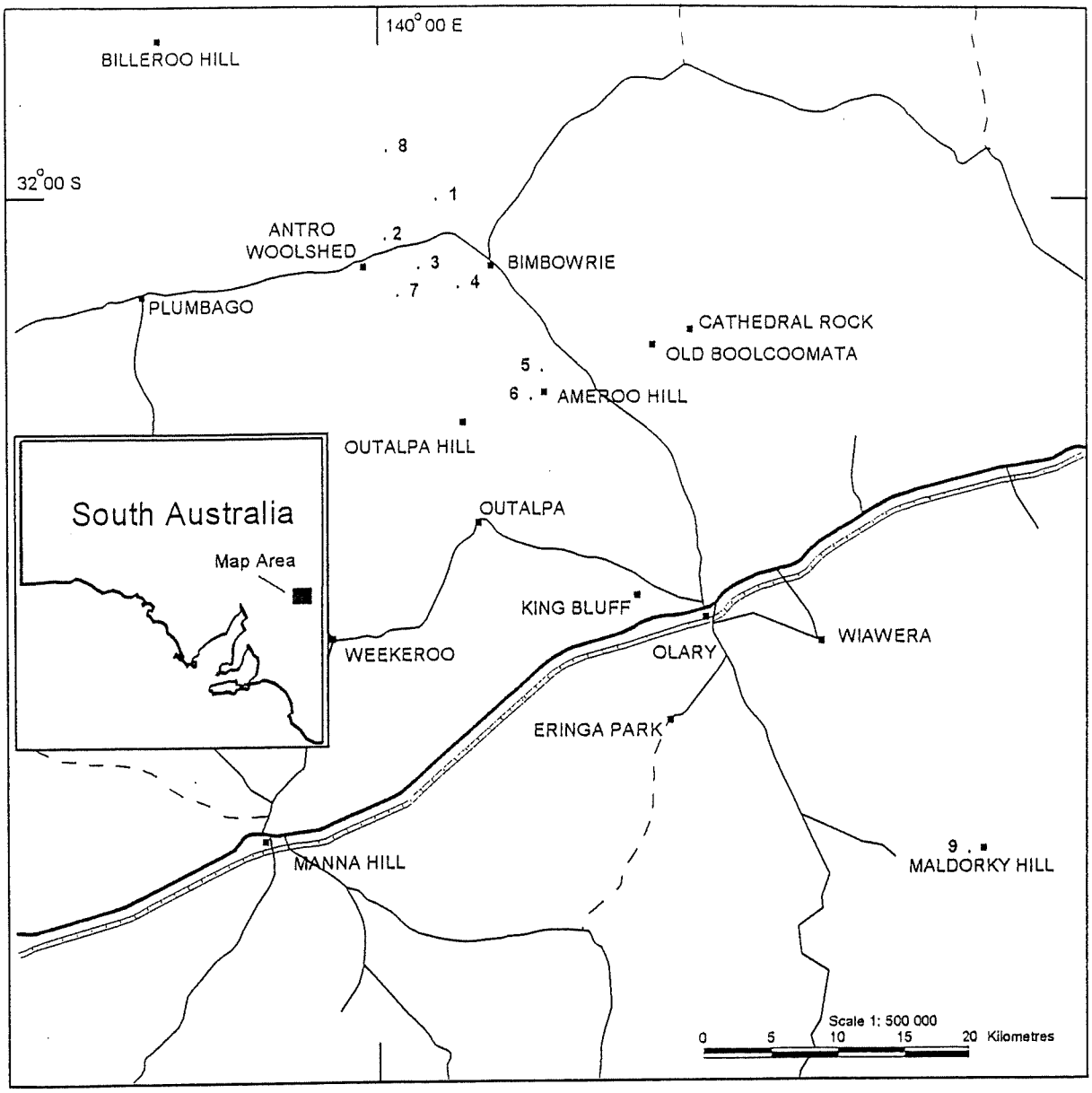

Fig 1.1 Loacality map of the Olary district, South Australia. Numbered points indicate location of outcrop in Table 1.1.

CHAPTER 2: REGIONAL GEOLOGY

2.1 Introduction

The Willyama Complex forms a series of partially detached Palaeoproterozoic inliers in western New South Wales (the Broken Hill Block) and eastern South Australia (the Olary Block; Fig.1.1). For more than a century the Broken Hill Block has been the focus of extensive mineral exploration and geological research, due to the impetus provided by the world class Broken Hill Pb-Zn-Ag deposit. In contrast, the Olary Block has received much less geological attention. Recently the Olary Block has been the focus of a new exploration initiative by various mineral exploration companies.

Mawson (1912) was the first to undertake a detailed investigation of the structural framework of the Olary Block and subsequently made a division between the regionally metamorphosed sediments of the crystalline basement, which he named the Willyama Complex, and the overlying Adelaidean sediments. Campana and King (1958) arranged the Palaeoproterozoic sequence into four broad stratigraphic units; migmatite and granite gneiss of Archaean origin (which was 'granitised' during the Palaeoproterozoic), the Outalpa Quartzites, the Ethiudna Calc-silicate Group and the Weekeroo Schist.

Talbot (1967) subsequently reversed the stratigraphy devised by Campana and King (1958) and placed the granitic terrain in the Weekeroo Inlier at the base of the sequence. Parker (1972) described a sequence in the Wiperaminga Hill area consisting of basal anatexites/quartzite/layered gneiss and schist/calc-silicate/mica schist. This became the basis for later stratigraphic proposals by Flint and Flint (1975) and Clarke *et al.* (1986). Flint and Parker (1993) provide an excellent summary of the geology of the Olary Block.

2.2 Regional Geology

The Willyama Supergroup in the Broken Hill Block has been interpreted by Willis *et al.* (1983) to represent a failed early Proterozoic rift. It has been proposed that the Olary Block portion of the Willyama Supergroup may represent a margin of this failed rift and although there is no conclusive palaeoenvironmental evidence for such a rift, it is generally thought that the stratigraphic sequence is consistent with deposition in an environment deepening upwards into marine strata (Cook and Ashley,1992; Ashley *et al.*, 1995).

Some parts of the stratigraphic framework established for the Olary Block can be correlated with similar features in the Broken Hill Block. This is depicted in Fig 2.2.1. Similarity exists between much of the Quartzofeldspathic Suite in the Olary Block and the Thackeringa Group in the Broken Hill Block, in addition to the Pelite Suite and Paragon Group (see below).

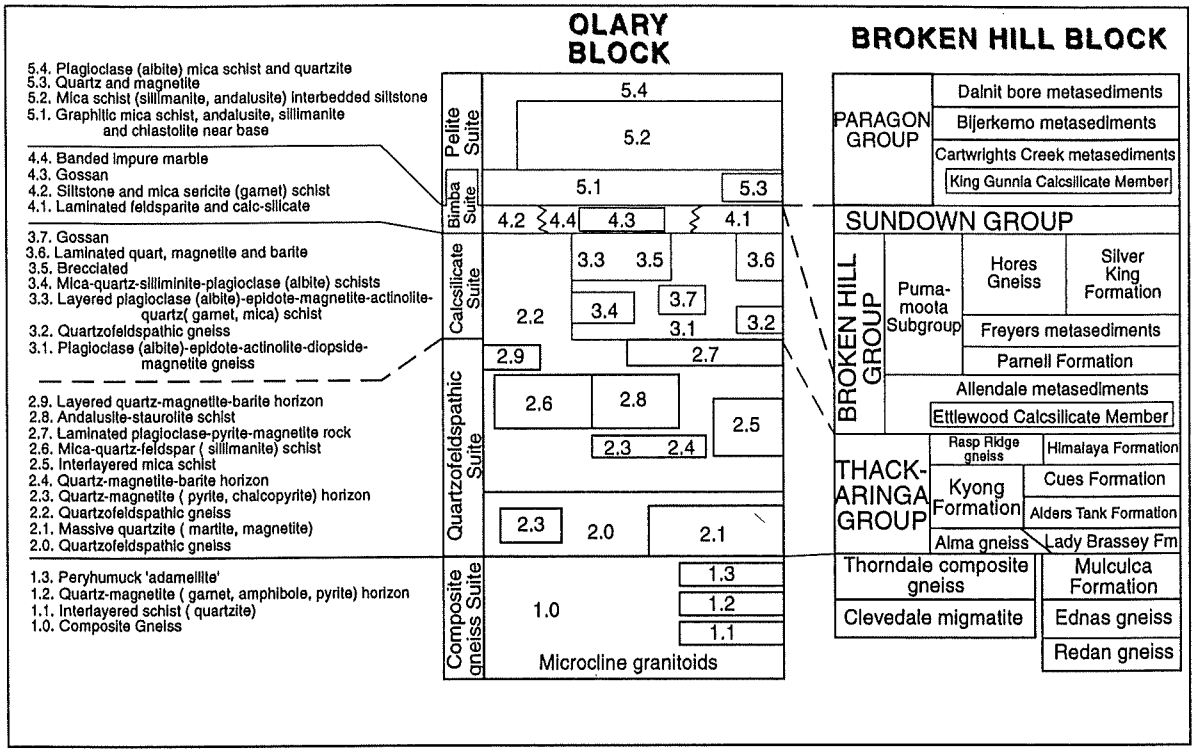

Fig 2.2.1 A tentative stratigraphic correlation between the Olary Block and Broken Hill Block (after Stevens *et al.*, 1990).

The Olary Block consists of medium (upper greenschist facies) to high (upper amphibolite facies) grade metamorphosed sediments in which primary layering is much better preserved than in the neighbouring Broken Hill Block, which exhibits even higher (granulite facies) metamorphic grades. A north to south increase in metamorphic grade in the Olary Block (Clarke *et al.*, 1987; Ashley *et al.*, 1995) is broadly consistent with the metamorphic isograds proposed for the Broken Hill Block (Phillips, 1980).

However, a major disparity between the Broken Hill Block and Olary Block exists in the absolute abundance of granitoids, in addition to the relative proportion of granitoids to mafic igneous rocks. Up to 10% of the outcropping Olary Block is granitoid (Ashley *et al.*, 1995) and mafic rocks are relatively scarce. In comparison, mafic rocks form a relatively major part of the Broken Hill Block.

2.3 Stratigraphy.

Clarke *et al.* (1986) proposed five main stratigraphic units for the Willyama Supergroup in the Olary Block which can be roughly correlated with stratigraphic equivalents in the Broken Hill Block (Fig.2.2.1). These stratigraphic units are individually discussed below.

Composite Gneiss Suite

The Composite Gneiss Suite is interpreted as the base of the Willyama Supergroup in the Olary Block. It is typically dominated by coarse grained and migmatitic quartz-feldspar-biotite ± garnet ± sillimanite gneiss.

Quartzofeldspathic Suite

The Quartzofeldspathic Suite is dominated by quartz-plagioclase (albite)-biotite±K-feldspar gneisses and massive quartzites, and can be correlated with the Thackaringa Group in the Broken Hill Block (e.g. Clarke *et al.*, 1986; Cook and Ashley, 1992; Flint and Parker, 1993). It has been informally divided into three components:

(i) A crudely layered "Lower Albite" unit; consisting typically of albite-quartz (± K-feldspar ± biotite ± muscovite ± magnetite ± pyrite) rocks. Granitoids exhibiting A-type affinities, have been observed within this unit (e.g. Buckley, 1993; Pierini, 1994).

(ii) A "Middle Schist" unit; of pelites, psammopelites and locally occurring composite gneiss.

(iii) A characteristically well laminated "Upper Albite" unit; with a variable mineralogy of albite-quartz (±K-feldspar ±biotite ±magnetite ±calc-silicates), occurs at the top of the suite.

Much of the Quartzofeldspathic Suite is thought to have a sedimentary origin involving felsic volcanoclastic precursors, (e.g. Flint and Parker, 1993).

Calcsilicate Suite

The base of the Calcsilicate Suite (and upper Quartzofeldspathic Suite) is characterised by laminated quartzofeldspathic rocks grading into massive (and brecciated) calcalbitite and calc-silicate rock. It appears possible that the "Upper Albite" unit of the Quartzofeldspathic Suite and much of the Calcsilicate Suite may be diachronous (Ashley *et al.*, 1995). The Calcsilicate Suite typically contains albite, actinolite, diopside, epidote and magnetite (± haematite ± sphene ± tourmaline ± zircon ± pyrite).

Cook and Ashley (1992) suggested an evaporitic origin in a lacustrine, playa lake, or sabkha setting for the calc-silicate rocks.

Bimba Suite

The Bimba Suite is a regionally extensive yet thin (≤50m) unit, comprising predominantly a quartz-albite-biotite rich, finely laminated metasiltstone, calc-silicate gneiss, pyritic gossan,

and impure marble (Fig 2.2.1). Bimba Suite gossans and surficial lag deposits are anomalous in Mn, Cu , Au, Pb, Ag, and Zn (Cook and Ashley, 1992).

The unit has been interpreted as representing a reduced, transitional lacustrine/sabkha/shallow marine environment (Flint and Parker, 1993; Ashley *et al.*, 1995).

Pelite Suite

The Pelite Suite is dominated by a more homogeneous mineralogy of quartz-biotite-feldspar ± muscovite±tourmaline. It is also characterised by basal occurrences of chiastolite porphyroblasts and by a graphitic facies of organic origin. The contact between the Pelite Suite and the underlying Bimba Suite is sharp, and provides a useful stratigraphic marker horizon (e.g. at the western base of Ameroo Hill).

The Pelite Suite is interpreted as a deep water (possibly turbiditic) deposit; a manifestation of continued Palaeo-Mesoproterozoic rifting.

2.4 Structure and Metamorphism in the Olary Block

Five major deformational events have been described to account for the folding and metamorphism of the Willyama Supergroup and Adelaidean sediments in the Olary Block (Berry *et al.*, 1978). Three of these phases (D_1 to D_3) affect the basement only, and are a manifestation of the Olarian Orogeny. The other two (D_4 and D_5) are also recognised in the Neoproterozoic (Adelaidean) cover, and can be attributed to the Cambro-Ordovician Delamerian Orogeny (Fig 2.4.1).

Clarke *et al.* (1987) proposed four metamorphic zones arising from a general north to south increase in grade. The relative timing of aluminosilicate assemblages implies an anticlockwise P-T-t path for the Olarian Orogeny; i.e. early-stage andalusite, middle-stage sillimanite and late-stage kyanite.

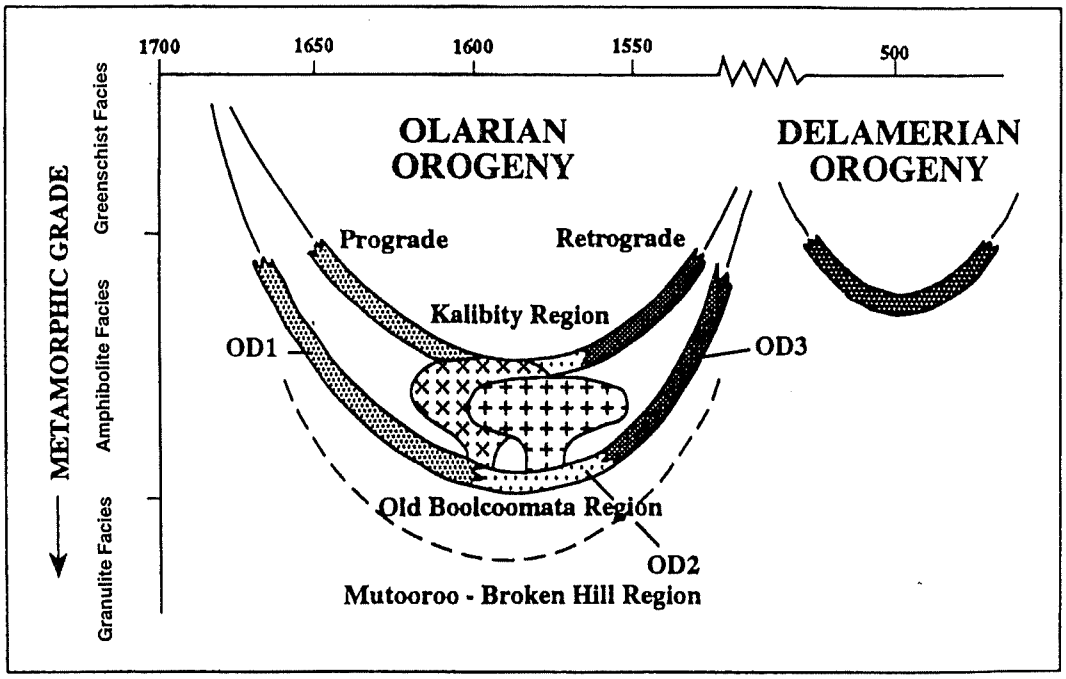

Fig 2.4.1 Metamorphism in the Olary Block; Metamorphic grade and timing of deformation . After Flint and Parker (1993).

2.5 Geochronological Constraints

Deposition of the Willyama metasediments is tentatively inferred from a U-Pb zircon analysis (on a banded albitite) to have initiated post ~1785 Ma (Fanning, 1995). The minimum age of sedimentation is not well constrained; a Mt Howden sample revealed a cluster at ~1775 Ma and one concordant grain at ~1630Ma, implying that sedimentation may have continued after 1630 Ma (Fanning, 1995).

Two quartzofeldspathic rocks with A-type affinities, a felsic metavolcanic rock and a meta-granitoid, have yielded U-Pb zircon ages of 1699±10 Ma and 1703±6 Ma respectively (Cook *et al.*, 1994). These dates are slightly older than that obtained by Page and Laing (1992) of 1690±5 Ma for a felsic volcanic rock metamorphosed to amphibolite grade from the Broken Hill Block. This slight difference is thought to be consistent with a contrast in stratigraphic position (Ashley *et al.*, 1995).

Intrusion of mafic rocks, frequently concordant with respect to primary layering, may have been a response to Early Proterozoic rifting. The age of sill/dyke emplacement is not well constained. A suite of I-type granitoids were emplaced at 1629±12Ma (Cook *et al.*, 1994). This sequence of metasediments, granites and mafic intrusives (volcanics?) was subsequently folded and metamorphosed during the Olarian orogeny from ~1600±8Ma to ~1500Ma±20Ma (e.g. Flint and Webb, 1980). A suite of massive to foliated S-type granites (e.g. the Bimbowrie granite; Benton, 1994), interpreted as the products of partial anatexis, accompanied this

deformation. A sample of this granite type from Triangle Hill has yielded a U-Pb zircon age of ~1590Ma.

A later suite of tholeiites is relatively unmetamorphosed and have geochemical affinities with the Wooltana Volcanics in the Adelaide Geosyncline (Ashley *et al,* 1995). These tholeiites are not observed to intrude the Neoproterozoic sediments, and are believed to have a pre-Adelaidean intrusive age.

Many previous attempts at Rb-Sr dating of granitoids in the Olary Block indicate the effects of post-magmatic alteration or metamorphism. For example, Flint and Webb (1980) obtained Rb-Sr dates of ~1460Ma-1500Ma for both the S-type granites and the Ameroo Hill A-type gneissic granitoid; probably indicating partial isotopic re-equilibration (Fanning, 1995). The Poodla Hill granitoid yielded a Rb-Sr 'isochron' of ~500Ma. Such a date possibly has implications for mobilisation of Rb and Sr during the Delamerian Orogeny, that deformed both the Adelaidean cover and Willyama Supergroup.

Table 2.4.1 below is a presentation of the relative timing of events in the Olary Block that is commonly adopted at present.

Table 2.4.1 (adapted from Ashley *et al.*, 1995)

Time (Ga)	Event	Source
500±20Ma	Delamerian Orogeny; D_4 & D_5	Ashley *et al.* (1995)
?800Ma	Pre-Adelaidean dolerite	Ashley *et al.* (1995)
1500±20Ma	D_3 .Minor granite, pegmatite emplacement. Retrograde metamorphism.	Flint & Webb (1980)
1600±8Ma	D_1-D_2; Amphibolite facies prograde metamorphism; S-type granites.	Page & Laing (1992)
1629±12Ma	Poodla granitoid and related I-Type granitoids.	Cook et al., (1994)
?1630Ma -1690Ma	Pelite Suite Bimba Suite Calcsilicate Suite	Fanning (1995)
1700Ma	A-type meta-felsic rocks Quartzofeldspathic Suite	Cook et al., (1994)
?1785Ma	Onset of sedimentation	Fanning (1995)
Archaean	recycling of old Archaean crust	

CHAPTER 3: PETROGRAPHIC AND FIELD DESCRIPTION OF THE MAFIC AND INTERMEDIATE ROCKS.

Regional mapping and sampling of the mafic and intermediate intrusives revealed five fundamentally different rock types, herein described as:

*Outalpa Amphibolite
*Poodla Granitoid
*Antro Granitoid (Benton, 1994)
*Olary Block dolerites and gabbros (3 types)
*Maldorky Lamprophyre

3.1 Outalpa Amphibolite

The Outalpa Amphibolite outcrops a as variably foliated, often highly weathered rock, principally composed of blue-green hornblende (50%-85%), plagioclase (albitised; 5-30%), opaques (magnetite, haematite and ilmenite; 5-10%), sphene(<5%), biotite(<5%) and minor quartz. The foliation is defined by the alignment of subhedral to euhedral hornblende (Plate 2e).

An outcrop of Outalpa Amphibolite about 1km west of Ameroo Hill was mapped at 1:5000 scale. This revealed a 1.2km long by 150m wide sill of plutonic or sub-volcanic nature. The sill has been emplaced within massive to crudely layered and locally brecciated calcalbitite rock which forms a topographic high at the western margin of the intrusive (Plate 1a). It is evident that this rock type has also been subject to post-magmatic alteration, evidenced by localised epidote-albite-actinolite assemblages (Plate 1b).

In the southern part of the outcrop the amphibolite is folded with the metasediments in an isoclinal D_2 syncline. It is also intruded by an Antro style granitoid of intermediate composition (Benton, 1994). Since the amphibolite has undergone high grade metamorphism and deformation, it is logical to assume that it was intruded prior to the Olarian Orogeny.

PLATE 1

(a) Concordant contact between the Outalpa amphibolite (top) and massive to crudely bedded calc-albitite (bottom) west of Ameroo Hill. Cross-cutting feature is a late stage pegmatite).

(b) Localised albite-epidote alteration in the Outalpa amphibolite (west of Ameroo Hill).

(c) Enclave of metasediment in the Poodla granitoid (arrow) west of Alconie Hill. (GR 0412396mE, 6462658mN).

(d) Tourmaline orbicule and smaller aggregates of biotite-epidote-sphene-magnetite in the Poodla granitoid. GR as for (c).

(e) Massive albite alteration in the Antro granitoid (GR 0412510 mE, 6457150 mN)

(f) Actinolte (enclosing albite) veins in the Antro granitoid.
GR as for (e).

(g) Pervasive epidote and albite veins in the Antro granitoid. GR as for (e).

(h) Ptygmatic folding of narrow pegmatite veins in quartzofeldspathic rocks (psammopelite) ~200m W of Ameroo Hill.


a


b


c


d

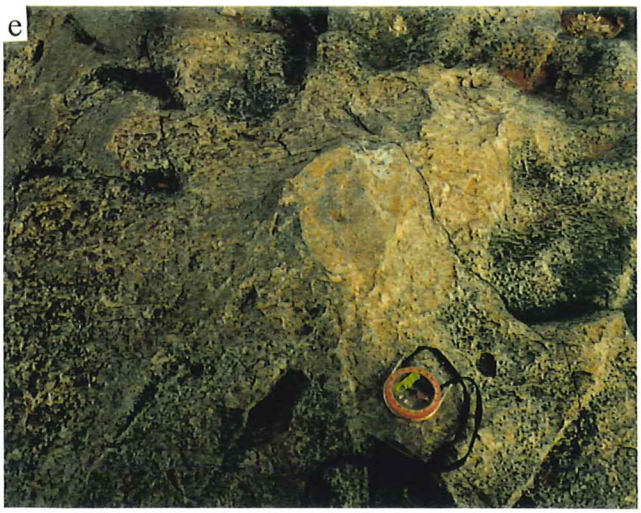
e

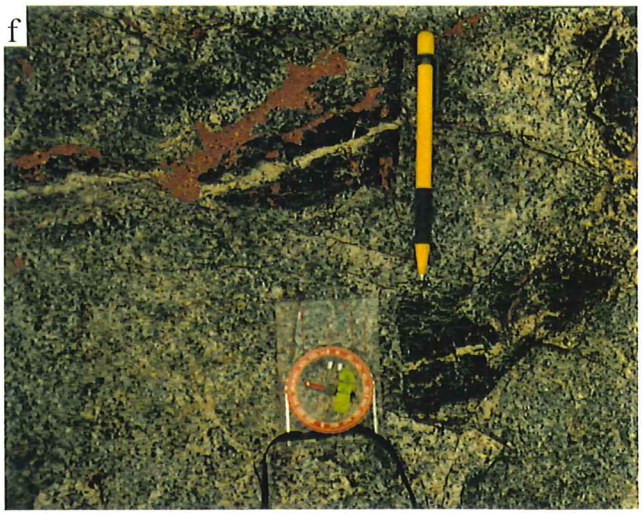
f


g


h

3.2 Antro Granitoid

Benton (1994) classified this rock type as a tonalite on the basis of modal plagioclase >50% and <5% K-feldspar. This study has also found it to possess mineralogy typical of quartz diorite and quartz monzodiorite. Modal compositions are variable; quartz~20%, plagioclase (variably albitised) 35%-50%, K-feldspar (checkerboard albite) <15% (Plate 2f), actinolite~5%, opaques~10%, sphene<5%, epidote~2% and minor biotite, chlorite, serpentine, limonite and zircon. A coarse granophyric texture is exhibited in an Antro quartz diorite outcropping north of Ameroo Hill (Plate 2g).

The Antro granitoid is clearly intrusive at an outcrop ~1km W of Ameroo Hill, where it crops out in a sill-like structure that intrudes the amphibolite, and is offset by a D_3 shear zone. It also crops out~2km NE of Antro Woolshed, at an isolated outcrop N of Ameroo Hill, near East Doughboy and on the western margin of a large 'Bimbowrie Granite' outcrop near Antro Woolshed. It is variably weathered in outcrop and exhibits three principle alteration styles; massive albite, pervasive epidote and actinolite (enclosing albite) veins (Plate 1e,f & g). Granitoid clasts in a calc-silicate breccia 2km NE of Antro Woolshed indicates post-magmatic brecciation (Plate 2c). A weak foliation can be distinguished in some outcrops.

Relationships with the surrounding metasediments are uncertain, due to of lack of exposure. Field relationships west of Ameroo Hill suggest that this intermediate intrusive is pre- to syn-orogenic. The Antro granitoid is related to the Poodla granitoid on geochemical grounds (Chapter 3) despite their contrasting petrographic nature (i.e. biotite poor versus biotite rich).

3.3 Poodla Granitoid

The Poodla granitoid contains K-feldspar (45%), quartz (20%), biotite (15%), magnetite (~7%), sphene (5%), epidote (5%) and zircon (<1%). It exhibits intergrowth of K-feldspar and albite: much of the original K-feldspar is now in the form of 'checkerboard' albite. Granular biotite occurs in ~6mm patches in association with epidote (often zoned: Plate 2h), magnetite, sphene and zircon. Biotite veining indicates post-magmatic K-enrichment (Plate 3a). According to the classification system of Streckeisen (1973) this rock is a syenogranite.

This lithology was sampled from a small outcrop west of Alconie Hill. Enclaves of metasediment (Plate 1c), large (~2cm) 'radial' patches (orbicules) of tourmaline (Plate 1d) and smaller (~1cm) aggregates of biotite and magnetite characterise this rock type. A weak foliation defined by aligned biotite aggregates was observed in outcrop . An unusual planar 'flow banding' phenomenon (centimetre scale) was also observed and may be indicative of either crystal settling or flow within a cooling magma. The relationship of this lithology with the surrounding metasediments is unknown due to lack of exposure.

PLATE 2

(a) Outcrop of the magnetic 'Rainy Day' dolerite ~2km NE of Antro Woolshed (in background).

(b) Sharp intrusive contact of a Maldorky Lamprophyre dyke with schistose Adelaidean siltstone, implying a post-Delamerian age for these potassic rocks.

(c) A clast of Antro granitoid in a calc-silicate and Fe-rich breccia; indicating post-magmatic brecciation. (At the outcrop ~2km NE of Antro Woolshed, near old Cu-pit).

(d) Thin section of the crenulated pelite (bt-qtz-tour-ap-zir) at the margin of the Rainy Day dolerite outcrop. Note how quartz grains are partitioned into the hinges of the crenulation folds. (X-polars; magnificationx1.5).

(e) Foliation in the Outalpa Amphibolite defined by the alignment of green hornblende crystals. (Plane light; magnificationx1.5).

(f) 'Checkerboard' albite in the Antro granitoid. This is inferred as evidence for the previous existence of K-feldspar in this granitoid. (Plane light; magnificationx10).

(g) A coarse, recrystallised granophyric texture in the Antro granitoid N of Ameroo Hill is further possible evidence for K-feldspar as a previous constituent. (X-polars; magnificationx1.5).

(h) Poodla granite: Zoned epidote crystal (arrow) in granular biotite-magnetite-sphene aggregate. (X-polars; magnificationx5).

a

b

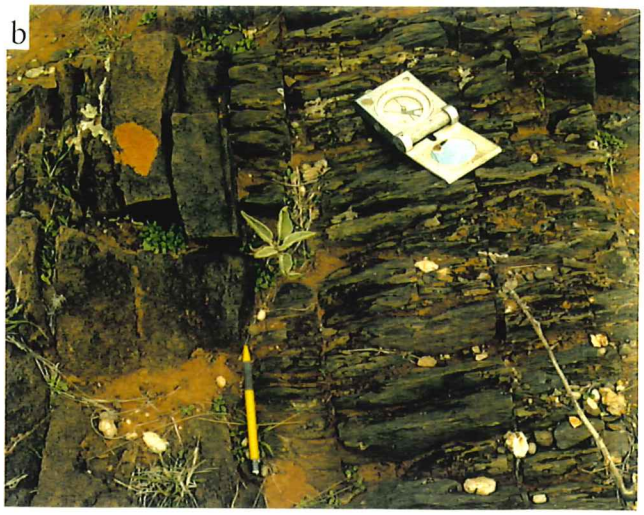

c

d

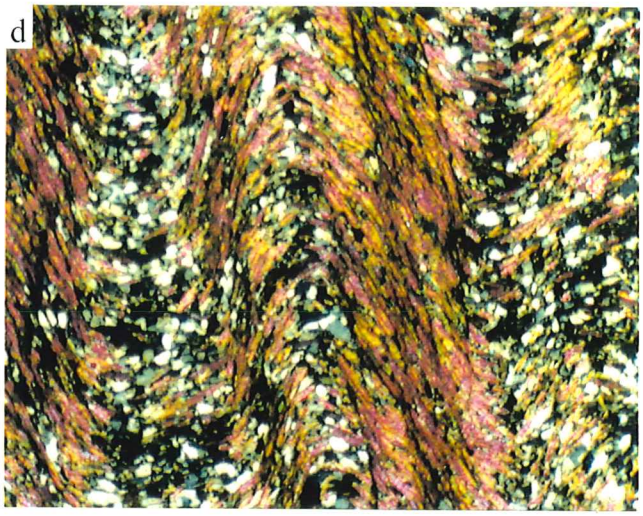

e

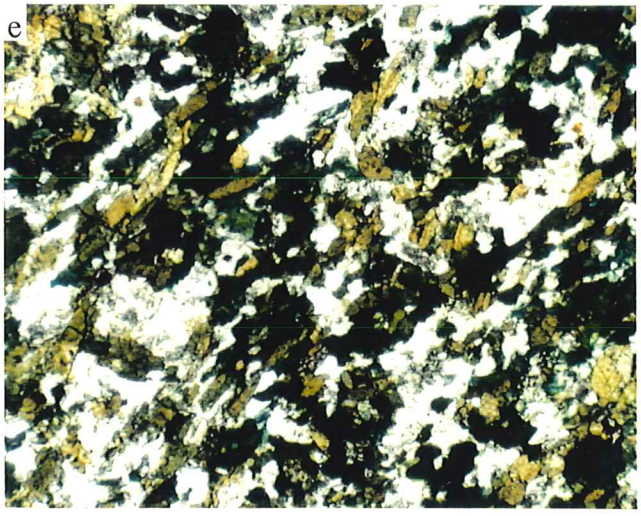

f

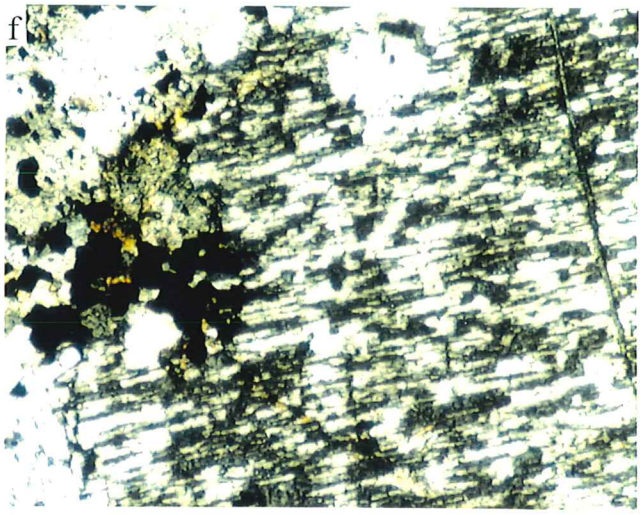

g

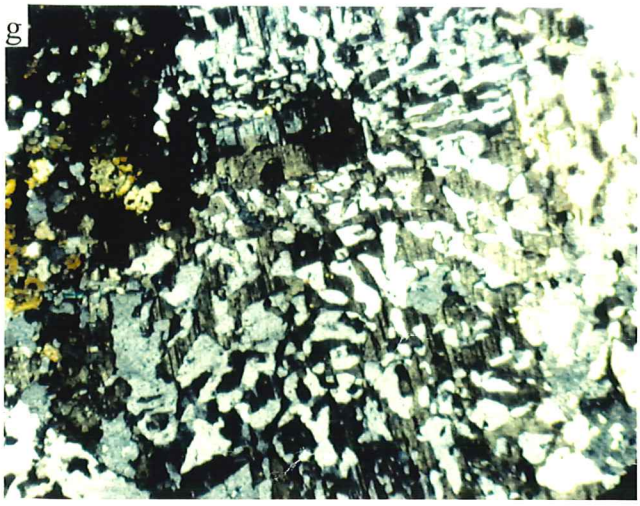

h

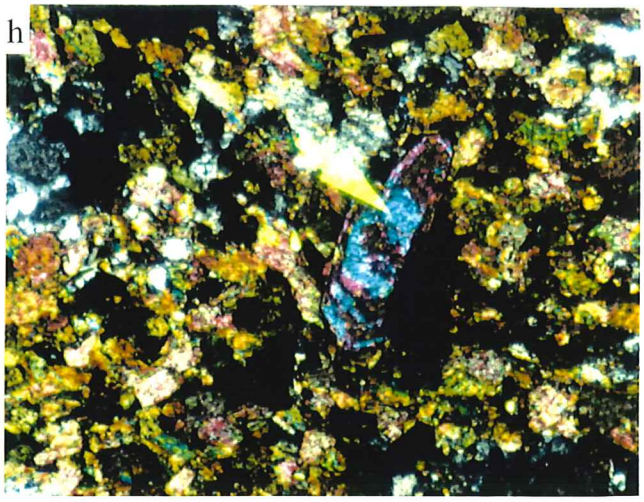

3.4 Olary Block Dolerites & Gabbros

Three types of post-Willyama variably albitised meta-dolerites have been distinguished by means of geochemical and isotopic analyses (Chapter 4 & Chapter 5). The first two have names describing their distinct geochemical characteristics; i.e. HPT (high P_2O_5 and TiO_2), LPT (low P_2O_5 and TiO_2). The third type is named after the outcrop 1-2km NE of Antro Woolshed. All types display distinct petrological characteristics:

(i) HPT dolerite

The most prominent constituents of these rocks are albitised plagioclase (20%-45%), actinolite (15%-40%) possibly after clinopyroxene, and opaque grains (magnetite+ilmenite+haematite 5%-22%). Minor constituents include sphene (<8%), epidote (<15%), chlorite, calcite and quartz. Sphene after ilmenite or Ti-magnetite is a common feature of these rocks. Biotite is highly variable (<1%-15%) and this appears to have important geochemical implications (Chapter 4). This lithology also exhibits variable textures; from sub-ophitic (gabbroic and doleritic; Plate 3b) to strongly recrystallised.

The HPT dolerites crop out at East Doughboy, Baxter's Bore, ~4km SW of Willow Well (near large outcrop of Bimbowrie granite), and at the northern most dolerite outcrop relative to the Antro Feldspar Mine. They intrude the Willyama metasediments but have not been observed intruding the Adelaidean metasediments.

(ii) LPT dolerite

The primary mineralogical difference of the LPT dolerites in comparison to the HPT dolerites is their opaque-poor nature (usually <3%; Plate 3c). They are generally plagioclase-amphibole-epidote rich and biotite/sphene poor. Epidotisation of plagioclase laths is a common alteration product and it is probable that the plagioclase is more Ca-rich relative to that in the HPT dolerites.

The LPT dolerite outcrops adjacent to the Antro Feldspar Mine, near Baxter's Bore and at Mt Howden (data of Menzies, 1992). Geochemically similar amphibolites crop out near Mutooroo. These mafics are clearly intrusive into the Willyama metasediments but not the Adelaidean cover. They are distinguished from the HPT dolerite by their consistently lower magnetic susceptibility and by geochemical discrimination (Chapter 4).

(iii) Rainy Day dolerite

In hand specimen this rock type exhibits a relict igneous texture. The mineralogy of the Rainy Day dolerite is clearly unlike the previous dolerites. Three types of amphibole minerals were identified, forming the basis of the distinction; primary brown hornblende (Plate 3d), cummingtonite and lesser riebeckite (at cummingtonite grain margins; Plate 3e), which comprise ~40% of the modal composition. Multiple twinned plagioclase (albitised, 30%),

biotite (7%), opaques(10-15%), and minor quartz and epidote are the other constituents. The Rainy Day dolerite is also characterised by a sub-ophitic texture.

The one known exposure of the Rainy Day dolerite is ~2km NE of Antro Woolshed (Plate 2a) where it outcrops in contact with an Antro granitoid (quartz monzodiorite). This contact appears gradational, with quartz content progressively increasing along a SE-NW transect, but the higher degree of alteration (albitisation) of the Antro style intrusive is suggestive of the later intrusion of the Rainy Day dolerite.

The contact of the Rainy Day dolerite with the metasediments (qtz-feld-bt-tour-zir: Plate 2d) is represented by a 'reaction zone' of albitised metasediment/ albitised dolerite at the margins of the intrusive body. Within the dolerite body pods of breccia and albitised dolerite outcrop, possibly indicating that the roof of the intrusion is presently exposed. Retrogressed andalusite porphyroblasts in the marginal metasediments could indicate relatively shallow crustal levels for the mafic intrusion.

3.5 Maldorky Lamprophyre

The Maldorky Lamprophyre is a potassic biotite/phlogopite-phyric rock of basic to intermediate composition. Its mineralogy is distinct, with the most characteristic feature in hand specimen being abundant biotite/phlogopite phenocrysts. These 5mm euhedral crystals contain needle-like apatite inclusions (Plate 3f) and comprise 30% of the modal composition. In the groundmass the prominent mineral is sericitised K-feldspar (orthoclase; 30%) and relict multiple twinning indicates minor plagioclase (<5%). Chlorite (after biotite; 8%), undulose quartz (<10%), and pale pink carbonate (calcite; <5%) are relatively minor groundmass phases. Opaque grains (10%) of ~6mm size exhibit conspicuous highly altered cores of biotite, chlorite, feldspar and carbonate (Plate 3g). This assemblage may indicate former olivine phenocrysts (as described by McDonald, 1992). The petrography of the Maldorky Lamprophyre is similar to that of the Truro lamprophyre (Muller *et al.*, 1993) and the lamprophyre dykes near Anabama Hill (McDonald, 1992).

This rock type outcrops south-east of the Olary township near Maldorky Hill in a series of N-S to NNE-SSW trending dykes, which intrude folded Adelaidean sandstones, siltstones and tillites (Plate2b). The dykes are variably exposed but are clearly transgressive with respect to inferred Delamerian structural features of the Adelaidean sediments. They have width of <1m to ~15m, and may strike for lengths up to several kilometres.

These rocks are considered equivalent to the Ordovician lamprophyres of Müller *et al.* (1993).

PLATE 3

(a) Poodla granite; Biotite veining (indicated by arrow) in typically diamond shaped sphene crystal, indicating potassic (post-magmatic) enrichment via interaction with K-rich fluids. (Plane light; magnificationx5).

(b) An example of the typical sub-ophitic texture observed in the HPT dolerites. Note the abundant opaque minerals. (X-polars; magnificationx5).

(c) Hornblende-plagioclase assemblage in the LPT dolerites. Note the lack of opaque minerals in comparison to the HPT dolerite (b). (Plane light; magnificationx5).

(d) Possible primary hornblende with good 120° cleavage in the Rainy Day dolerite. (Plane light; magnificationx10).

(e) Fe-rich amphibole (cummingtonite; blue & yellow birefringence) rimmed by sodic amphibole (arrow; riebeckite) in the Rainy Day dolerite. (X-polars; magnificationx10).

(f) Euhedral phlogopite phenocryst containing needle-like apatite inclusions, in the Maldorky Lamprophyre. (Plane light; magnificationx5).

(g) Biotite/phlogopite phenocrysts; K-feldspar groundmass; and opaque grain with altered core (centre), possibly representing former olivine in the Maldorky Lamprophyre. (Plane light; magnificationx1.5).

(h) Polished Section: Unusual alteration style of opaque grain in the HPT dolerite. Core is possibly goethite, whilst the darker outer laminae are haematite. (Plane light; magnificationx10).

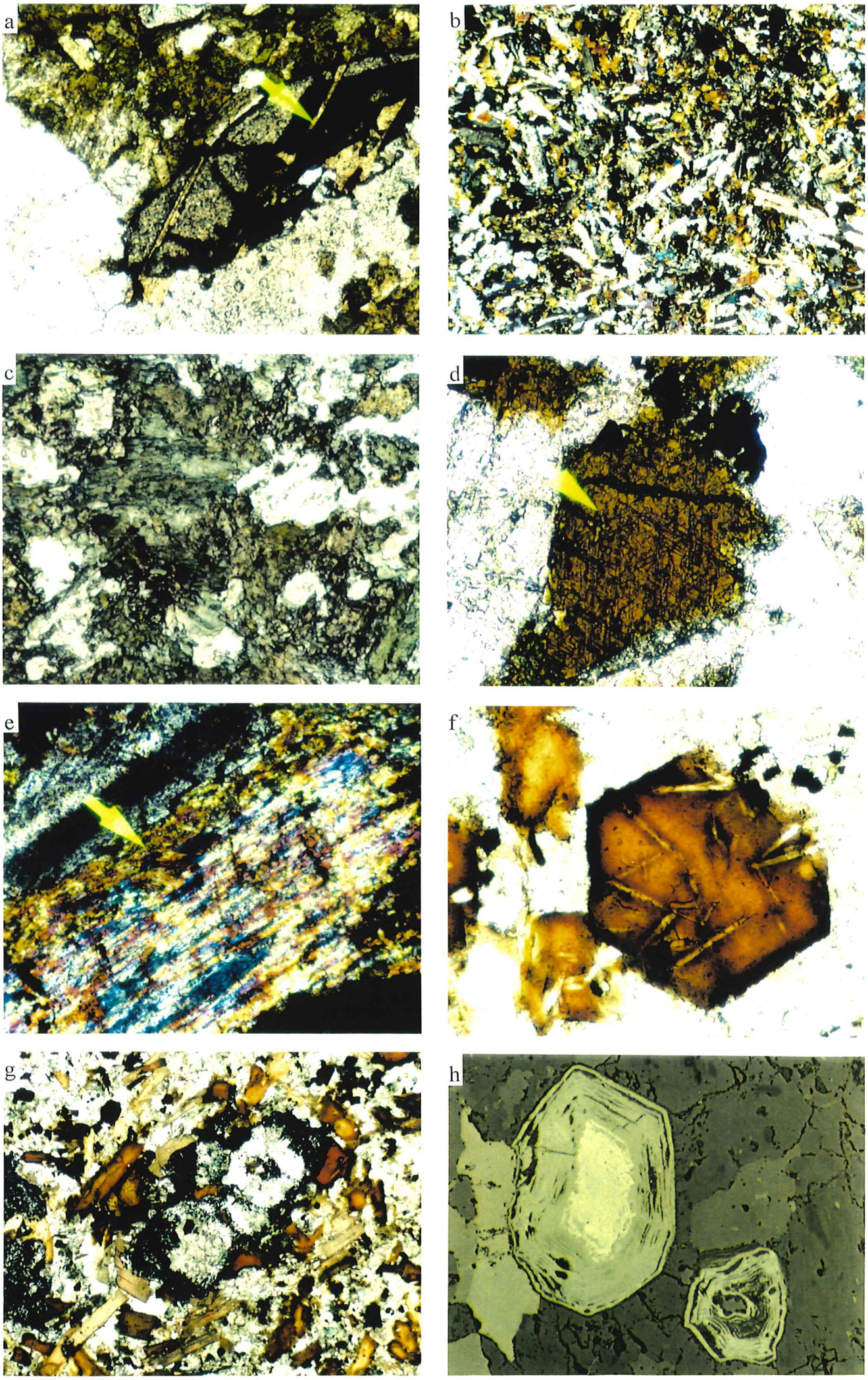
a
b
c
d
e
f
g
h

CHAPTER 4: GEOCHEMISTRY

4.1 Introduction

The study of petrogenesis in basic igneous rocks involves the determination of source characteristics, manner of partial melting, subsequent modification of magmas during ascent, identification of tectonic regime and characterisation of those features with implications for non-genetic (e.g. alteration) processes. Major and trace element geochemistry is the primary tool used to resolve of these problems.

In the Olary Province it is possible to discriminate the mafic and intermediate rocks by utilising major, trace and REE analyses. In metamorphosed terrains such as the Olary Block, complications arise in interpreting rock chemistries due to the mobility of many elements during metamorphic and metasomatic events. Major emphasis has been placed upon the application of those trace elements considered to be immobile during metamorphism and alteration: e.g. Ti, Nb, Y, Zr (Winchester & Floyd, 1975).

Thirty eight whole rock major and trace element analyses (Appendix C) were integrated with analyses provided by North Ltd and the data of previous workers.

This chapter aims to characterise the geochemistry of the Olary Block mafic rocks, to gain insight to processes involving partial melting, fractional crystallisation, crustal interaction, post-magmatic alteration; and to provide interpretations of the tectonic environments active during magmatism.

4.2 Outalpa Amphibolite

4.2.1 General

The Outalpa Amphibolite can characterised by SiO_2~50 wt%, moderate TiO_2 levels (~1.3wt%), high Na/K ratios and high total Fe (as Fe_2O_3) of ~15 wt%. MgO levels (>6wt%) are notably higher than the Cathedral Rock amphibolites of Pierini (1994) which, apart from one unusual sample (AMPH -256) do not have >5.5 MgO (wt%). Values for Mg# (Mg# $=Mg^{2+}/Fe^{2+}+Mg^{2+}$) of <0.5 are indicative of moderate degrees of fractionation of ferromagnesian minerals. On Fig. 4.2.1 the amphibolite plots within the sub-alkaline basalt and basaltic andesite fields. This characteristic, along with high Fe levels and other major element geochemistry (below), indicates a tholeiitic basalt precursor.

Sample No.	1060-055	AMPH-256	AMPH-UC1	R72900	Ave of 14
Rock type	Amphibolite	Amphibolite	Amphibolite	Amphibolite	Amphibolite
source/	this study	Pierini,1994	Pierini,1994	Eykamp, 1993	Flint&Parker, 1993
location	Ameroo Hill W	Cathedral Rock	Cathedral Rock	Outalpa	Weekeroo type
Major(wt%)					
SiO_2	49.28	46.53	48.79	50.16	51.48
TiO_2	1.34	0.71	2.92	1.43	1.64
Al_2O_3	13.54	13.02	11.61	14.34	14.28
Fe_2O_3	15.15	15.57	19.28	4.80	14.08
FeO				7.20	
MnO	0.22	0.24	0.19	0.15	0.18
MgO	6.31	9.94	4.19	6.88	5.89
CaO	9.67	9.44	6.29	10.29	7.93
Na_2O	3.42	2.79	4.33	2.35	3.68
K_2O	0.48	0.28	0.11	0.51	0.53
P_2O_5	0.15	0.02	0.31	0.14	0.05
SO_3	0.01	0.31	0.18	0.01	–
LOI	0.77	1.26	1.47	1.63	–

Table 4.2.1 Major element comparison between Olary Block amphibolites, showing a major element correlation between the Outalpa /Weekeroo amphibolites.

4.2.2 Comparison of Outalpa and Cathedral Rock samples

Table 4.2.1 above clearly illustrates a correlation between the Outapla amphibolite samples from this study and those from the study of Eykamp (1993) and Peterson (1993). In comparison nearly all the Cathedral Rock amphibolites have much higher total Fe (up to 20wt%), Ti (>2wt%) and P and lower Mg, Al and Ca.

The Outalpa amphibolite exhibits a very flat primordial mantle-normalised incompatible trace element pattern (Fig.4.2.2a) in accordance with the descriptions of Turner *et al.*, (1992) and Foden *et al.* (1995; in prep.) for the Palaeo-Mesoproterozoic mafic rocks of the Gawler Craton. A comparison between the Outalpa and Cathedral Rock amphibolites reveals a similarly flat but more incompatible element enriched pattern for the latter; with consistently higher Nb, P, Ti, Zr and Y levels (Fig 4.2.2b). Ni and Cr levels in the Outalpa rocks are far greater than in the Cathedral Rock amphibolites and this is consistent with a comparison of Mg# (0.35-0.5 and <0.27 respectively).

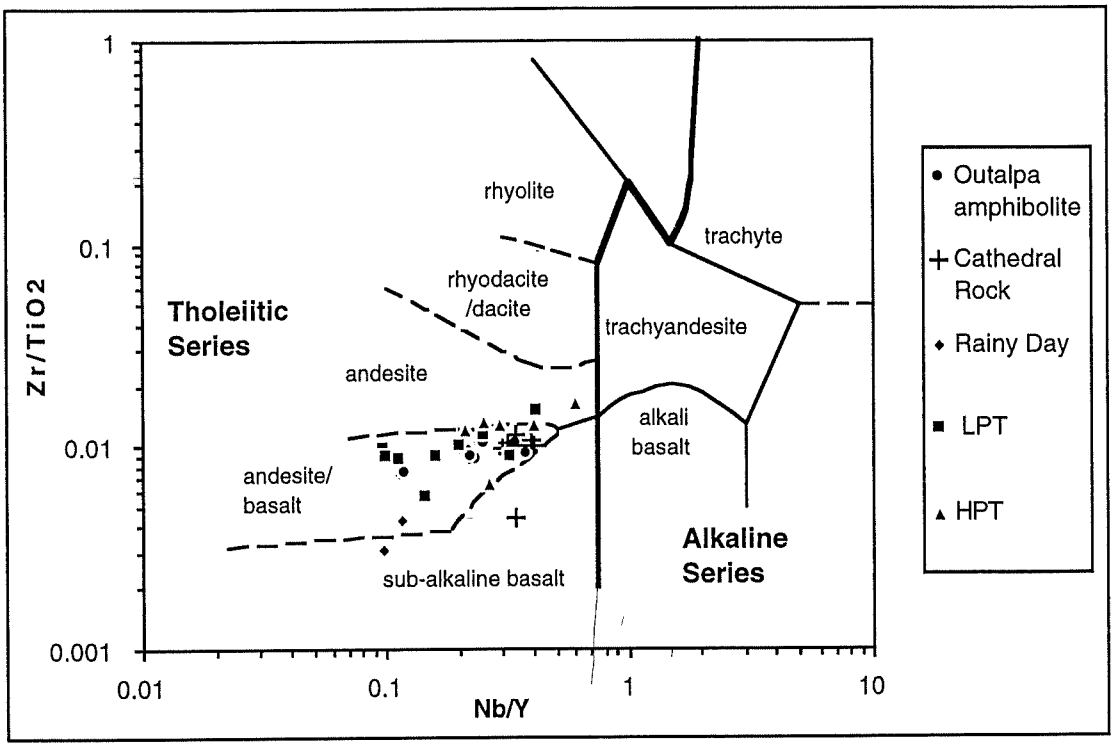

Fig 4.2.1. Zr/TiO2vNb/Y classification of volcanic rocks (after Floyd & Winchester, 1977).

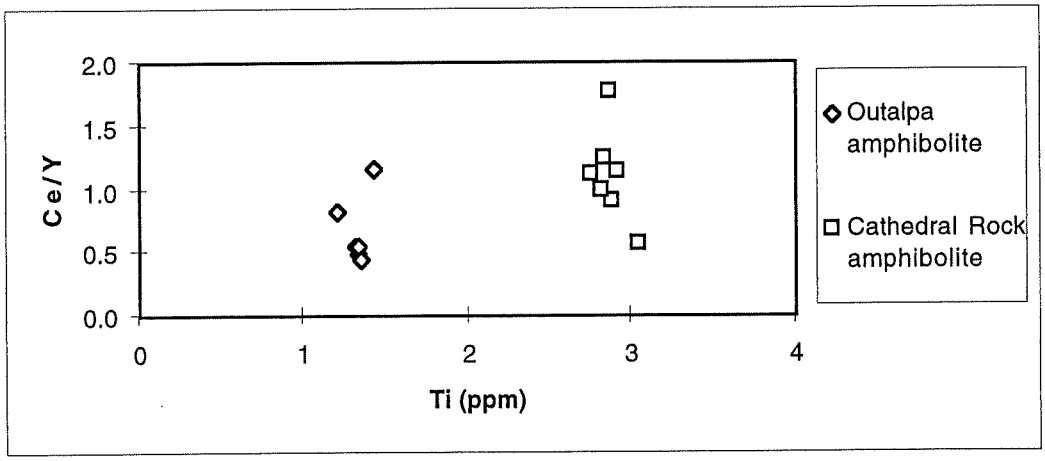

Fig 4.2.3 Ce/YvTiO2 discrimination of the Olary Block amphibolites.

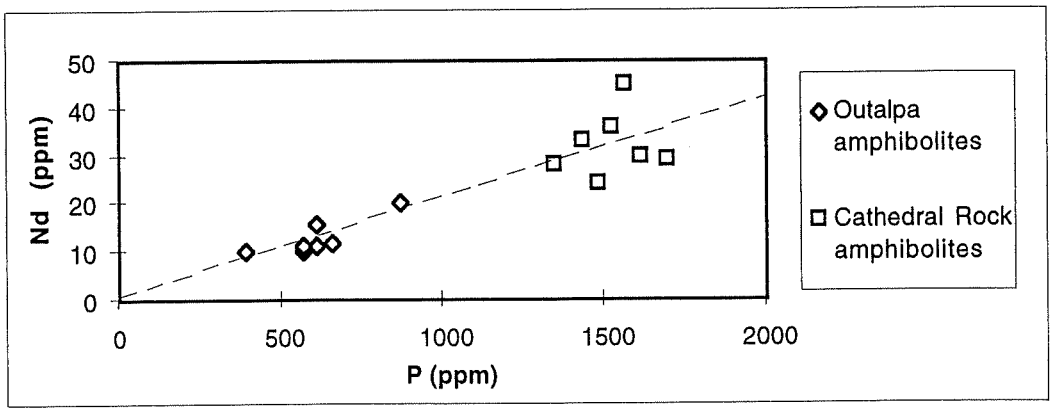

Fig 4.2.4 NdvP discrimination of the Olary Block amphibolites.

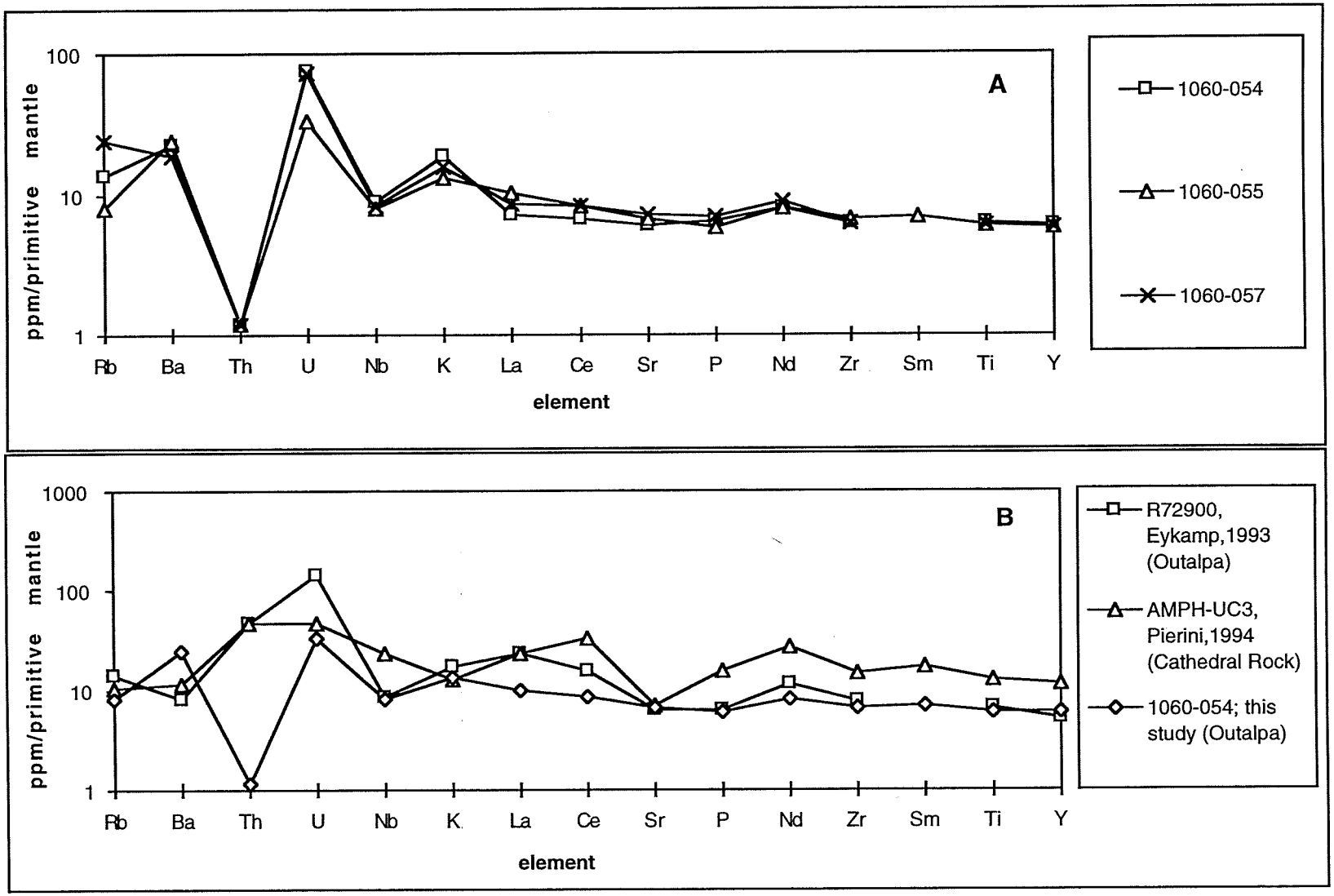

Fig 4.2.2 (A) Primitive mantle -normalised trace element pattern for the Outalpa amphibolite.

(B) Incompatible trace element comparison of the Olary Block amphibolites.

Several lines of evidence eliminate the possibility that the two amphibolite types are related by fractionation.

A plot of Ce/YvTi (Fig 4.2.3) clearly reveals different concentrations of Ti at similar values of Ce/Y for the two groups (Ce/Y is equivalent to LREE/HREE). Ce levels are mostly ~10x primitive mantle values for the Outalpa amphibolites in comparison to 25-40x primitive mantle for those of Pierini (1994). Fractionation of these tholeiites equivalent to 2-4 times for LREE would generate intermediate or acid magmas, not basalts or baslatic andesites with flat primitive mantle-normalised trace element patterns. Similarly a plot of NdvP (Fig 4.2.4) produces a straight line through the origin, but there is a considerable gap in absolute trace element concentrations, indicating that whilst the two rock types may have a similar source, either; (i) the source is heterogeneous, (ii) mixing between source components has occurred, (iii) or there has been variable degrees of partial melting of this source.

Significantly, this problem is resolved by plotting Y/NbvZr/Nb (Fig 4.2.5); on which the amphibolites lie on an array between an enriched plume-like source and a depleted MORB source, approximating the position of E-type MORB. Also significant is the closer proximity of the Cathedral Rock samples to an enriched source.

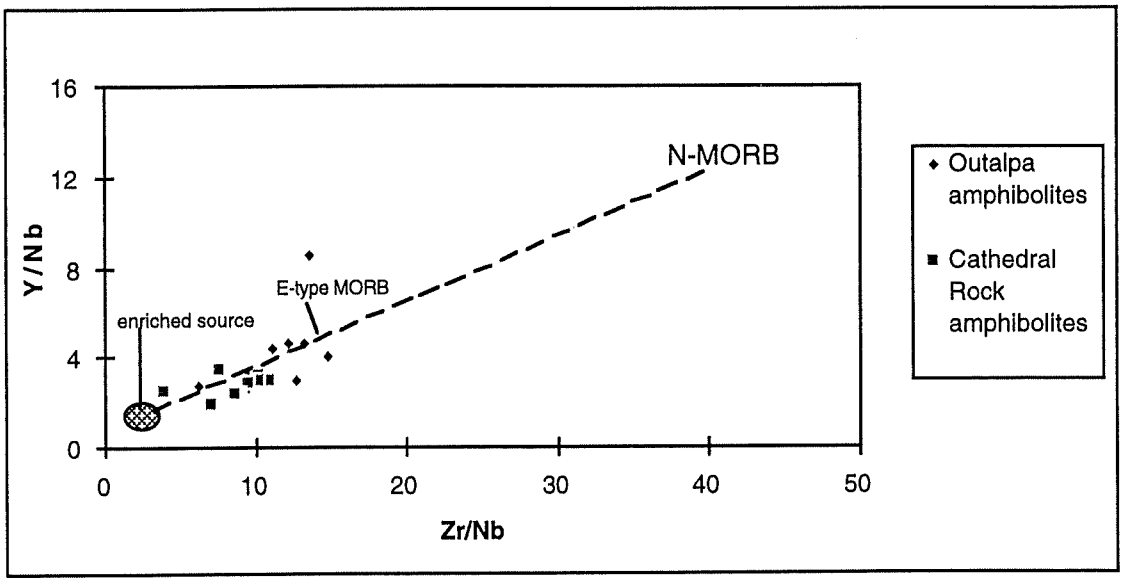

Fig 4.2.5 Y/NbvZr/Nb for the Olary Block amphibolites (adapted from Wilson, 1989).

4.3. Antro and Poodla granitoids

4.3.1 General

The Antro and Poodla granitoids are charactarised by intermediate compositions (SiO_2 range of 50-70wt%; precluding A-type affinities) and high total Fe (>5wt%). They are easily distinguished by alkali abundances. The Poodla granite is potassic (K_2O>4.5wt%) in marked contrast to the Antro granite which contains <1wt% K_2O. This is consistent with the biotite content of these rock types as discussed in section 3.2-3. The Antro granitoid is Na_2O-rich in comparison to the Poodla granite and this is attributed to the effects of Na and K metasomatism (see Appendix for discussion).

Other major element oxides that have not been affected considerably by this alteration, MgO and TiO_2, show negative correlations with respect to SiO_2, indicative of a fractionating magma series (Fig 4.3.1a&b). The Poodla granite is relatively Al-rich and Ca- and Fe-poor in comparison to the Antro granite. High Na, Al Index<1.1, CIPW normative diopside, and accessory CPX, hornblende and sphene are all indicators of an I-Type origin for the Antro granitoid (Chappell & White, 1974). Tourmaline, biotite, and normative corrundum~1% indicate that the Poodla granitoid is transitional I- to S-type; it has probably undergone greater crustal interaction than the Antro granite.

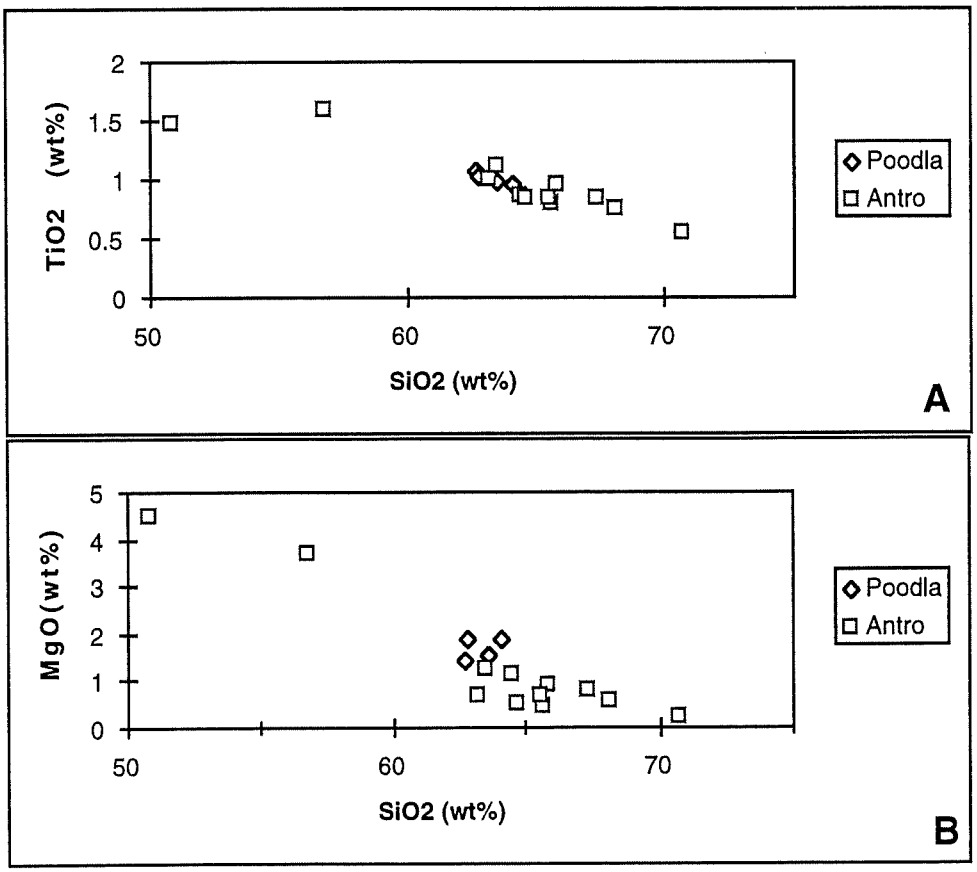

Fig 4.3.1a&b Major oxides (wt%) v SiO_2 for the Antro and Poodla granites.

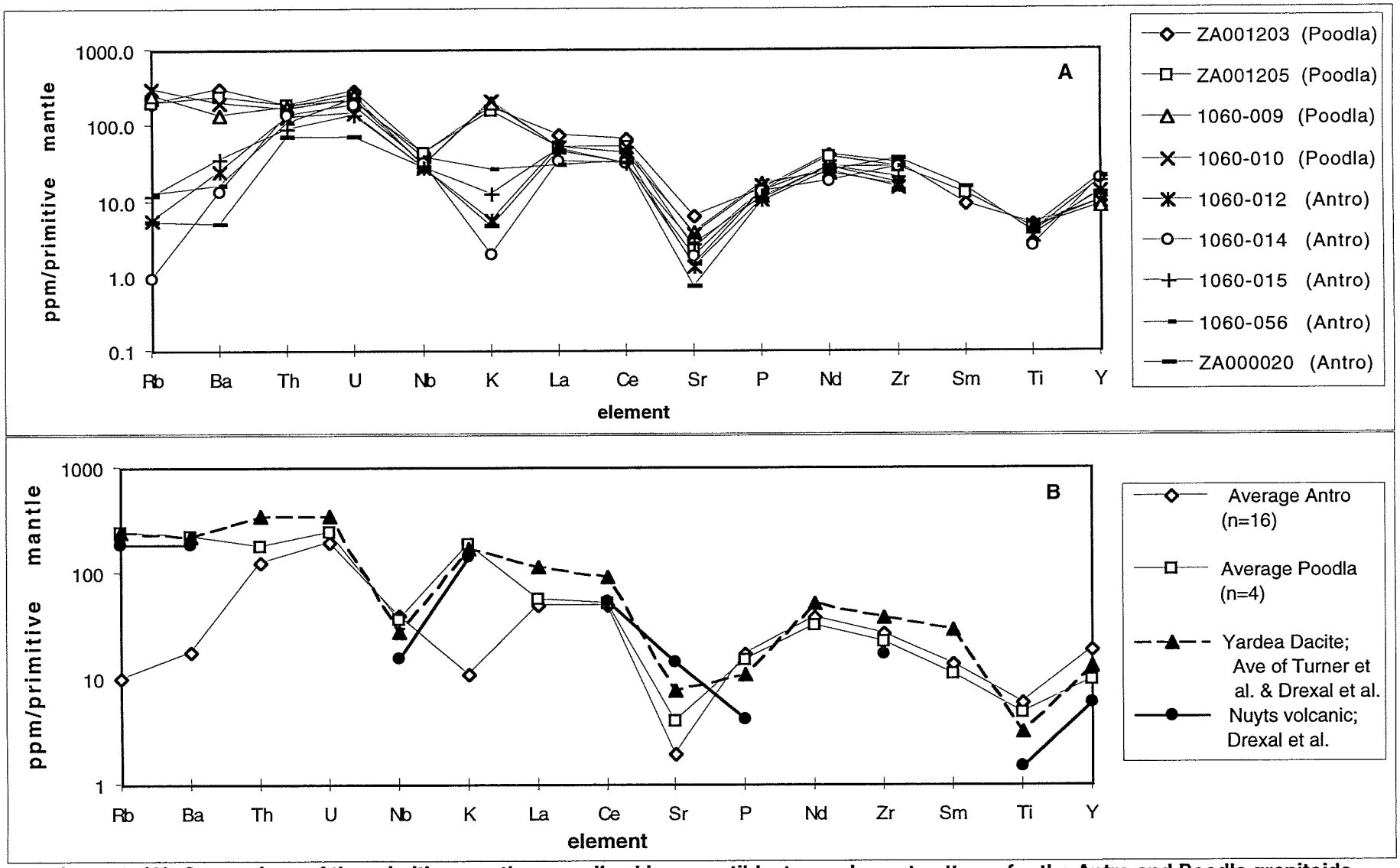

Fig 4.3.2 (A) Comparison of the primitive mantle-normalised incompatible trace element patterns for the Antro and Poodla granitoids. (B) Interregional correlation of Olary Block I-type granites with Gawler Block felsic rocks.

4.3.2 Trace element comparison

On a primitive mantle-normalised incompatible trace element diagram (Fig 4.3.2a) the Antro and Poodla granitoids appear chemically similar apart from discrepancies involving the mobile LIL elements Rb, Ba and K. Striking features for the Poodla granite are distinct Nb and Sr depletions, resulting from crustal interaction (evidenced by enclaves and tourmaline) and plagioclase fractionation, respectively. Geochemical comparison between the Olary intermediate rocks and Gawler Craton granitoids reveals good correlations between the Poodla granitoid, the Nuyts Volcanics (which have a similar SHRIMP age; Flint, 1993) and the Yardea Dacite (Fig 4.3.2b).

4.3.3 Tectonic discrimination

Pearce *et al.* (1984) used abundances of Nb, Y, Yb, Ta and Rb to discriminate between granites of different tectonic settings. Fig 4.3.3 shows a within-plate setting for the mafic granitoids using the Nb-Y scheme of Pearce *et al.* (1984). Furthermore, all samples plot beneath the upper compositional boundary (dashed line) for granites from anomalous ridge segments.

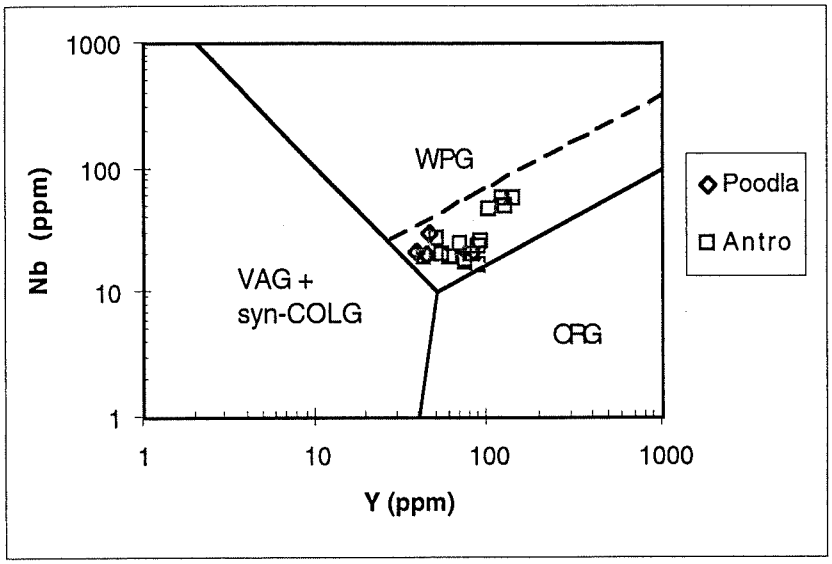

Fig 4.3.3 NbvY tectonic discrimination of granitoids (SiO_2=56-80 wt%), after Pearce et al. (1984). Volcanic arc granite (VAG), syn-collisional granite (syn-COLG), within-plate granite (WPG), ocean ridge granite (ORG); dashed line is upper limit for granites from anomalous ridge segments.

4.4 Olary Block dolerites

4.4.1 General

A simple discrimination of the three dolerite types can be obtained through use of major elements (e.g Fig 4.4.1). The HPT dolerites are characterised by high TiO_2 (~1.5wt%), Fe_2O_3 (~14wt%), Na_2O, P_2O_5 (~0.15wt%), and variable K_2O (0.11-1.83 wt%). The LPT dolerites are characterised by low TiO_2 (<1wt%), P_2O_5 (<0.1wt%), Fe_2O_3 and high Al_2O_3, MgO and CaO. The Rainy Day dolerite is typically SiO_2-, P_2O_5- and Al_2O_3-poor, but with very high Fe_2O_3 (~20wt%) and high TiO_2 (~2.3wt%). The HPT dolerites have transitional to tholeiitic compositions (Nb/Y~0.2-0.7) in contrast to the LPT and Rainy Day dolerites which are strongly tholeiitic (Nb/Y<0.2).

According to the classification scheme of Winchester and Floyd (1977) all the dolerite suites are intrusive equivalents of a tholeiitic basaltic andesite precursor (Fig 4.2.1).

As can often be expected from dyke-type rocks, linear bivariate trends suggestive of fractional crystallisation are difficult to obtain. Nevertheless, good correlations were found using Fe_2O_3/MgO, Mg# and SiO_2 indices (Fig 4.4.2a-d), possibly verifying cpx+plag fractionation.

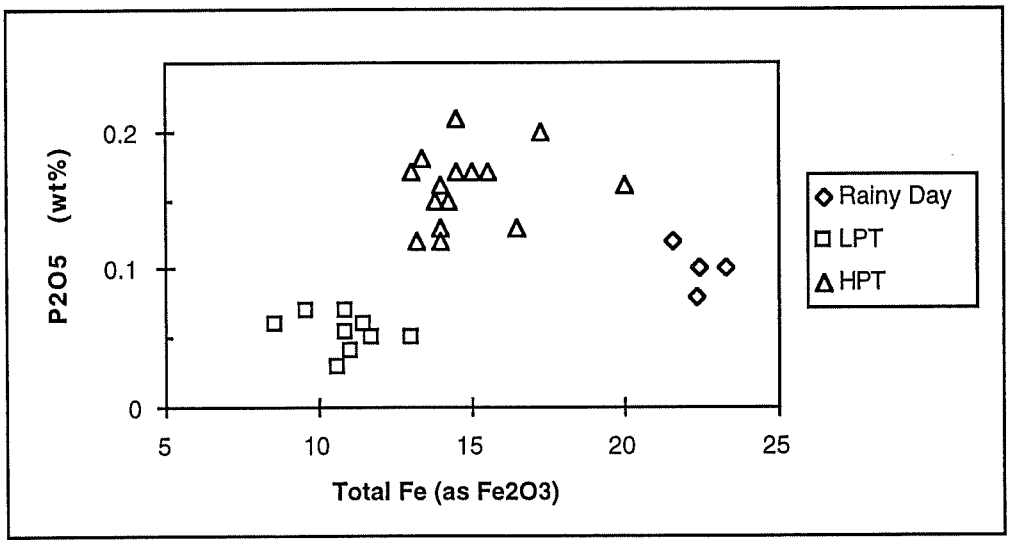

Fig 4.4.1 P_2O_5vFe_2O_3 discrimination between the three types of dolerites.

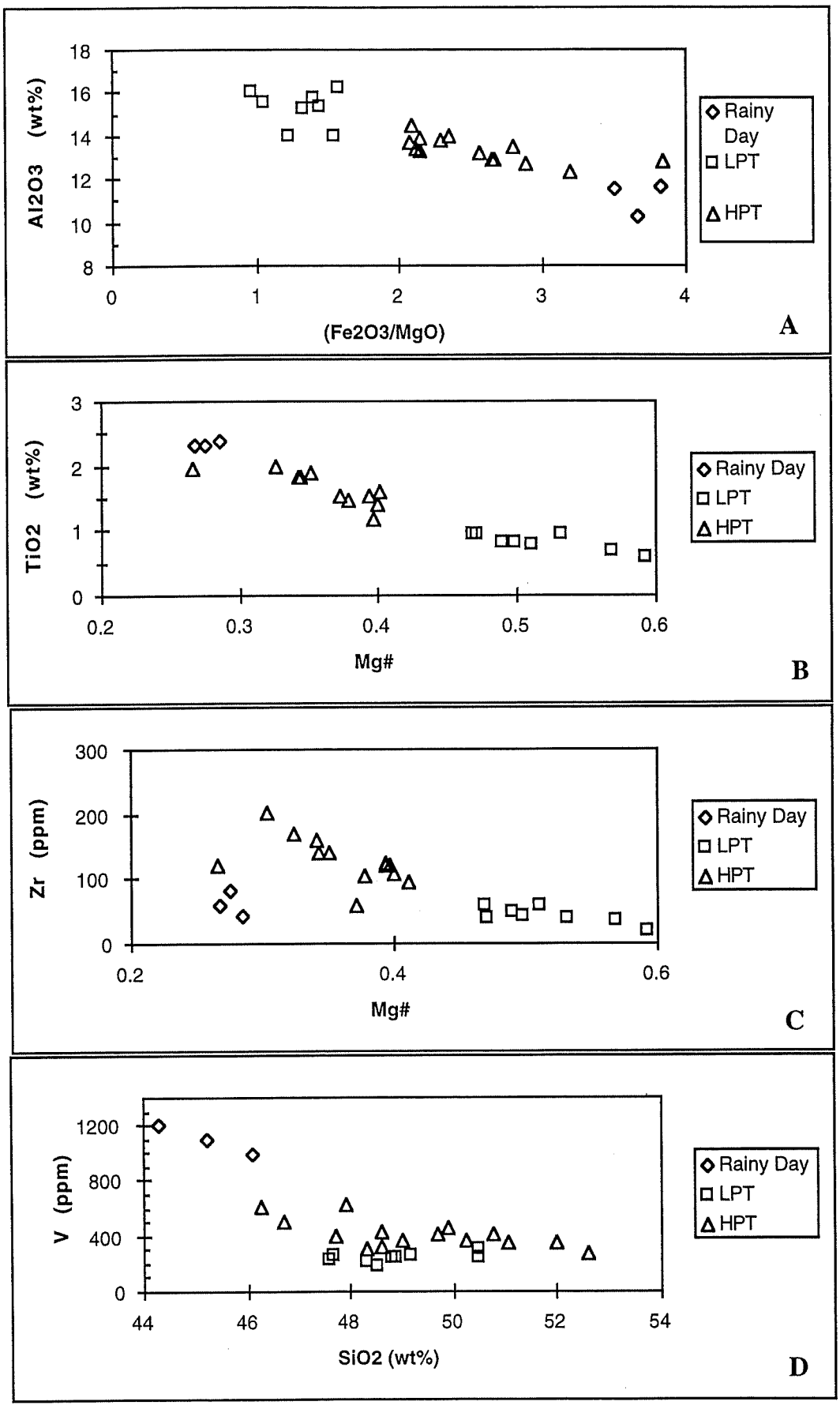

Fig 4.4.2.a-d Bivariate trace element and oxide plots for the Olary Block dolerites.

4.4.2 Incompatible trace elements

Primordial mantle-normalised trace element diagrams are illustrated in Figs.4.4.4a and 4.4.5a, for the HPT dolerites and LPT/Rainy Day dolerites respectively. Th and U have been excluded from these diagrams as they have been mobile during metamorphism/alteration.

The HPT dolerites exhibit relatively flat patterns with normalised HFSE abundances ~10x primitive mantle. These samples may be further sub-divided into high-K and low-K types (with corresponding high and low Rb), the cause of which is attributed to post-magmatic alteration. The samples of Pierini (1994), in particular, resemble the Wooltana metabasalts which are considered temporal but altered (high K-Rb) equivalents of the Gairdner dykes on the Stuart Shelf (Smith, 1992). In comparison the HPT dolerites have higher Nb and La and slightly higher Zr, Nd, and Sm. Good correlations are also made with OIT's and a Deccan basalt for the HPT rocks, indicating a probable plume source component.

The equivalent diagram for the other two dolerite groups also reveals flat patterns with slight absolute enrichment of HFSE of the Rainy Day dolerites relative to the LPT dolerites, but overall depletion of both, compared to the HPT dolerites is noted. Enrichments in K, Ba and Rb and P-depletion (apatite fractionation) are the most imposing features of the LPT patterns, whilst the main difference between the two groups is $(Ti/Y)_n$: Rainy Day >1, LPT <1. The LPT dolerites may have patterns approximating those of the 'IP1ES' basalts of the Brazilian continental margin (Fodor and Vetter, 1984) and of some depleted Cambrian samples from Mt Pleasant (Foden et al. 1995, in prep.);

Normalised REE patterns provide further evidence for the relative enrichment of the mafic groups (Fig 4.4.5b). The HPT, Rainy Day and LPT have $(La/Yb)_n$ of ~5, ~4 and <2 respectively. For similar reasons described in respect to the amphibolites in Section 4.2, it is clear that the LPT dolerites and the HPT dolerites are not related by fractional crystallisation.

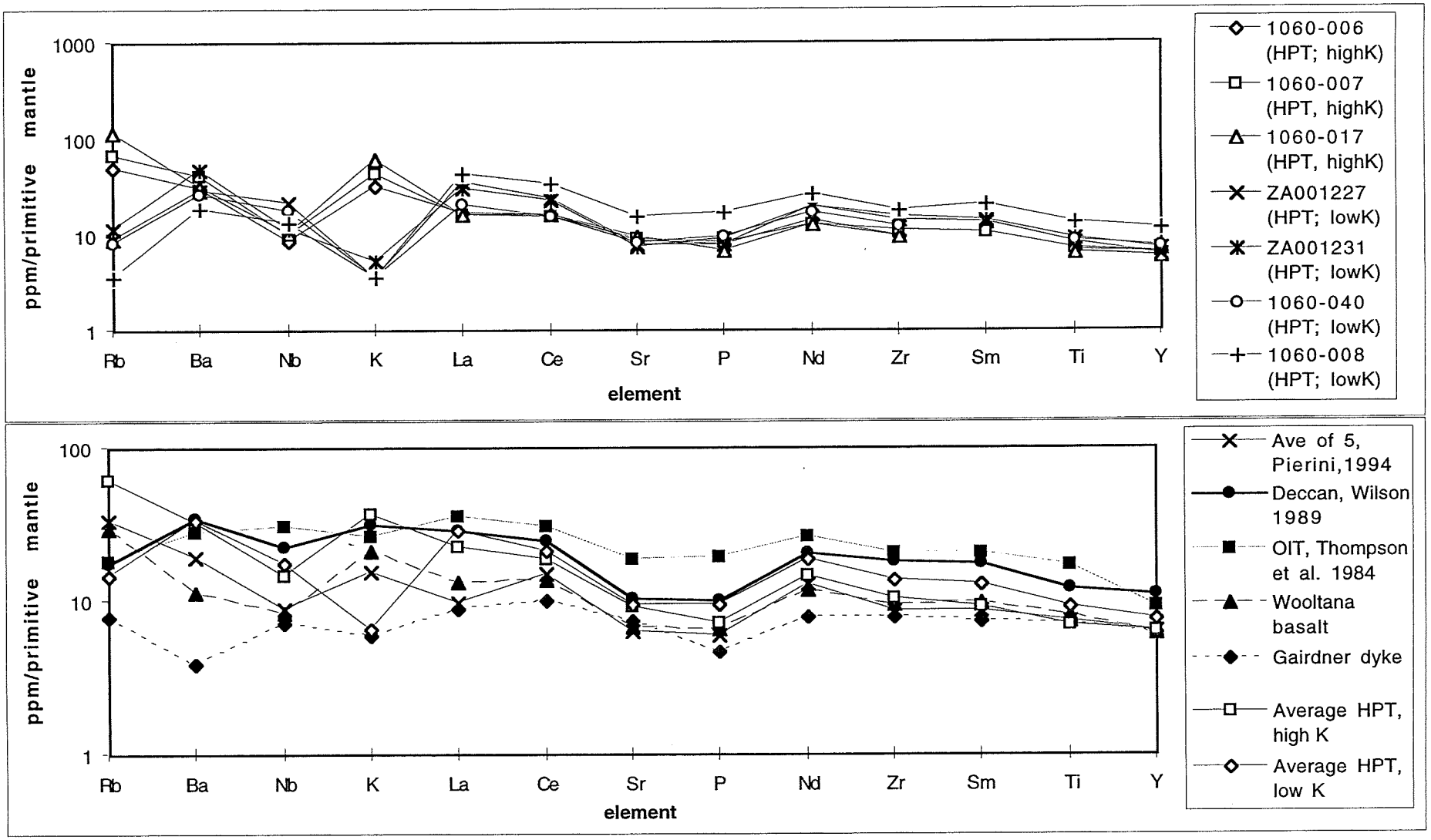

Fig 4.4.4 (A) Primitive mantle-normalised incompatible trace element diagram for the HPT dolerites. High and low-K types.

(B) Trace element comparison between HPT dolerites, OIT's and South Australian Neoproterozoic basalts.

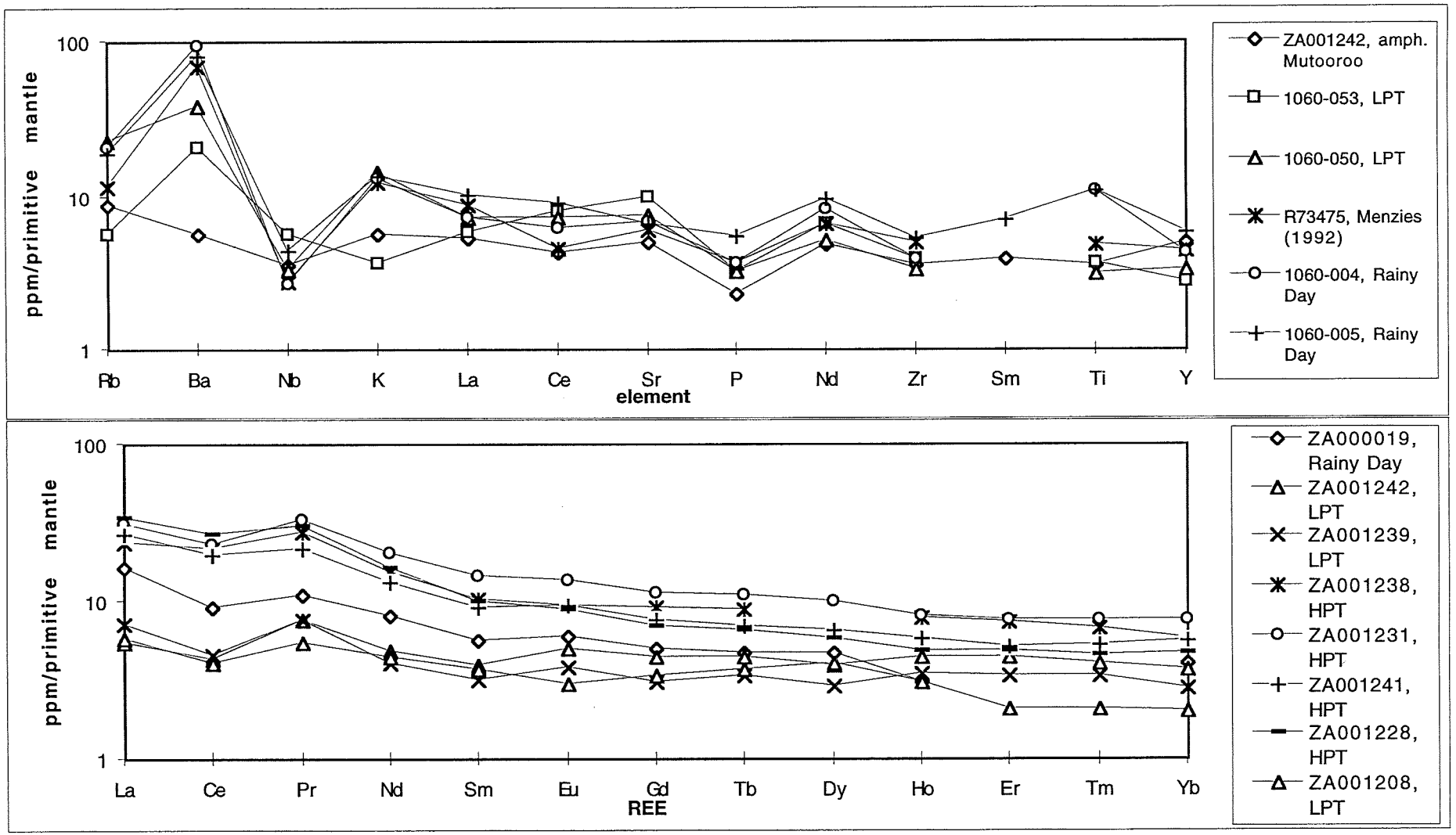

Fig 4.4.5 (A) Normalised incompatible trace element diagram for the Rainy Day and LPT dolerites.

(B) Primitive mantle-normalised REE pattern for the dolerites illustrating varialbe LREE enrichment.

4.4.4 Source characteristics and crustal contamination; dolerites v amphibolites

The La/Nb ratio has often been used to elucidate crustal contamination in basic igneous rocks (e.g. Thomson *et al.* 1984). Fig 4.4.6 reveals $(La/Nb)_n$ <1.5 for most of the Olary Block amphibolites, probably indicating minor crustal interaction of the dyke/sill rocks. Perhaps significant, though, is the greater value of $(La/Nb)_n$ for two of the Outalpa samples compared with any of the Cathedral Rock samples. It is plausible that the relatively depleted Outalpa amphibolite samples were derived via greater percent partial melting of the same source as the Cathedral Rock amphibolites. These 'hotter' partial melts would then be expected to assimilate more crust on their passage through the lithosphere. The dolerites have (La/Nb)n dominantly <2, which suggests a slightly greater lithospheric component than for most of the amphibolites.

Also on this diagram, the $(Zr/Nb)_n$ ratio suggests affinities with an enriched asthenospheric (MORB/OIT) source for all the mafic rock types. However, source component contrast between the amphibolites and dolerites is unclear. The next section tackles this problem by relating source charactaristics to tectonic setting.

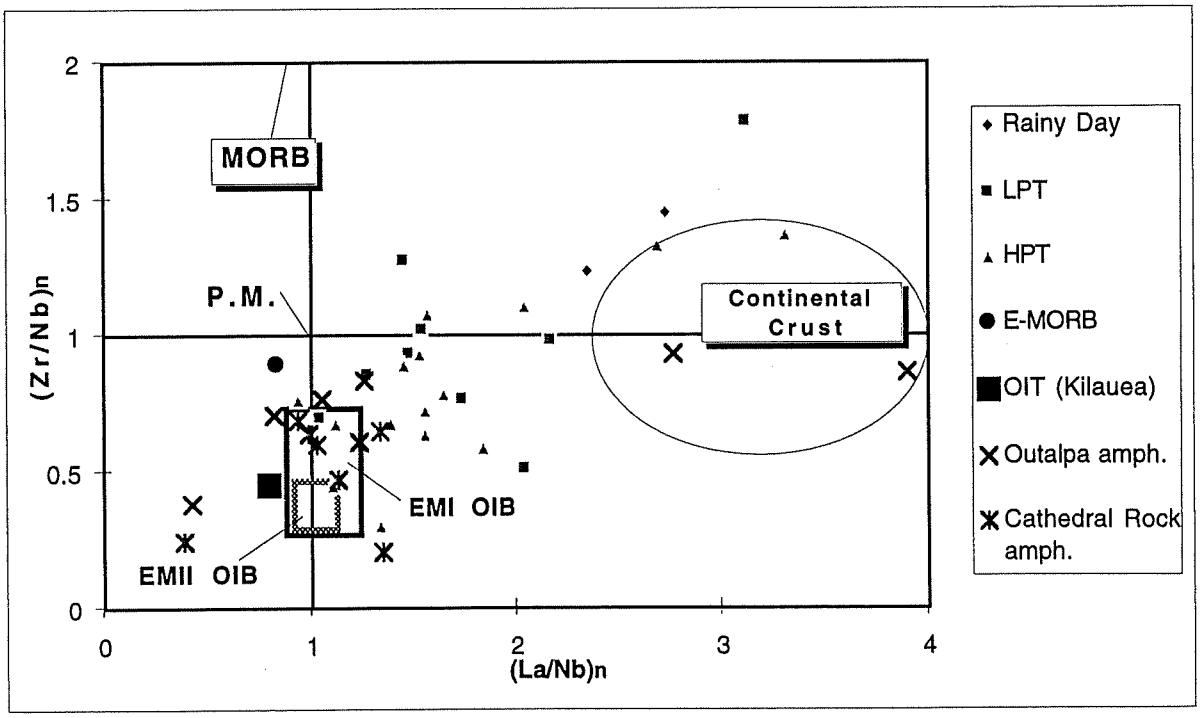

Fig 4.2.6 Source characteristics and crustal contamination of the Olary Block amphibolites and dolerites; $(La/Nb)_n$ ratio is used as an indicator of crustal contamination; $(Zr/Nb)_n$ ratio indicates affinities with an an enriched MORB/OIT source and enriched mantle components EMI and EMII (Saunders *et al.*, 1988). PM=Primordial mantle.

4.4.4 Tectonic Discrimination

Fig 4.4.7 depicts an OIT-normalised correlation of the HPT dolerites with a typical Deccan basalt (composition from Wilson, 1989). These patterns are for the most part nearly identical, thus indicating an affinity with intra-continental flood basalt magmatism for the HPT dolerites. This evidence combined with Figs.4.4.4(b) and 4.4.6 indicate similarities with an enriched plume source. Once again it is clearly shown that the Rainy Day and LPT samples are depleted with respect to the HPT rocks, but they display similarly flat patterns normalised to OIT. One can speculate that these depleted tholeiites are a product of source component mixing involving an enriched plume-like component and depleted mantle. Higher Rb, Ba and K in the dolerites relative to OIT probably represent the effects of hydrothermal alteration.

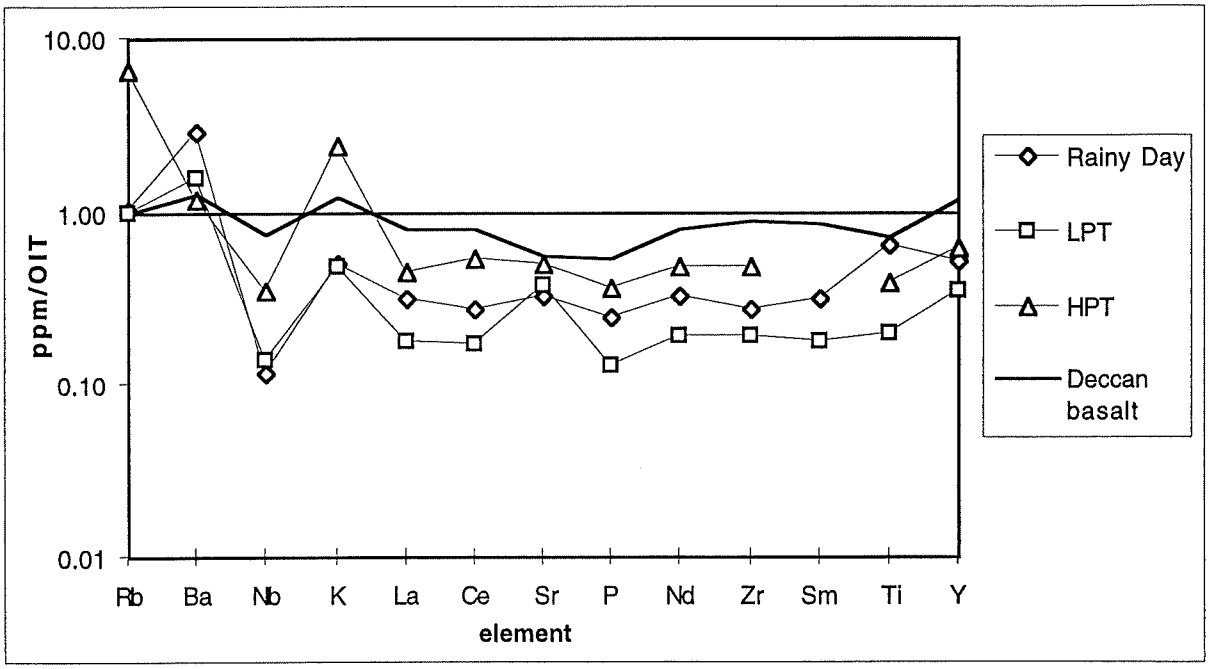

Fig 4.4.7 OIT-normalised incompatible element diagram for the three dolerite types indicating similar flat patterns relative to ocean-island basalts. (OIT composition after Thompson et al. 1984).

Two tectonic discrimination diagrams were used to investigate the possible tectonic setting of the mafic rocks (Appendix H). The HPT dolerites dominantly plot in the within-plate field of the 2Nb-Zr/4-Y and Y/15-La/8-Nb/8 discrimination diagrams of Meschede (1986) and Cabanis and Lecolle (1989) respectively. The LPT and Rainy Day samples primarily plot in the fields of extensional settings; MORB and back-arc basins; confirming their more tholeiitic nature. The amphibolites yield points in the MORB and E-MORB fields for both diagrams, which is consistent with the interpretation of Fig 4.2.5.

4.5 Maldorky Lamprophyre

The Maldorky Lamprophyre is characterised by low CaO (~5wt%), intermediate SiO_2 (~53 wt%), high K/Na, TiO_2, P_2O_5 and a very high LOI (upto 7wt%). They have low Mg# (~0.4) and low Ni (Fig 4.5.1a), indicating a considerable degree of fractionation, involving ferromagnesian minerals. This relatively fractionated condition together with a scarcity of contact metamorphic effects would seem to suggest a relatively low temperature of emplacement (Rock, 1987). Decreasing Fe_2O_3T with SiO_2 is indicative of an alkaline magma series (Figs.5.5.1b; Miyashiro and Shido, 1975). Using the classification scheme of Rock (1987), K/(Na+K) (at.%) ratios of >70 for these rocks define an ultrapotassic, lamproiitic affinity.

Furthermore, this lamprophyre exhibits a similar incompatible element pattern to the lamprophyres from the Karinya syncline (Fig 4.5.2). Muller *et al.* (1993) defined two petrographic groups for the lamprophyres from this region; (I) *phlogopite-phyric* and (II) *apatie-phlogopite-phyric*. The main geochemical distinction between these groups is P_2O_5 content. The Maldorky rocks have $(P/Nd)_n$ <1 and predominantly higher Nb than the group II rocks, indicating a closer association to petrographic group I of Müller *et al.* (1993).

Other distinguishing geochemical features are high concentrations of Rb, Th, U and Ba and high HFSE (e.g. Zr, Nd, Y), confirming the alkaline nature of these rocks. On Fig.4.5.2 they exhibit very prominent Nb depletion relative to La. This feature is probably diagnostic of an enriched source within the sub-continental lithospheric mantle, rather than crustal contamination. High values of La/Nb are charactaristic of calc-alkaline lamprophyres and lamproites in destructive plate margin regimes (Rock, 1987). However, these rocks clearly plot in the within-plate field for lamprophyres in Figure 4.5.3 , and in the absence of subduction indicators such as ophiolites or blueschists, a continental intra-plate tectonic setting is suggested (Müller *et al.*, 1993).

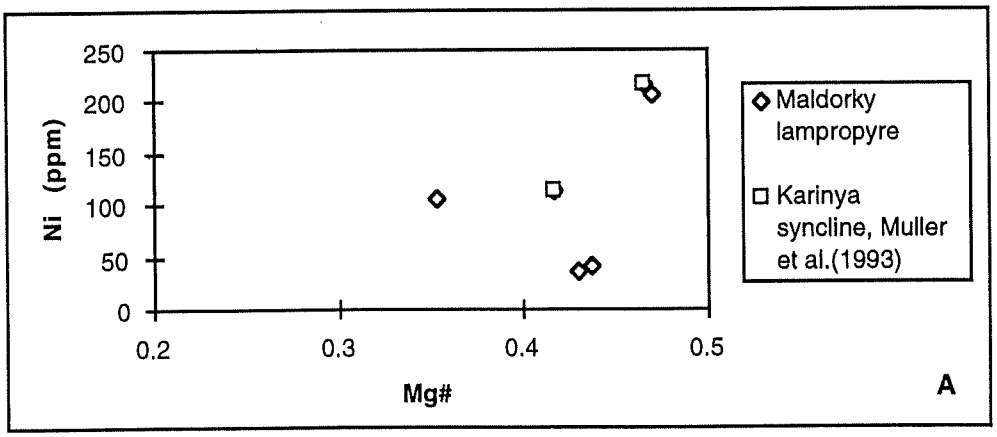

Fig 4.5.1 (A) Low Ni (ppm) for the Maldorky lamprophyre,indicating considerable degrees of fractionation of ferromagnesian minerals.

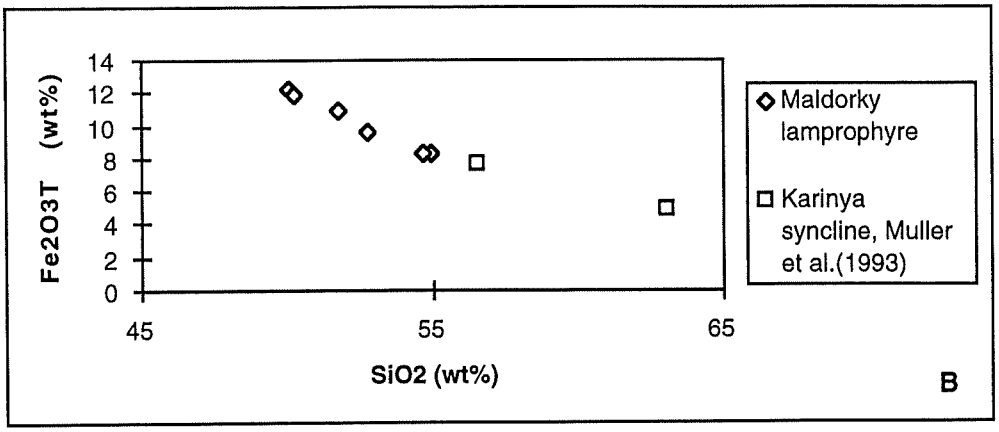

Fig 4.5.1 (B) Decreasing Fe2O3T (wt%) and V (ppm) with SiO2 (wt%) indicative of an alkaline magma series.

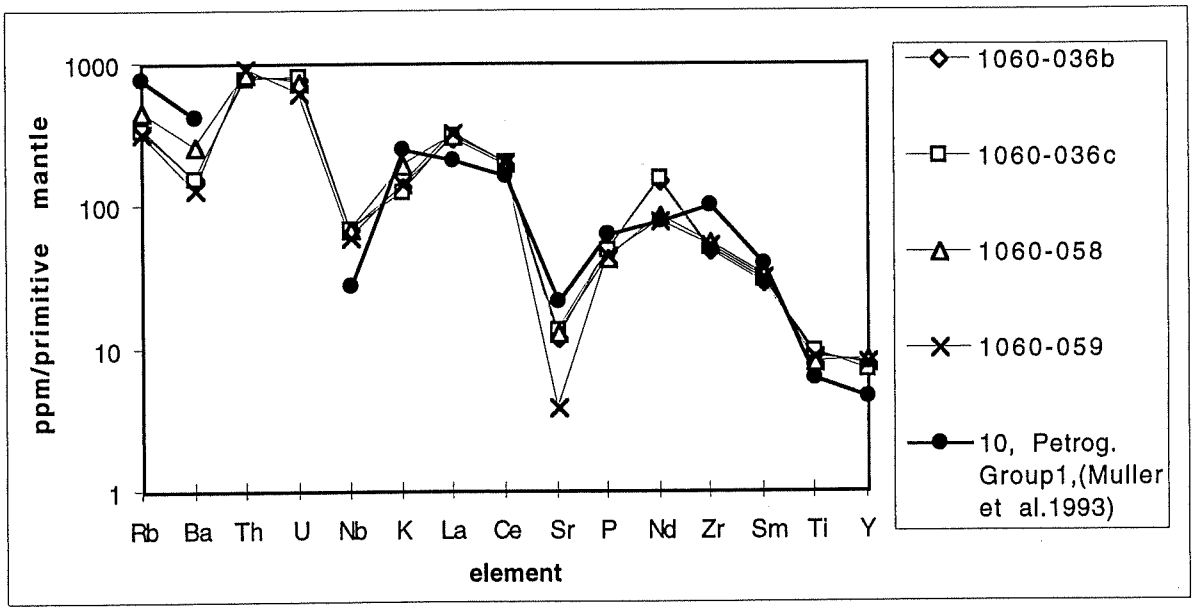

Fig 4.5.2 Incompatible trace element pattern for the Maldorky Lamprophyre and comparison to Ordovician lamprophyre of the Adelaide Fold Belt.

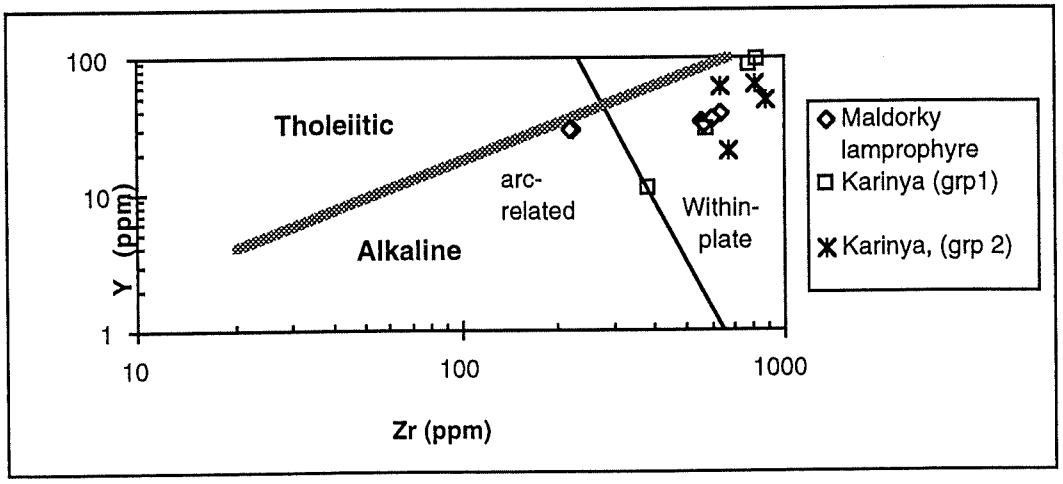

Fig 4.5.3 Y v Zr; Tectonic discrimination of Maldorky Lamprophyre (after Müller*et al.*, 1992).

4.6 Summary

The Outalpa Amphibolite has lower Fe_2O_3, TiO_2, HFSE and higher MgO, Al_2O_3 and CaO than the Cathedral Rock samples of Pierini (1994). They may represent the products of variable mixing of MORB and OIB source components.

The Antro and Poodla granitoids are I-type and transitional I-S-type respectively. They exhibit remarkable geochemical similarity except for discrepancies involving the mobile LILE. They can be categorised as within-plate granites according to the discrimination diagram of Pearce *et al.* (1994).

The HPT dolerites have higher P, Zr, Y, Nb and LREE than the LPT and Rainy Day dolerites. They exhibit extremely variable Rb and K and this is attributed to hydrothermal alteration. They have similar trace element charactaristics to ocean island basalts and are categorised as within-plate basalts. In contrast the LPT and Rainy Day dolerites have a more depleted and tholeiitic geochemistry.

The Maldorky Lamprophyre has an ultrapotassic (lamproitic) geochemistry characterised by high abundances of K_20 and incompatible elements . They are geochemically similar to the Truro lamprophyres of Müller *et al.* (1993).

CHAPTER 5: ISOTOPES

5.1. Introduction to Isotope Systematics.

The first and major use of isotopes in geochemical studies is the determination of rock ages through geochronology (e.g. crystallisation, metamorphic, alteration and crustal residence ages). More recently, isotopic data have been utilised to characterise and distinguish petrogenetic processes and sources. A result of this development is that geochemists are now able to sample the Earth's mantle, a vital step towards constraining the chemical and physical nature of basalt petrogenesis. This study employs two parent/daughter isotope systems: ^{87}Rb-^{87}Sr and ^{147}Sm-^{143}Nd.

The Rb-Sr system is one of the most widely adopted isotope systems for rock dating. However, the results of such analyses are often difficult to interpret, due to limited spread of Rb/Sr ratios and variable crustal contamination (Zhao and McCulloch, 1993). Rb and Sr are both highly mobile under the influence of hydrothermal fluid influx. Even for internal mineral isochrons Rb and Sr are often prone to post-magmatic hydrothermal and metamorphic effects (Patchett, 1979). More often, for older rocks, a Rb-Sr isochron can be attributed to an alteration or metamorphic event.

The evolution of the Sm-Nd isotope system in the Earth is summarised by a model known as CHUR ("chondritic uniform reservoir"; DePaolo and Wasserberg, 1976). This model is dependant on the condition that terrestrial Nd has evolved in a reservoir with Sm/Nd and initial $^{143}Nd/^{144}Nd$ equivalent to that of chondritic meteorites.

Partial melting necessarily results in reduction of Sm/Nd relative to CHUR or the depleted mantle (DM). Rocks that crystallise from such a magma will exhibit low concentrations of radiogenic Nd and low $\varepsilon Nd(T)$. Remelting of the residue produces rocks exhibiting relatively radiogenic Nd. Figure 5.1.1 depicts the isotopic evolution of Nd for CHUR and the depleted mantle through time. The evolutionary line for CHUR represents those parts of the chondritic reservoir that have remained unaffected by magma generation, and production of radiogenic Nd has therefore been uninterrupted to the present. However, for most crustal rocks, derivation from a depleted mantle source seems more likely, as this reservoir has been present for most of Earth history (since ~3.96Ma; Bowring *et al.*, 1989).

The depletion history of the Earth's upper mantle can be defined by a Nd isotopic evolution curve, constructed by plotting the most radiogenic initial Nd isotopic compositions available through time. Recent isotopic studies in Archaean terrains have provided new data that indicates a non-linear evolution of Nd in early Earth history (e.g. Chase and Patchett, 1988;

Collerson *et al.*, 1991; Bennett *et al.*, 1993). However, this new estimate of Nd isotopic evolution only differs significantly from the linear model prior to ~2.7Ga. As all of the depleted mantle model ages calculated for this study are ≤2.7Ga the linear Nd evolution model is considered adequate.

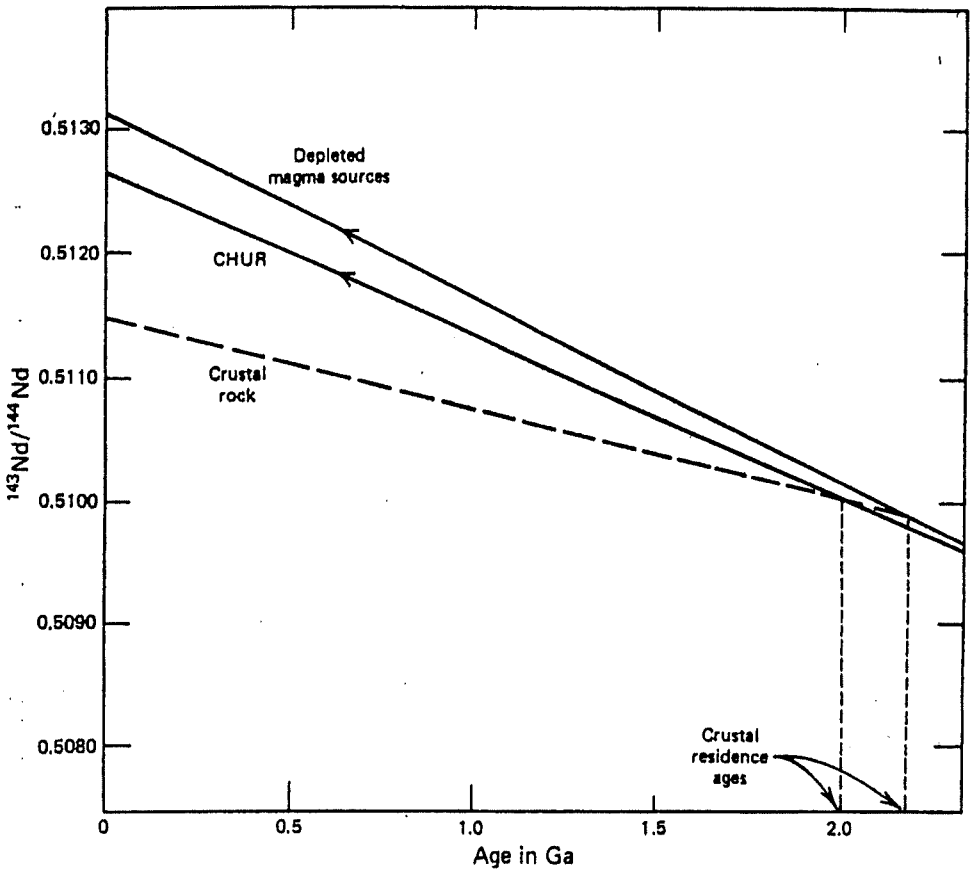

Fig.5.1.1 Isotopic evolution of Nd in a chondritic uniform reservoir and depleted mantle. $T_{dm}>T_{chur}$; from Faure (1977).

5.2. Isotopic data.

Seven mafic samples were analysed by mass spectrometry for $^{143}Nd/^{144}Nd$, $^{87}Sr/^{86}Sr$, Nd (ppm) and Sm (ppm). Concentrations of Rb and Sr were obtained by accurate XRF analysis. A summary of the data collected is compiled in Appendix E.

5.2.1 Comparison of the Mafic Suites

It should be noted that mafic rock model ages are often suspect due to limited deviation from mantle values of $^{147}Sm/^{144}Nd$ following partial melting. Therefore interpretation of such data is difficult, and commonly multiple hypotheses may be appropriate for a given data set. Bearing this in mind, the Olary Block isotopic data generally support the geochemical characterisation of the mafic rocks described in Chapter 4.

The HPT dolerites have measured $^{143}Nd/^{144}Nd$ values of 0.511928-0.511983, with DM model ages ranging from 2.24-2.7 Ga. The significantly greater model age and higher $^{87}Sr/^{86}Sr$ of sample A1060-007 can be attributed to the affects of crustal contamination or hydrothermal alteration, geochemical evidence favouring the latter. It is therefore believed that the lower model age is a better indication of mantle separation time for this suite. Similarly, an old model age (2.69Ga) and very high $^{87}Sr/^{86}Sr$ (0.7701) for the LPT sample relative to the other mafic rocks is indicative of hydrothermal alteration (crustal contamination appears unlikely considering the depleted nature of this suite). The Outalpa amphibolite probably has a similar model age to the HPT and LPT dolerites. The Rainy Day sample has a similar model age to the mafic granitoids (i.e. 2.44-2.49Ga) and $\varepsilon Nd(T)$ comparable to the Outalpa amphibolite.

Low and very high $^{87}Sr/^{86}Sr$ for the Poodla granitoid compared to the Antro granitoid is consistent with its K-Rb-rich nature. (It is thought that the low $^{87}Sr/^{86}Sr(T)$ calculated for the Poodla sample is a consequence of hydrothermal K-Rb enrichment, evidenced by biotite veining). These model ages are slightly younger than those of the regional S-type granitoids and the metasediments from which they were derived (T_{DM}~2.6Ga; Benton, 1994). Comparatively higher initial εNd for the Rainy Day, Outalpa and LPT samples is consistent with either a more depleted source or relatively minor contamination compared to the HPT dolerites.

Fig 6.2.1 is a plot of εNd v time(Ga). On this diagram the most depleted suites according to trace element characteristics (Chapter 4; LPT dolerites, Outalpa amphibolites and Rainy Day dolerites), exhibit enhanced evolution of Nd since extraction from the mantle, in comparison with the other suites; a manifestation of near chondritic $^{147}Sm/^{144}Nd$ (0.170-0.181).

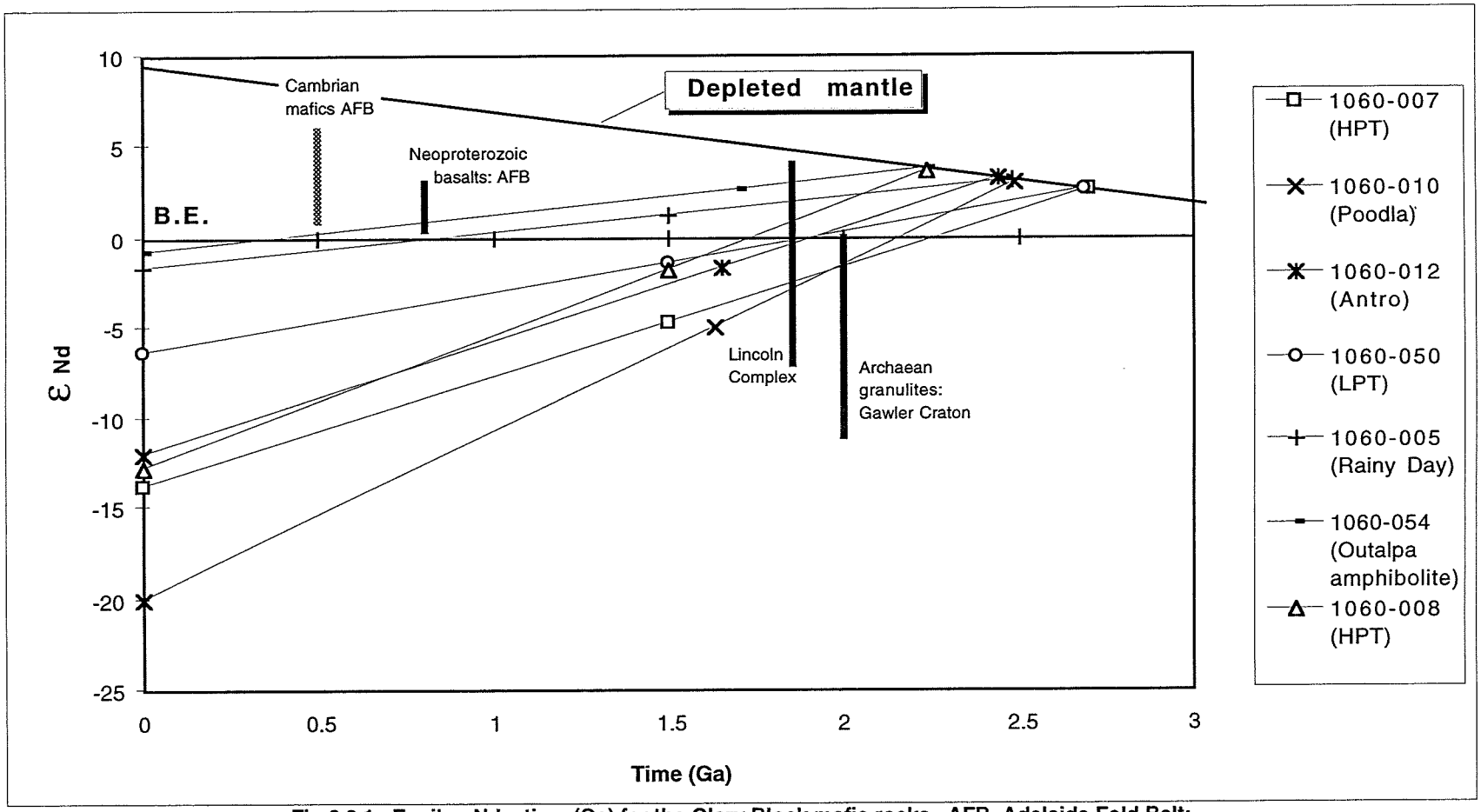

Fig 6.2.1. Epsilon Nd v time (Ga) for the Olary Block mafic rocks. AFB=Adelaide Fold Belt; B.E.=Bulk Earth. Gawler Craton and AFB data from Turner *et al.* (1992) and Foden *et al.* (1995).

5.2.2 Interregional Comparison.

The Nd isotopic compositions of the HPT dolerites (-007, -008) contrast markedly with those of the Gairdner dykes, Wooltana Volcanics and Beda Volcanics. Even the Wooltana basalts, considered altered equivalents of the Gairdner dykes, have considerably higher εNd(T) than the Olary Block HPT dolerites at similar values of $^{87}Sr/^{86}Sr$ (e.g. data of Turner *et al.*, 1992). The difference is portrayed in Fig.6.2.1, which also delineates Gawler Craton Palaeo-Mesoproterozoic Nd isotopic characteristics for all the Olary samples.

The HPT dolerites have values for εNd (800Ma) of ~-10 that contrast considerably to εNd (800Ma)~+0.5-+4 for the Palaeoproterozoic rocks. To achieve this degree of relative enrichment a large amount of assimilation of old crust is required. Theoretically these negative εNd values could be inherited through assimilation of Archaean granulite crust with long term low Sm/Nd. However, this degree of assimilation cannot be reconciled with the observed major and trace element data (e.g. sample 1060-008 has SiO_2 of only 46 wt%). Nor can alteration (unlikely to considerably affect REE ppm) account for such differences. Consequently, the HPT dolerites are proposed to have a Mesoproterozoic age of emplacement.

5.2.3 Isochrons

Ambiguous results were obtained from the plotting of Sm-Nd and Rb-Sr isochrons (Appendix. The most remarkable result obtained was a Sm-Nd whole rock 'isochron' date of 2400Ma± 90Ma that includes all seven mafic samples. This age is approximately equivalent to an average T_{DM} calculated for the data of 2.47Ga. A similarly remarkable result was obtained by Zhao and McCulloch (1992) for Sm-Nd analyses of the Stuart and Kulgera dyke swarms in central-southern Australia. These authors attributed this phenomenon to fractionation of Sm and Nd in the underlying CLM.

A two point Rb-Sr isochron plotted for the HPT dolerites yielded a date of 1534Ma±6Ma. It must be noted that extreme depletion in Rb due to alteration in sample 1060-008 has inhibited the production of radiogenic Sr, whereas Rb enrichment in sample 1060-007 enhanced radiogenic Sr production. This date is tentatively attributed to a greenschist facies metamorphic event that caused mobilisation of Rb and Sr (e.g. M_3 of the Olarian Orogeny; Clarke *et al.* 1986). If this interpretation is correct then it would tend to confirm a Palaeo-Mesoproterozoic intrusive age for the HPT dolerites.

5.3. Pb/Pb zircon evaporation

Three zircon evaporation analyses were performed on an Antro granitoid sample from the outcrop 2km NE of Antro Woolshed (Sample A1060-012). These revealed a major 'pre-Hiltaba' population at 1679Ma±13Ma. This is interpreted as a magmatic age. A smaller

population at 1652±17Ma was obtained from the rim of one grain. This younger age is attributed to mixing of magmatic and metamorphic (Olarian or Delamerian) Pb/Pb signatures (see Fig 5.3.1).

The implications of this age are twofold. Firstly, it contrains the emplacement age of the Outalpa amphibolite (that the Antro granitoid intrudes) to post-1700Ma and .pre-1680Ma. Secondly, this age is statistically indistinguishable from the 1689±5Ma and 1680±13Ma SHRIMP ages obtained from low and high grade rocks in the Broken Hill Block (Page and Laing, 1992). This result appears to reinforce post-1700Ma/ pre-1600Ma magmatic episodes in the Broken Hill Block and Olary Block (Fanning, 1995).

(A summary of the Pb/Pb zircon evaporation results is given in Appendix F).

Fig 5.3.1 Summary of Pb-Pb zircon evaporation data for the Antro Granitoid

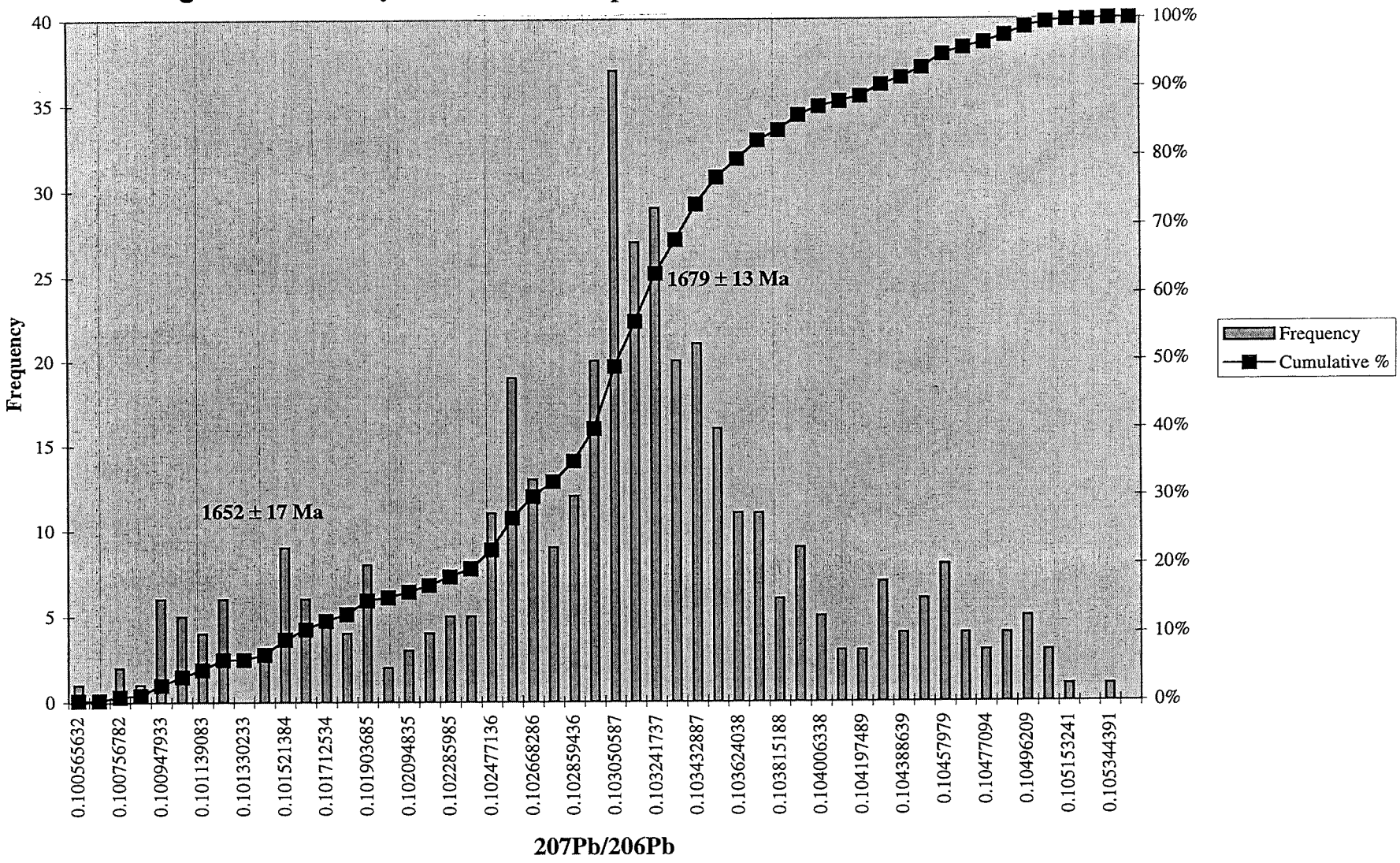

5.4 Conclusion

The isotopic data for the Olary Block mafic rocks is generally consistent with the geochemical comparisons made in Chapter 4.

Compared to the LPT dolerites, the HPT dolerites have lower εNd(T) values that are consistent with derivation from a plume source. The relatively depleted Outalpa amphibolites, Rainy Day and LPT dolerites all have εNd(T)>1. This is attributed to the involvement of mixed depleted mantle and plume source components.

The isotope data of this study has revealed a likely Palaeo-Mesoproterozoic age of emplacement for the greenschist facies (HPT, LPT and Rainy Day) dolerites. Whole rock Rb-Sr isochron dating of the HPT dolerites yielded an age of 1534±6Ma that is tentatively attributed to greenschist facies metamorphism during D_3 of the Olarian Orogeny.

Initial εNd values obtained for the Antro and Poodla granitoids suggest a larger degree of crustal contamination for the latter. This is consistent with the petrographic and geochemical features described in Chapters 3 and 4. The DM model ages of the granitoids are slightly younger than those obtained for the regional granitoids (Benton, 1994).

Three Pb/Pb zircon evaporation analyses of the Antro intrusive ~2km NE of Antro Woolshed have yielded a 'pre-Hiltaba' magmatic age of 1679±13Ma. A smaller population derived from the rim of one grain yielded a younger (mixing) age of 1652±17Ma.

Clearly more extensive isotope studies of all the suites would confirm (and constrain) or preclude petrogenetic processes such as source mixing.

CHAPTER 6: PETRO-TECTONIC MODELS FOR CONTINENTAL THOLEIITE GENERATION

6.1 Possible Sources of Continental Tholeiites

Early work by Thompson *et al.* (1977) suggested that an asthenospheric source for continental flood basalts (CFB) similar to that proposed for oceanic basalts, with crustal contamination invoked as a probable cause of relatively enriched isotopic and geochemical features. DePaolo and Wasserburg (1979) used Nd isotopes to reinforce a sub-lithospheric origin although they advocated an OIB-like source within the lower mantle. Later work (e.g. Hawkesworth *et al.,* 1983) utilised mantle xenolith data to propose that some tholeiites were derived from an enriched source within the lower lithosphere.

However, it now appears generally accepted that most, if not all, CFB provinces are related to mantle plume activity (Saunders *et al.,* 1992). Any model implementing considerable melting of a thin lower lithosphere must also account for the voluminous nature of CFB provinces, in addition to the fact that melting of such material is usually associated with volatile-rich (amphibole-mica-rich), alkaline products, such as lamprophyres (Menzies, 1992). This latter reality must be reconciled with the dominantly tholeiitic nature of CFB's.

6.2 Lithospheric thickness and mantle temperature

Decompressional melting of an asthenospeheric source can be achieved through rifting of the lithosphere (mechanical boundary layer). The amount of melting of asthenospheric material is controlled by (i) the temperature of the mantle, (ii) the degree of lithospheric extension. Production of MORB crust is a manifestation of unlimited extension combined with melting at 'normal' mantle temperatures. This is depicted in Fig 6.2.1, which also illustrates that melting at abnormally high mantle temperatures (e.g. above a mantle plume) and high degrees of lithospheric extension result in the production of voluminous continental flood basalts, and oceanic plateau basalts. Thus, thickness of the lithosphere can be seen to play an obvious role in determining both the amount of melt generated as well as the geochemical nature of the melt.

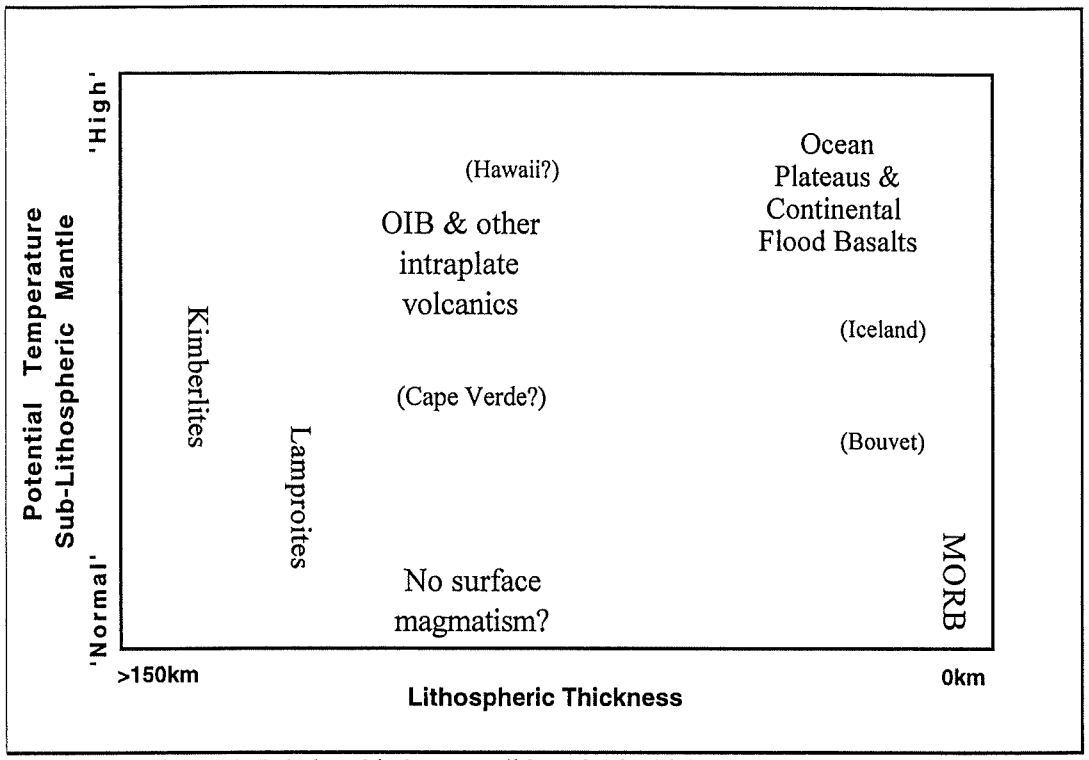

Fig 6.2.1 Relationship between lithospheric thickness, mantle potential temperature and magma volume. Predicted from the models of McKenzie & Bickle (1988), Watson & McKenzie (1991). After Saunders *et al.* (1992).

6.3 Plume impact Vs Plume incubation

Melting within a plume is essentially controlled by lithospheric thickness. For example, Watson and McKenzie (1991) suggested that melt generation of a plume source is essentially prevented if the thickness of the mechanical boundary layer exceeds ~100km. For models proposing impact of a plume at the base of 'normal' lithosphere , significant transformation of the thermal structure of this lithosphere is unlikely within the (estimated) ~10Ma time span before first generation of melt.

Saunders *et al.* (1992) used a simple model of a lithospheric plate moving across a stationary plume to describe the nature of plume incubation. They calculated that for a slow moving plate (~1cm a^{-1}) then a point at the base of the lithosphere could be in contact with a developing plume head for well in excess of 50Ma. Moreover, a plume head with a rate of expansion greater than the plate velocity would be in contact with the base of the lithosphere indefinitely. Naturally, the thermal contribution of the plume to the overlying lithosphere would decrease with time, unless new material from the lower mantle was continuously or episodically injected. Therefore, plume incubation is a virtual necessity for any model involving plume impingement on the base of relatively thick lithosphere (Saunders *et al.*, 1992).

6.4 Implications for the Olary Block Mafic Rocks & Proterozoic plume dynamics

Considering the field and isotopic evidence it is proposed that the Outalpa amphibolites were emplaced during development of the Willyama Supergroup at ~1700Ma. A model invoking plume impingement at the base of a rifting lithosphere may explain the geochemical contrast between the amphibolites. In this model the amphibolites are derived from different degrees of partial melting of an enriched plume source at the base of the lithosphere. A spatial relationship between the High Ti/low Mg# (Cathedral Rock) and low Ti/high Mg# (Outalpa) amphibolites is suggested: high Ti magmas are derived from low percent partial melting of the plume material, followed by emplacement into the relatively cool lithosphere above the plume flanks, causing rapid evolution to low values of Mg#. Low Ti magmas are a product of high percent partial melting at the centre of the plume head and may therefore experience continuous replenishment in lithospheric magma chambers (Fodor, 1987), resulting in retarded magma evolution. The model requires lithospheric rifting and deposition of at least part of the Willyama Supergroup before plume impingement.

Alternatively, two component source mixing involving depleted MORB mantle and a plume may account for the patterns seen. In this scenario one would expect a transition to lower εNd values for the Cathedral Rock amphibolites. However, addition of a significant component of continental crust to the Cathedral Rock amphibolites cannot be reconciled with their observed major and trace element geochemistry. The amphibolites may therefore be sampling a heterogeneous mantle source. Clearly, further isotopic studies would confirm or eliminate or this possibility.

A Palaeo-Mesoproterozoic intrusive age for the HPT dolerites is proposed given the data of this study (Section 5.2). This interpretation solves several problems, the most significant being the lack of evidence for intrusion of these rocks into the Neoproterozoic cover.

The most plausible explanation for the generation of these relatively enriched magmas involves melting of a previously underplated source. It is conceivable that an ascending mantle plume (that was sourced by earlier amphibolites) could ascend and freeze at the Moho during the final stages of rifting. This could then provide a source for the later dolerites, during the waning stages of the Olarian Orogeny. The differing chemistry of the LPT dolerites and HPT dolerites can be accounted for by differing degrees of partial melting or by a gradual shift from transitional-tholeiitic to strongly tholeiitic melts, just prior to or at the cessation of deformation. This is similar to the scenario described by Foden *et al.* (1995) for the latter stages of the Delamerian Orogeny in the Adelaide Fold Belt.

CHAPTER 7: CONCLUSION

The Willyama inliers form a series of partly exposed inliers in eastern South Australia (Olary Block) and western New South Wales (Broken Hill Block). The Olary Block consists of a fining upward sequence of medium to high grade metasediments (Willyama Supergroup), voluminous granites and a minor mafic rock component. In comparison, the Broken Hill Block has a larger mafic component and less granitoids.

The Willyama Supergroup sediments were deposited during a Palaeoproterozoic rifting event. These sediments were subsequently deformed and metamorphosed in three distinct phases during the Mesoproterozoic Olarian Orogeny. The Willyama Supergroup and Neoproterozoic (Adelaidean) sediments later experienced greenschist facies metamorphism during the Cambro-Ordovician Delamerian Orogeny.

Seven compositionally different mafic and intermediate lithologies have been revealed by geochemical and isotopic analyses in the vicinity of Bimbowrie-Outalpa Stations and south of Olary, near Maldorky Hill.

The Outalpa Amphibolite is a variably foliated rock, often highly weathered and altered, primarily composed of plagioclase and hornblende. It was intruded/erupted as a sill/flow, concordant with respect to the regional statigraphy (upper Quartzofeldspathic Suite). Field relationships suggest that this rock type pre-dates a later suite of I-type granitoids. The Outalpa Amphibolite is proposed to have an age of emplacement between ~1700Ma and 1680Ma. This rocktype contrasts significantly with the Cathedral Rock amphibolites of Pierini (1994), which have higher Ti, P, Fe, LREE and HFSE and lower Ca, Mg, and Al.

The Antro Granitoid is a variably weathered, albite-rich/biotite-poor I-type granitoid. Field relationships west of Ameroo Hill suggest that this lithology is pre- to syn-orogenic, and this is consistent with a 'pre-Hiltaba' Pb/Pb zircon age of 1679±13Ma. This age is identical (within experimental `error) to ~1680Ma-1690Ma magmatic zircon SHRIMP ages in the Broken Hill Block (Page and Laing, 1992).

The Antro Granitoid exhibits remarkable geochemical similarity to the Poodla Granitoid except for discrepancies involving LILE (Rb, Ba and K), that are attributed to post-magmatic Na-K metasomatism. High K_2O, enclaves of metasediment, tourmaline, normative corundum ~1% and low $\varepsilon Nd(T)$ compared to the Antro granitoid indicate greater degrees of crustal contamination for the Poodla Granitoid. These rocks are categorised as within-plate granites according to the discrimination diagram of Pearce *et al.* (1984).

Three types of greenschist facies dolerites have been identified by petrographic and geochemical means. The HPT (high phosphorus & titanium) dolerites have higher concentrations of LREE and HFSE and lower Mg# compared to the LPT (low phosphorus & titanium) dolerites. The Rainy Day dolerite exhibits geochemical and isotopic features similar to the LPT dolerites (i.e. low HFSE and LREE, and high εNd), but has much higher Fe_2O_3 and TiO_2. The HPT dolerites exhibit geochemical characteristics similar to typical continental flood basalts, whereas the Rainy Day and LPT dolerites have trace element concentrations characteristic of extensional settings (e.g.MORB and back arc basins).

One of the main conclusions to come from this work is the proposal that the HPT dolerites have a Mesoproterozoic crystallisation age as inferred from the isotope data. Values of εNd(800) of ~ -10 are considered outside the range of conventional plume-derived melts, and consideration of major element data precludes the possibility of crustal contamination. However, εNd(1500) values of -1 to -4 are comparable to initial εNd values for the plume associated Paraná basalts of South America. A two point Rb-Sr isochron date of 1534±6Ma is tentatively inferred to represent greenschist facies metamorphism during D_3 of the Olarian Orogeny.

The biotite/phlogopite-phyric Maldorky Lamprophyre crops out south of the Olary township in a series of N-S trending dykes that intrude Adelaidean sediments. It exhibits cross cutting relationships with the inferred Delamerian structures of the sediments, constraining their age to Ordovician. This rock is basic-intermediate and ultrapotassic, defining lamproitic affinities. Field, petrographic and geochemical evidence suggest a correlation with the post-Delamerian Ordovician lamprophyres near Anabama Hill (McDonald, 1992) and Truro (Müller *et al.* 1993).

In summary, the early amphibolites were emplaced during rifting and development of the Willyama Supergroup, between 1700Ma and 1680Ma. The Antro I-type granitoids were intruded at 1679±13Ma. This age may indicate some relation between the generation mechanism of of the I-type and A-type granites (e.g. Ameroo Granite). The initial stages of convergent deformation are probably recorded by the transitional I- to S-type Poodla Granitoid (~1630Ma). High grade metamorphism at ~1600Ma culminated in the generation of abundant S-type granites (e.g. Benton, 1994). Magmatism then became bimodal with generation of 'within-plate' transitional-tholeiitic melts in the waning stages of the Olarian Orogeny. The mechanism by which these melts were generated is problematic as is the relative timing of emplacement of the LPT dolerites.

Given the data of this study, a plume source component for the HPT dolerites is proposed. In addition, mixing between a dominant plume-like component and depleted MORB mantle is suggested to account for the observed amphibolite compositions. Such models invoking

impingement of a plume at the base of relatively thick lithosphere may require incubation of the plume, to achieve significant transformation of the thermal structure of the lithosphere.

Further work should be concentrated on the acquisition of crystallisation ages and the generation of new isotopic data for the dolerite and amphibolite suites. Rb-Sr methods are likely to give metamorphic or metasomatic ages rather than a true crystallisation age. The Sm-Nd internal mineral isochron method (e.g. Stuart and Kulgera dyke swarms; Zhao & McCulloch, 1993) is expected to be the most successful method of dating for these enigmatic rocks.

REFERENCES

Ashley, P.M., Cook, N.D.J., Lawie, D.C., Lottermoser, B.G. and Plimer, I.R., 1995. Olary Block geology and field guide to 1995 excursion stops. Department of Mines and Energy South Australia, Report Book 95/13.

Bennett, V.C., Nutman, A.P. and McCulloch, M.T., 1993, Nd isotopic evidence for transient, highly depleted mantle reservoirs in the early history of the earth. *EPSL* 119, 299-317.

Benton, R.Y., 1994. A petrological, geochemical and isotopic investigation of granitoids from the Olary Province of South Australia-implications for Proterozoic crustal growth. B.Sc. Honours thesis, University of Adelaide, (unpublished).

Berry, R.F., Flint, R.B. and Grady, A.E., 1978, Deformational history of the Outalpa area and its applicaiton to the Olary Province, South Australia. *Roy. Soc. S. Aust. Transactions*, 102, 43-54.

Bowring, S.A., King, J.E., Housh, T.B., Isachsen, C.E. and Podosek, F.A., 1989. Neodymium and lead isotope evidence for enriched early Archaen crust in North America, *Nature* 340, 222-225.

Buckley, P.M., 1993. The geology and mineralisation of Abminga Station, Olary Block, South Australia. B. Sc. Honours thesis, University of New England (unpublished).

Cabanis, B. and Lecolle, M., 1989. Le diagramme La/10-Y/15-Nb/8: un outil pour la dicrimination des series volcaniques et la mise en evidence des processus de melange et/ou de contamination crustale. C.R. Acad. Sci. Ser. II, 309, 2023-2029.

Campana, B. and King, D., 1958. Regional geology and mineral resources of the Olary Province. *Geol. Surv. S.A.* Bulletin 34, 133pp.

Chappell, B.W. and White, A.J.R., 1974. Two contrasting granite types. *Pacif. Geol.* 8, p.173-174.

Chase, C.G. and Patchett, P.J., 1988, Stored mafic/ultramafic crust and early Archaean mantle depletion, *EPSL* 91, 66-72.

Clarke, G.L., Burg, J.P. and Wilson, C.J.L., 1986. Stratigraphic and structural contraints on the Proterozoic tectonic history of the Olary Block, South Australia. *Precambrian Research* 34, 107-137.

Clarke, G.L., Guiraud, M., Powell, R. and Burg, J.P., 1987. Metamorphism in the Olary Block, South Australia: compression with cooling in a Proterozoic fold belt. *J. Metamorpic Geol.* 5, 291-306.

Collerson, K.D., Campbell, L.M., Weaver, B.L. and Palacz, Z.A., 1991, Evidence for extreme fractionation in early Archaean ultramafic rocks from northern Labrador, *Nature* 349, 209-214.

Cook, N.D.J. and Ashley, P.M., 1992. Meta-evaporite sequence, exhalative chemical sediments and associated rocks in the Proterozoic Willyama Supergroup, South Australia: implications for metallogenesis. *Precambrian Research* 56, 211-226.

Cook, N.D.J., Fanning, C.M. and Ashley, P.M., 1994. New geochronological results from the Willyama Supergroup, Olary Block, South Australia. In: Australian Research Ore Genesis Symposium, AMF, 19.1-19.5.

DePaolo, D.J. and Wasserburg, G.J., 1976, Nd isotope variations and petrogenetic models. *Geophys. Res. Lett.* 3, 249-252.

DePaolo, D.J. and Wasserburg, G.J., 1979. Petrogenetic mixing models and Nd-Sr isotopic patterns. *Geochim. Cosmo. Acta* 43, 615-627.

Dilles, J.H. and Einaudi, M.T., 1992. Wall-rock alteration and hydrothermal fluid paths about the Ann-Mason porphyry copper deposit, Nevada - A 6-Km vertical reconstruction, *Econ. Geol.* 87, 1963-2001.

Eykamp, W.R., 1993. A Proterozoic basement and cover sequence in the Outalpa area, Olary Block, South Australia. B. Sc. Honours thesis, University of New England (unpublished).

Fanning, C.M., 1995. Geochronological synthesis of southern Australia. Part I. The Curnamona Province. *Prise.* Report prepared for the Department of Mines and Energy, South Australia. April 1995.

Faure, G., 1977, *Principles of Isotope Geology*, John Wiley & Sons, New York.

Flint, D.J. and Webb, A.W., 1980. Geochronological investigations of the Willyama Complex, South Australia. *South Australia. Department of Mines and Energy. Report Book* 79/136.

Flint, R.B., 1993. Nuyts Volcanics: In Drexel, J.F., Preiss, W.V. and Parker, A.J. (eds.), The geology of South Australia. Volume 1, The Precambrian, *Geol Surv. S.A.*, Bulletin 54, p. 69.

Flint, R.B. and Flint D.J., 1975. Preliminary geological investigations on the Curnamona 1:250 000 sheet. *South Australia. Department of Mines and Energy. Report Book* 75/124.

Flint, R.B. and Parker, A.J., 1993. Willyama inliers: In Drexel, J.F., Preiss, W.V. and Parker, A.J. (eds.), The geology of South Australia. Volume 1, The Precambrian, *Geol Surv. S.A.*, Bulletin 54, p. 82-93.

Foden, J.D., Song, S.H., Smith, P.B. and Van der Steldt, B., 1995. Geochemical evolution of the lithospheric mantle beneath S.E. South Australia, (in prep.)

Fodor, R.V., 1987. Low- and high-TiO2 flood basalts of southern Brazil: origin from picritic parentage and a common mantle source. *EPSL* 84, 423-430.

Fodor, R.V. and Vetter, S.K., 1984. Rift-zone magmatism: Petrology of basaltic rocks transitional from CFB to MORB, southeastern Brazil margin. *Contrib. Min. Petrol.* 88, 307-321.

Mawson, D., 1912. Geological investigations into the Broken Hill area. *Roy. Soc. S.A., Memoirs.* 2, 211-319

McDonald, G., 1992. The petrology, geochemistry and geochronolgy of the Anabama Granite and associated igneous activity, Olary region, South Australia: Implications for the southern Adelaide Fold Belt, Antarctic and the Lachlan Fold Belt of N.S.W. B. Sc. Honours thesis, University of Adelaide, (unpublished).

McKenzie, D., and Bickle, M.J., 1988. The volume and composition of melt generated by extension of the lithosphere. *J. Petrol.* 29, 625-679.

Menzies, D.C., 1992. The Willyama Supergroup in the Billeroo area, South Australia- with special emphasis on the quartz-magnetite and meta-basic rocks. B. Sc. Honours thesis, University of New England.

Menzies, M.A., 1992, The lower lithosphere as a major source for continental flood basalts: a re-appraisal. In: Story, B.C., Alabaster, T. and Pankhurst, R.J. (eds), *Magmatism and the Causes of Continental Break-up,* Geol. Soc. Special Publication 68, 31-39.

Merino, E., Nahon, D. and Wang Yifeng, 1993. Kinetics and mass transfer of pseudomorphic replacement: Application to replacement of parent minerals and kaolinite by Al, Fe and Mn oxides during weathering. *Am. J. Sci.* 293, 135-155.

Merino, E., Wang Yutian, Wang Yifeng and Nahon, D., 1994. Implications of pseudomorphic replacement for reaction-transport modeling in rocks. *Mineral Mag.* 58A, 599-600.

Merino, E., 1995. Comment on "Geochemistry of tectonically expelled fluids from the northern Coast ranges, Rumsey Hills, California, USA" by M.L. Davisson, T.S. Presser and R.E. Criss. *Geochim. et Cosmo. Acta* 59, 1871-1872.

Meschede, M., 1986. A method of discriminating between different types of mid-ocean ridge basalts and continental tholeiites with the Nb-Zr-Y diagram. *Chem. Geol.* 56, 207-218.

Miyashiro, A. and Shido, F., 1975. Tholeiitic and calc-alkaline series in relation to the behavoirs of titanium, vanadium, chromium and nickel. *Am. Jour. Sci.* 2775, 265-277.

Müller, D., Rock, N.M.S and Groves, D.I., 1992. Geochemical discrimination between shoshonitic and potassic volcanic rocks from different tectonic settings: a pilot study. *Mineral. Petrol.* 46, 259-289.

Müller, D., Morris, B.J. and Farrand, M.G., 1993. Potassic alkaline lamprophyres with affinities to lamproites from the Karinya Syncline, South Australia. *Lithos* 30, 123-137.

Page, R.W. and Laing, W.P., 1992. Felsic metavolcanic rocks related to the Broken Hill Pb-Zn-Ag orebody, Australia: geology, depositional age and timing of high grade metamorphism. *Econ. Geol*, 87, 2138-2168.

Parker, A.J., 1972. A petrological and structural study of a portion of the Olary Province, west of Wiperaminga Hill, South Australia. B. Sc. Honours thesis, University of Adelaide, (unpublished).

Patchett, P.J, Van Breeman, O. and Martin, R.F., 1979. Sr isotopes and the structural state of feldspars as indicators of post-magmatic hydrothermal activity in continental dolerites. *Contrib. Min. Petrol.*, 69, 65-73.

Pearce, J.A., Harris, N.B.W. and Tindle, A.G., 1984. Trace element discrimination diagrams for the tectonic interpretation of granitic rocks. *J. Petrol.* 25, 956-983.

Peterson, M.J., 1993. Geology of the Outalpa-Tommie Wattie Bore area with special reference to migmatite formation during low pressure, high temperature amphibolite grade metamorphism. B. Sc. Honours thesis, University of Melbourne, (unpublished).

Phillips, G.N., 1980. Water activity changes across an amphibolite-granulite facies transition, Broken Hill, Australia. *Contrib. Min. Pet.* 75, 377-386.

Pierini, M., 1994. Amphibolites, piemontite and the geology of the Cathedral Rock-Drew Hill Area, Olary Block, South Australia. B. Sc. Honours thesis, University of Melbourne, (unpublished).

Rock, N.M.S., 1987. The nature and origin of lamprophyres: In Fitton, J.G. & Upton, B.G.J. (eds), Alkaline Igneous Rocks, *Geol. Soc. Special Publication* 30, 191-226.

Saunders, A.D., Norry, M.J. and Tarney, J., 1988. Origin of MORB and chemically depleted mantle reservoirs: trace element constraints. *J.Petrol.,* Special Lithosphere Issue, 415-445.

Saunders, A.D., Story, M., Kent, R.W. and Norry, M.J., 1992. Cosequences of plume-lithosphere interaction In: Story, B.C., Alabaster, T. and Pankhurst, R.J. (eds), *Magmatism and the Causes of Continental Break-up,* Geol. Soc. Special Publication 68, 31-39.

Smith, P.B., 1992, The alteration history of the Late Proterozoic Wooltana Volcanics of the Mt Painter Province, South Australia. B. Sc. Honours thesis, University of Adelaide, (unpublished).

Stevens, B.P.J., Barnes, R.G. and Forbes, B.G., 1990. Willyama Block-regional geology and minor mineralisation. In: Hughes, F.E. (ed.), Geology of the mineral deposits of Australia and Papua New Guinea. *Australaisian Institute of Mining & Metallurgy. Monograph Series* 14: 1065-1072.

Streckeisen, A., 1973. Plutonic rocks: Classification and nomenclature recommended by the IUGS. Subcommision on the systematics of igneous rocks. *Geotimes Oct.,* 26-30.

Sun, S.S. and McDonough, W.F., 1989. Chemical and isotopic systematics of ocean basalts: implications for mantle composition and processes. In: Sauders, A.D. and Norry, M.J. (eds). *Magmatism in the Ocean Basins. Geol. Soc. London,* Special Publication 42, 313-345.

Talbot, J.L., 1967. Subdivision and structure of the Precambrian (Willyama Complex and Adelaide system), Weekeroo, South Australia. *Roy. Soc. S.A. Transactions,* 91, 45-58.

Thompson, R.N., Morrison, M.A., Henry, G.L. and Parry, S.J., 1984. An assesment of the relative roles of crust and mantle in magma genesis: an elemental appraoch. *Philos. Trans. Roy. Soc. London,* A310, 549-590.

Thompson, R.N., 1977. Columbia/Snake River-Yellowstone magmatism in the context of westen USA. Cenozoic geodynamics. *Tectonophysics*, 39, 621-636.

Turner, S.P., Foden, J.D., Sandiford, M. and Bruce, D., 1992. Sm-Nd isotopic evidence for the provenance of sediments from the Adelaide Fold Belt and southeastern Australia with implications for episodic crustal addition. *Geochim. et Cosmo. Acta.* 57, 1837-1856.

Watson, S. and McKenzie, D., 1991. Melt generation by plumes: a study of Hawaiian volcanism. *J. Petrol.* 32, 501-537.

Whalen, J.B., Currie, K.L. and Chappell, B.W., 1987. A-type granites: geochemical characteristics discrimination and petrogenesis. *Contrib. Min. Petrol.* 95, 407-419.

Williams, P.J. and Blake, 1993. Alteration in the Cloncurry District, roles of recognition and interpretation in exploration for Cu-Au and Pb-Zn-Ag deposits, Contribution 49, Economic Geology Research Unit, James Cook University.

Williams, P.J. and Blake, 1995. Alteration in the Cloncurry District, 1995 lecture notes.

Willis, I.L., Brown, R.E., Stroud, W.J. and Stevens, B.P.J., 1983. The early Proterozoic Willyama Supergroup: stratigraphic subdivision and interpretation of high to low-grade metamorphic rocks in the Broken Hill Block, New South Wales. *J. Geol. Soc. Aust.* 30, 195-224.

Wilson, M., 1989. *Igneous Petrogenesis*. Chapman & Hall, London, U.K.

Winchester, J.A. and Floyd, P.A., 1975. Geochemical magma type discrimination: Application to altered and metamorphosed basic igneous rocks.

Winchester, J.A. and Floyd, P.A., 1977. Geochemical discrimination of different magma series and their differentiation products using immobile elements. *Chem. Geol.* 20, 325-343.

Zhao, J.X. and McCulloch,M.T., 1993b. Melting of a subduction-modified continental lithosphere: Evidence from Late Proterozoic mafic dike swarms in central Australia, *Geol.* 21, 463-466.

Zhao, J.X., McCulloch, M.T. and Korsch, R.J., 1994. Characterisation of a plume related ~800Ma magmatic event and its implications for basin formation in central-southern Australia. *EPSL* 121, 349-367.

APPENDIX A:

ANALYTICAL TECHNIQUES

X-Ray Fluorescence (XRF)

All samples chosen for XRF analysis were cut with a diamond saw to rid of weathered surfaces and then washed with water. These cleaned rock fragments were crushed in a steel jaw crusher. A fine powder was produced using a tungsten carbide mill.

Trace element anlysis involved thourough mixing of ~5g of rock powder with approximately 0.8mL of PVA solution. Pressed pellets were made by enclosing the mixed powder within a boric acid casing.

Major element analysis involved drying of a few grams of rock powder in an oven at ~100°C for 1-2hrs. Samples were ignited in a furnace at ~1000°C for 8-9hrs and LOI (loss on ignition) was subsquently measured by taking the before and after weight difference. One gram of the ignited powder was mixed with four grams of flux and mixed thoroughly. This blend was heated in a Pt crucible until complete fusion (and homogenisation) of the sample had been obtained. The liquid was poured into Pt mould and cooled with a jet of air.

Major and trace elements were were measured on the Phillips PW 1480 XRF spectrometer.

Nd and Sr Isotope Analysis

Digestion of 200mg of rock powder was achieved by a series of HF/HNO_3 dissoltions in teflon containers. For samples containing refractory zircon, teflon bombs were placed in metal jackets and placed in an oven at 180°C for $2^{1/2}$ days, to enable complete dissolution. One drop of Sm-Nd spike was added to each of the dissolved solutions to enable measurement of element concentrations. Sr, Nd and Sm were separted from the sample by cation exchange columns.

Nd and Sm IC and ID analyses were loaded onto degassed filaments with a 'double' configuration. Sr IC samples were loaded onto 'single' configuration tantalum filaments. Isotopic compositions, Nd and Sm concentrations were measured on the Finnigan MAT 261 mass spectrometer. Rb and Sr concentrations were measured by extended XRF analysis (see above).

Pb/Pb Zircon Evaporation

One sample with relatively high Zr concentrations was chosen for Pb/Pb zircon evaporation. The rock sample was washed thoroughly with water to rid of surface contaminants, and crushed in a steel jaw crusher until the entire sample passed through a 1mm sieve. An initial heavy mineral separate was achieved using a Wilfley table. The heavy fraction was drained and then soaked in ethanol to enhance drying of the sample. A hand magnet was run over the sample to separate a large magnetic component.

The final step involved heavy liquid separation. The light fraction was rich in feldspars and quartz, whilst the heavy fraction contained zircon, sphene, apatite, epidote, magenetite, and rare gold. Rhenium filaments were bent into a 'canoe' shaped configuration and degassed. Selection of zircons involved choosing of grains that were pale pink, translucent, with sharp crystal edges and with as few fractures as possible. Those crystals with inclusions or a metamict appearance were disregarded. Zircons were selected for analysis and placed in the degassed filament. The filament was closed up almost completely, leaving a tiny hole in the top through which Pb would be evaporated.

The filaments were loaded onto a carousel with opposing Rhenium ionisation filaments, and loaded into the MAT 261 mass spectrometer. Pb isotopic compositions were measured in a number of heating steps (or depositions); First Pb was evaporated from the zircon and deposited on the ionisation filament. The evaporation then ceased and the ionisation filament was turned up until a steady Pb beam was obtained. Measurement of the Pb/Pb ratio continued until the size of the beam became too small. Depositions continued, gradually burning into the core of the zircon from the outside.

APPENDIX B:

THIN SECTION DESCRIPTIONS

Sample No.: 1060-009 (Poodla)

Location: west of Alconie Hill, on track between Koolka Hut and Antro Woolshed.

Thin Section Description:

Dominantly cross hatched rounded K-feldspar (microcline) intergrown with albite is abundant in this slide comprising ~45-50% of the modal composition. Smaller recrystallised quartz grains exhibiting undulose extinction are also common and usually occur in patches a few mm across. Ferromagnesian aggregates up to 5mm across are comprised primarily of granular biotite (probably after amphibole) exhibiting pleochroic haloes, epidote crystals displaying complex zoning of interference colours (5%), fractured (originally euhedral) magnetite (5%), and grey-brown sphene in large (~1mm) typically diamond shaped subhedral crystals. Significantly, there is also evidence for interaction with K-rich alteration fluids in the form of biotite veins. Tourmaline observed in outcrop in discrete patches (to a few cms) is not observed in this thin section. This rock is classified as a syenogranite.

K-feldspar (microcline) and Albite	50%
Quartz	20%
Biotite	15%
Magnetite	5%
Epidote	5%
Sphene	5%
Zircon	tr

Sample No.: 1060-005 (Rainy Day dolerite)

Location: 2km NE of Antro Woolshed, to south of outcropping mafic granitoid.

Thin Section Description:

This thin section is composed mainly of amphibole; possibly primary brown hornblende exhibiting a strong 120 degree cleavage, twinned Fe-rich amphibole (cummingtonite, which accounts for the Fe-rich nature of this rock); and lesser pale green riebeckite on the rims of other amphibole grains, indicating Na-rich alteration. Plagioclase exhibits multiple twinning and comprises 30% of the section. Minor constituents are fine grained magnetite (as well as late stage Fe-rich veins), biotite after hornblende, quartz and epidote.

Amphibole	45%
Plagioclase	30%
Magnetite	10%-15%
Biotite	5%
Epidote	<2%
Quartz	minor

Sample No.: 1060-017 (HPT dolerite)

Location: in creek bed <1km west of East Doughboy Bore.

Thin Section Description:

Elongate (3mm) albitised plagioclase laths dominate this thin section. Large 2mm grains of magnetite are intimately associated with sphene, and often associated with aggregates of actinolite, biotite after actinolite, and fine granular epidote. Quartz is minor or absent. Actinolite and biotite occur in roughly equal proportions. Epidote is also an alteration product in plagioclase laths. This rock was originally a dolerite or gabbro.

Albite	45%
Actinolite	15%
Biotite	15%
Magnetite	10%
Sphene	5%
Epidote	5%

Sample No.: 1060-006 (HPT dolerite/gabbro)

Location: near Baxter's Bore; northern-most outcrop.

Thin Section Description:

This slide is similar to 1060-017 except the modal percentages of actinolite and plagioclase are roughly reversed. It exhibits a sub-ophitic texture with plagioclase laths (2.5mm; 20%) interstitial with respect to actinolite aggregates (2mm; 40%). This sample contains very fine grained epidote in association with plagioclase (alteration of plagioclase). Biotite occurs as complex fine grained aggregates most commonly in association with actinolite and the opaque minerals. Some sphene growth can be observed on the rims of opaque grains probably indicating the presence of Ti-magnetite or ilmenite. The opaques are subhedral to anhedral and appear highly fractured. Some albite rich veins are also present.

Actinolite	40%
Plagioclase	20%
Opaques	15%
Epidote	12%
Biotite	10%
Sphene	3%
Chlorite	tr

Sample No.: 1060-008 (HPT dolerite)

Location: near Baxter's Bore (western outcrop).

Thin Section Description:
Fine grained plagioclase grains (<1mm) are abundant along with pale green, slightly pleochroic actinolite (<1.5mm). Rare quartz (elongated grains to 1mm) exhibits undulose extinction. Sphene is very common and occurs chiefly as a replacement of Ti-magnetite or ilmentite. Many opaque grains not rimmed with sphene are probably magnetite, and account for the high magnetic susceptibility of this sample. Greenish-yellow epidote is common in this slide and is associated primarily with amphibole where it may exhibit some zoning of its interference colours. In contrast to 1060-007 or -017 biotite is an extremely minor phase.

Plagioclase	30%
Actinolite	30%
Opaques	20%
Epidote	12%
Sphene	5%
Biotite	<1%
Quartz	tr

Sample No.: 1060-049 (HPT dolerite ?)

Location: Northern most outcrop near Antro Feldspar Mine.

Thin Section Description:
This is a strongly recrystallised fine grained equigranular dolerite composed of albite-actinolite-magnetite-biotite-qtz.

Sample No.: 1060-050 & 1060-053 (LPT dolerites).

Location: near Antro Feldspar Mine.

Thin Section Description:

These samples are clearly different from the other greenschist facies meta-dolerites and gabbros. Sample -050 has a sub-ophitic texture with possibly zoned plagioclase grains (elongate and mostly ~1mm), indicating that some may be of primary igneous origin. Most grains however are epidotised. Sample -053 appears to be more recrystallised and altered; denoted by a greater abundance of epidote, and the lack of a sub-ophitic texture. Green hornblende forms relatively large aggregates up to a few mm diameter in both samples, and is apparently after CPX. Consistent with these samples' geochemistry (i.e. low Fe_2O_3 and TiO_2), and their low magnetic susceptibility, there are very few opaque grains (<3%); especially in comparison to other metadolerite samples. An average modal composition is set out below.

Plagioclase(Albite)	45%
Hornblende (after CPX)	40%
Epidote	10%
Opaques	<3%
Quartz	minor/absent

Sample No.: 1060-012 (Antro)

Location: 2km NE of Antro Woolshed

Thin Section Description:

This rock has a felsic mineralogy with abundant plagioclase and quartz, accessory CPX, actinolite, magnetite, sphene, epidote and trace amounts of limonite, biotite and zircon. Two principal types of feldspar are characterised by different twinning styles. Multiple twinned plagioclase is dominant but there is a significant component of probable albitised K-feldspar in the form of 'checkerboard albite'. Feldspar grains are <3mm in size. Recrystallised rounded quartz grains exhibit undulose extinction and dominantly occur in large patches with individual grains not exceeding 4mm. Actinolite (possibly after CPX) occurs in small patches of <1mm. Sphene exhibits an association with these mafic aggregates as do the opaque minerals, minor biotite after actinolite and fine, disseminated epidote. Limonite is slightly pleochroic and exhibits red-brown colours. The opaques are disseminated and exhibit grain sizes from 0.5mm-0.05mm. With a significant K-feldspar precursor component this sample is classified as a quartz monzodiorite.

Plagioclase	40%
K-spar ('checkerboard albite')	15%
Quartz	20%
Opaques	8%-12%
Actinolite	4%
Sphene	3%
Epidote	2%-3%
Limonite	1%-2%
Biotite	<1%
Zircon	tr

Sample No.: 1060-014 (Antro)

Location: 2km NE of Antro Woolshed, eastern outcrop.

Thin Section Description:

This slide is very similar to 1060-012 except that it has a much greater content of modal quartz (consistent with SiO_2 content) and less checkerboard albite. Quartz (which can be clearly observed in hand specimen) occurs as large (6mm) rounded grains that exhibit undulose extinction. This knowledge combined with lower modal proportion of checkerboard albite suggests either an original tonalitic to granodioritic composition for this rock type or significant SiO_2 enrichment during alteration, the latter being more likely.

Quartz	35%
Plagioclase	35%
Opaques	8%-10%
'Checkerboard albite'	7%
Actinolite	3%
Sphene	3%
Limonite	<2%
Zircon	tr

Sample No.: 1060-015 (Antro)

Location: 1-2km N of Ameroo Hill (NE most outcrop).

Thin Section Description:

Quartz grains (0.5mm) commonly occur in patches to 3mm. Multiple twinned albite is the dominant constituent of this rock. Minor amphibole is pleochroic, light to dark green, and is the major constituent of isolated patches that include magnetite (<1mm), sphene, biotite (after amphibole), epidote and minor apatite. Amphibole is probably after minor CPX. Some yellow epidote grains are as large as 0.5mm and exhibit complex interference patterns. Light brown to red-brown biotite, exhibiting straight extinction, is invariably associated with amphibole. Minor apatite exhibits high relief relative to quartz and feldspar. Some sphene aggregates contain opaque inclusions. This rock is given a classification of quartz diorite.

Plagioclase	50%
Quartz	25%
Amphibole	5%
Opaques	5%
Sphene	4%
Biotite	2%
Epidote	2%
K-spar	minor

Sample No.: 1060-016 (Antro)

Location: 1-2km N of Ameroo Hill (SW most outcrop).

Thin Section Description:

This is a Quartz, plagioclase, hornblende, magnetite-bearing rock. Quartz occurs both as very large grains (5mm) and as finer recrystallised grains intergrown with albitised feldspar (probably K-spar) defining a 'granophyric texture'. 5mm grains of euhedral-anhedral plagioclase exhibits multiple twinning and is less common in this slide than in 1060-015. Amphibole (hornblende?) occurs in association with fine to medium grained magnetite (0.05mm-1mm), fine grained sphene (0.05mm) and zoned epidote crystals (<1.5mm) in 5mm long elongated lenses. This rock is classified as a quartz monzodiorite.

Plagioclase	40%
Quartz	18%
Amphibole	10%
Opaques (magnetite)	8%
Sphene	5%
Epidote	<2%
K-spar	(?) ~10%

Sample No.: 1060-018 (Antro)

Location: near East Doughboy; 'Horse Paddock'.

Thin Section Description:
This sample has a more mafic mineralogy. It is characterised by a gabbroic texture in thin section. Quartz is rare in comparison to samples 1060-015 & -016, and occurs as smaller grains to 1.5mm, but mostly <0.5mm. Sodic plagioclase are multiple twinned and are laths to 4mm. Dark green 3mm hornblende grains are displayed in aggregates with minor CPX, epidote, sphene and magnetite. Anhedral sphene grains (2mm) often contain inclusions of magnetite.

Albite	30%
Hornblende & CPX	30%
Opaques	10%
Sphene	5%
Epidote	<5%
Apatite	<1%
K-spar	minor
Biotite	absent

Sample No.: 1060-056 (Antro)

Location: 1km West of Ameroo Hill.

Thin Section Description:
Similar to other mafic granitoid samples (e.g. 1060-012 & -014), except it contains more amphibole and biotite. A foliation observed in hand specimen is not evident in this thin section. Despite uncertainty over K-feldspar content this sample is classified as a granodiorite-tonalite.

Na-Plagioclase	40%
Quartz	28%
Amphibole	14%
Opaques	7%
K-spar	(?) 5%
Sphene	3%
Biotite	3%
Apatite	tr

Sample No.: 1060-031 (Outalpa Amphibolite)

Location: 1km East of Ameroo Hill

Thin Section Description:

Subhedral to euhedral diamond shaped blue-green hornblende crystals to 1mm define an obvious mineral foliation in this sample. These crystals may contain relict cores of pyroxene that exhibit high birefringence. Plagioclase grains of similar size rarely exhibit multiple twinning, and contain abundant inclusions of fine grained, granular epidote, yellow in colour (Epidotisation of plagioclase). Magnetite is definitely present due to the relatively high magnetic susceptibility of the hand specimen. Sphene is not common but is invariably associated with opaque minerals, probably Ti-magnetite and ilmenite.

Hornblende	45%
Plagioclase(Albite)	38%
Opaques	7%
Epidote	7%
Sphene	3%
Quartz	?

Sample No.: 1060-036a

Location: near Maldorky Hill

Thin Section Description:

Large euhedral grains of biotite and hexagonal phlogopite (5mm grains) are the most notable feature in hand specimen. In thin section these grains, containing needle-like inclusions of apatite, give this rock its porphyritic nature. The main feldspar is K-Feldspar, which has now been largely sericitised, although rare relict multiple twins suggest that plagioclase may have formally been a minor component. Chlorite is dominantly after biotite. 6mm long opaque grains exhibit highly altered cores consisting of chlorite, feldspar and carbonate (probably calcite). These assemblages may represent former olivine phenocrysts. Although difficult to confirm some fine grain quartz may also be displayed in this section.

Biotite/Phlogopite	30%
K-spar (largely sericitised)	30%
Opaques	12%
Chlorite	8%
Quartz	(?) 5%
Carbonate (calcite)	<5%
Apatite	2-3%
Plagioclase	minor
Epidote	tr

REFLECTIVE MICROSCOPY

Sample No.: 1060-064 (Outalpa amphibolite); MAGNETIC

Location: West of Ameroo Hill

Polished Thin Section Description:
This hand specimen of this sample is highly magnetic. The polished section contains abundant opaques that define a mineral lineation. Brown/purple isotropic magnetite is the major Fe oxide phase. Abundant veinlets of anisotropic haematite occur within magnetite grains. Rare magnetite grains display haematite rich rims. Ilmenite occurs in larger aggregates associated with magnetite grains and is observed to replace sphene. Haematite veins and rims are interpreted as secondary alteration effects.

Magnetite : Haematite : Ilmenite
= 70 : 15 : 15

Sample No.: 1060-064 (Outalpa amphibolite): NON-MAGNETIC

Location: West of Ameroo Hill

Polished Section Description:
This section contains less Fe/Ti oxides than the previous section. Also magnetite is a minor phase in comparison to haematite. Some euhedral haematite grains exhibit concentric zoning, with a blue-white anisotropic core and slightly anisotropic concentric rims. Almost all previous magnetite appears to have been altered to haematite.

Sample No.: 1060-061 (HPT dolerite): MAGNETIC.

Location: Northern-most dolerite outcrop north of Antro feldspar mine.

Polished Section Description:
Abundant fine grained subhedral to euhedral magnetite grains are fractured and contain veinlets of haematite (very similar to 1060-064). Minor grey ilmenite is also commonly present within these magnetite-haematite assemblages. Very minor fine grained pyrite and chalcopyrite is present.

Sample No.: 1060-062 (HPT dolerite): NON-MAGNETIC

Location: as for -061

Polished Section Description:
Fe-Ti oxides are much less common in this sample (<5% of total rock). They are mainly fine grained anhedral haematite grains and magnetite is very minor. This oxide assemblage probably represents an almost total replacement of magnetite by haematite although it is also likely also that a significant amount of Fe has been leached from the rock entirely.

APPENDIX C:

NORMALISATION FACTORS AND XRF WHOLE ROCK DATA

Normalisation Factors

Primordial mantle- and OIB-normalised incompatible trace element diagrams in the main text are all normalised to the data of Sun and McDonough, 1989. These data are set out in the table below.

Element	Primitive mantle	OIB
Rb	0.635	31
Ba	6.989	350
Th	0.085	4
U	0.021	1.02
Nb	0.713	48
K	250	12000
La	0.687	37
Ce	1.775	80
Sr	21.1	660
P	95	2700
Nd	1.345	38.5
Zr	11.2	280
Sm	0.444	10.0
Ti	1300	17200
Y	4.55	29
REE	**Primitive mantle**	**OIB**
Pr	0.276	9.70
Eu	0.168	3.00
Gd	0.596	7.620
Tb	0.108	1.050
Dy	0.737	5.600
Ho	0.164	1.06
Er	0.480	2.62
Tm	0.074	0.350
Yb	0.493	2.16

Sample No.	1060-004	1060-005	ZA000019	AVERAGE	LPT	ZA001241	ZA001242	1060-053
Rock type	dolerite	dolerite	Dolerite	RAINY DAY	DOLERITES	amphibolite	amphibolite	dolerite
Location E	Rainy Day	Rainy Day	North Ltd	DOLERITE		North Ltd	North Ltd	w. of Antro
N			Rainy Day			Mutooroo	Mutooroo	feldspar mine
Major(wt%)								
SiO2	44.28	46.1	45.2	45.19		50.5	50.5	49.16
TiO2	2.37	2.33	2.3	2.33		0.68	0.76	0.8
Al2O3	11.5	11.62	10.3	11.14		14	14	15.74
Fe2O3T	22.33	21.53	23.3	22.39		11	13	10.88
MnO	0.26	0.26	0.28	0.27		0.21	0.23	0.09
MgO	6.37	5.62	6.35	6.11		8.98	8.37	7.8
CaO	9.81	9.15	9.2	9.39		12.5	11.5	8.03
Na2O	2.02	2.17	1.65	1.95		1.43	1.83	4.6
K2O	0.39	0.41	0.36	0.39		0.25	0.17	0.11
P2O5	0.08	0.12	0.1	0.10		0.04	0.05	0.07
SO3	0.02	0.01		0.02				0.02
LOI	0.6	0.57	0.85	0.67		1.3	0.04	2.72
Total	100.03	99.89	99.89	99.94		100.89	100.45	100.02
Mg#	0.28	0.27	0.27	0.28		0.53	0.47	0.50
trace(ppm)								
Pb	18	14.31	13	15		8	8	5
Ba	667	566	410	548		380	40	144
Th	0	0	2.5	0.8		0.4	0.4	0.0
U	0.1	2.2	<0.5	1.2		0.1	0.1	0.3
Nb	2	3	<10	2.50		2	3	4
K	3236	3402	2987	3209		2074	1411	913
La	5	7	11	7.67		3	3.7	4.0
Ce	11	16	16	14		6	8	14
Pb	1	8	<4	4.30		3	4.0	1.6
Sr	143	139.13	100	127		120	105	206
P	349	524	437	436.62		175	218	306
Nd	11	10.24	11	11		5	7	9
Zr	43	60	80	61		40	40	44
Sm		3.07	2.5	2.8		1.5	1.8	
Ti	14208	13968	13788	13988		4077	4556	4796
Y	20	27	20	22		21	23	13
Sc	56	53	50	53		50	50	35
Cr	2	4	<50	3		155	115	325
V	1206	982	1100	1096		240	300	253
Co	85	76	60	74		46	49	51
Ga	23	22	26	23		16	16	15
Cu	675	361	390	475		115	200	18
Zn	146	157	50	118		74	93	26
Ni	66	43	85	65		85	91	101

Sample No.	1060-050	ZA001230	ZA001208	ZA001209	ZA001239	AVERAGE	R73475	R66559
Rock type	dolerite	Qtz Gabbro	Gabbro	Dolerite	Gabbro	LTP	metadolerite	metadolerite
Location E	414413	North Ltd	North Ltd	North Ltd	North Ltd	DOLERITE	Dibben 1990	Dibben 1990
N	6452210	Double Dam	Feldspar Mine	Feldspar Mine	Baxter's Bore		Mt Howden	Mt Howden
Major(wt%)								
SiO2	47.66	48.3	47.6	48.8	48.5	48.88	48.61	50.97
TiO2	0.68	0.66	0.77	0.83	0.59	0.72	1.06	1.05
Al2O3	15.57	16.2	15.3	15.4	16	15.28	14.40	12.53
Fe2O3T	9.61	10.6	11.7	11.5	8.54	10.85	12.67	13.60
MnO	0.06	0.2	0.14	0.16	0.08	0.15	0.18	0.17
MgO	9.08	6.75	8.8	7.95	8.91	8.33	7.77	6.70
CaO	11.08	12.2	8.25	10.9	10.5	10.62	11.63	11.12
Na2O	3.28	2.04	3.62	3	2.62	2.80	2.28	2.70
K2O	0.43	0.3	0.28	0.23	1.24	0.38	0.37	0.48
P2O5	0.07	0.03	0.05	0.06	0.06	0.05	0.08	0.10
SO3	0.06					0.04	0.02	0.03
LOI	2.29	0.83	2.1	1.32	2.23	1.60	1.14	0.97
Total	99.87	98.11	98.61	100.15	99.27	99.67	100.21	100.42
Mg#	0.57	0.47	0.51	0.49	0.59	0.52	0.46	0.41
trace(ppm)								
Pb	20	16.00	4	3	61	15	10	8
Ba	270	330	440	680	90	297	476	923
Th	0	1	7.0	2.0	1.1	1.4		
U	0	0.2	1.0	<0.5	0.2	0.3	7.0	1.0
Nb	2	5	<10	<10	3	3	2	6
K	3568	2489	2323	1909	10289	3122	3070	3983
La	5.0	5.5	4.0	4.0	4.9	4.2	6.0	10
Ce	13	9	7	9	8	9	8	19
Pb	0.0	5	4.0	5.0	1.0	2.9	<2	2
Sr	154	135.00	135	170	170	149	127	208
P	306	131	218	262	262	235	349	437
Nd	5.90	6	6	9	6	7	9	14
Zr	37	60	60	50	20	44	56	72
Sm	1.67	1.58	0.5	0.5	1.4	1.3		
Ti	4077	3957	4616	4976	3537	4324	6355	6295
Y	15	11	10	10	18	15	20	24
Sc	35	35	30	30	40	38		
Cr	354	80	320	270	185	226		
V	254	220	230	240	180	240		
Co	44	40	60	60	38	49		
Ga	15	16	20	18	14	16		
Cu	10	230	55	65	8	88		
Zn	8	75	18	20	26	43		
Ni	126	75	120	80	110	99		

HPT	Sample No.	ZA001204	ZA001238	1060-006	1060-007	1060-017	ZA001228	ZA001207
DOLERITES	Rock type	Gabbro	Gabbro	gabbro	gabbro	dolerite	Dolerite	Gabbro
high K	Location E	North Ltd	North Ltd	416923	416935	E.Doughboy,	North Ltd	North Ltd
	N	Baxter's Bore	Baxter's Bore	6459622	6459602	in creek bed	Doughboy	Willow Well
	Major(wt%)							
	SiO2	47.9	49	49.67	51.04	50.25	48.3	52
	TiO2	1.83	1.52	1.47	1.54	1.4	1.18	1.6
	Al2O3	12.9	14	13.78	13.92	14.44	13.4	13.7
	Fe2O3T	16.5	14	14.45	13.38	13.8	13.2	13
	MnO	0.16	0.14	0.16	0.14	0.09	0.12	0.06
	MgO	6.2	5.96	6.31	6.24	6.62	6.25	6.25
	CaO	9	7.67	8.4	7.23	5.98	9	4.82
	Na2O	3.46	3.47	3.47	4.06	4.65	4.48	6.1
	K2O	0.75	1.1	1	1.31	1.83	1.03	0.6
	P2O5	0.13	0.16	0.17	0.18	0.15	0.12	0.17
	SO3			0.01	0.01	0.01		
	LOI	1.15	1.12	1.28	1.01	0.73	1.36	2.04
	Total	99.98	98.14	100.17	100.06	99.95	98.44	100.34
	Mg#	0.34	0.37	0.38	0.39	0.40	0.40	0.40
	trace(ppm)							
	Pb	25	51	43	57.82	101	60	35
	Ba	220	80	213	292	224	280	240
	Th	4.5	4.3	1.7	3.4	2.5	3.0	7.0
	U	0.5	0.7	1.3	0.9	1.0	0.9	5.5
	Nb	10	13	6	7	8	13	15
	K	6223	9128	8298	10870	15185	8547	4979
	La	14	16	12	11	11	23	20
	Ce	35	38	29	28	29	47	35
	Pb	8	1	3	2	2	4	4
	Sr	220	180	186	192.40	200	250	110
	P	568	699	742	786	655	524	742
	Nd	17	21	19	18.86	17	22	25
	Zr	140	60	106	123	109	120	160
	Sm	3.0	4.6		4.66		4.5	3.5
	Ti	10971	9112	8813	9232	8393	7074	9592
	Y	25	48	29	29	26	21	25
	Sc	40	35	42	40	45	40	40
	Cr	50	55	75	68	142	150	80
	V	620	360	411	356	368	310	350
	Co	65	45	54	59	49	38	40
	Ga	25	22	20	21	17	18	25
	Cu	110	115	127	123	34	85	6
	Zn	15	26	29	28	27	26	3
	Ni	75	50	63	56	72	60	65

Sample No.	AVERAGE	HPT	ZA001210	ZA001227	ZA001231	1060-008	1060-040	ZA001225
Rock type	HPT, High K	DOLERITES	Gabbro	Dolerite	Gabbro	dolerite	dolerite	Qtz dolerite
Location E		low K	North Ltd	North Ltd	North Ltd	415443	413894	North Ltd
N			Willow Well	Willow Well	Willow Well	6459624	6454643	Pimponda Mine
Major(wt%)								
SiO2	49.74		46.7	47.7	48.6	46.25	49.87	48.6
TiO2	1.51		1.96	1.81	2	2.94	1.88	1.38
Al2O3	13.73		12.8	12.9	12.7	12.29	13.2	13.3
Fe2O3T	14.05		20	15	17.2	17.14	14.51	14
MnO	0.12		0.06	0.17	0.2	0.09	0.1	0.23
MgO	6.26		5.2	5.6	5.95	5.37	5.66	6.55
CaO	7.44		5.7	7.35	9.1	11.5	7.42	10.6
Na2O	4.24		5.6	5.55	1.19	3.61	5.28	2.1
K2O	1.09		0.26	0.11	0.16	0.11	0.11	0.44
P2O5	0.15		0.16	0.17	0.2	0.37	0.21	0.12
SO3	0.01					0.01	0.02	
LOI	1.24		1.91	1.63	0.51	0.89	1.45	0.55
Total	99.58		100.35	97.99	97.81	100.57	99.71	97.87
Mg#	0.38		0.27	0.34	0.32	0.30	0.35	0.39
trace(ppm)								
Pb	53		11	8	10	2.14	7	36
Ba	221		150	210	340	133	188	360
Th	3.8		2.0	4.9	2.1	4.0	3.6	2.6
U	1.5		2.0	2.4	0.9	7.2	6.4	0.6
Nb	10		10	16	8	9	13	17
K	9033		2157	913	1328	913	913	3651
La	15		9	24	21	30	14	18
Ce	34		18	43	40	60	28	34
Pb	3		5	9	3	3	4	6
Sr	191		180	165	155	325.45	174	200
P	674		699	742	873	1615	917	524
Nd	20		20	27	27	40.03	23	18
Zr	117		120	160	170	203	140	120
Sm	4.1		3.0	5.9	6.3	9.24		4.1
Ti	9027		11750	10851	11990	17625	11271	8273
Y	29		30	28	33	53	35	27
Sc	40		35	30	40	40	36	40
Cr	89		40	40	130	110	14	170
V	396		500	400	420	607	452	320
Co	50		40	44	50	38	56	44
Ga	21		20	22	23	20	18	18
Cu	86		2	55	70	62	18	200
Zn	22		8	40	60	21	25	120
Ni	63		55	48	48	63	50	70

Sample No.	AVERAGE	R72903	R72901	R70742	AVERAGE OF	1060-049	1060-039
Rock type	HPT low K	metadolerite	metadolerite	metadolerite	5 SAMPLES	?	?
Location E		Eykamp,1993	Eykamp,1993	Menzies,1992	Pierini,1994	414907	413967
N		Outalpa	Outalpa	Billeroo	Cathedral Rock	6452911	6453916
Major(wt%)							
SiO2	47.95	49.07	49.28	49.49	49.17	50.76	52.57
TiO2	2.00	1.69	1.55	1.43	1.60	1.48	1.91
Al2O3	12.87	13.72	13.57	13.68	13.50	13.45	14.61
Fe2O3T	16.31	13.65	13.00	14.12	13.98	15.48	10.65
MnO	0.14	0.22	0.21	0.21	0.24	0.12	0.05
MgO	5.72	6.51	7.18	6.70	7.03	5.52	4.93
CaO	8.61	10.77	10.79	10.81	10.82	7.76	5.64
Na2O	3.89	1.87	1.89	2.06	1.86	4.68	6.59
K2O	0.20	0.31	0.43	0.41	0.46	0.35	0.81
P2O5	0.21	0.14	0.13	0.15	0.13	0.17	0.28
SO3	0.02	0.02	0.02	0.06	0.00	0	0.01
LOI	1.16	1.91	1.88	0.79	1.31	0.3	1.61
Total	99.05	99.88	99.93	99.91	100.10	100.07	99.66
Mg#	0.33	0.40	0.43		0.41	0.33	0.39
trace(ppm)							
Pb	12	14	25	21	28	2.9	49.5
Ba	230	139	472	1246	135	316	240
Th	3.2					9.4	4.4
U	3.2	3.0	3.0	4.0	-	1.9	8.4
Nb	12	7	6	12	6	8.8	22
K	1646	2572	3568	3402	3817	2904	6721
La	19	16	11	25	7	20	67
Ce	37	20	26	27	27	45	139
Pb	5	7	13	2	0	2.2	2.5
Sr	200	145	154	211	134	59.3	84.7
P	895	611	568	655	568	742	1223
Nd	25	16	17	20	17	24	57
Zr	152	101	94	89	96	121.1	159
Sm	5.7				3.8		
Ti	11960	10132	9292	8573	9592	8873	11450
Y	34	30	28	27	29	44	62
Sc	37					45	35
Cr	84					76	25
V	450					409	368
Co	45					52	27
Ga	20					20	16
Cu	68					52	9
Zn	46					12	12
Ni	56					53	37

Sample No.	ZA001203	ZA001205	1060-009	1060-010	AVERAGE	ANTRO	1060-012	1060-013
Rock type	Poodla	Poodla	Poodla	Poodla	POODLA	GRANITOIDS	Antro	Antro
Location E	North Ltd	North Ltd	412396	412406	(n=4)		Rainy Day	Rainy Day,
N	Sth Willow	W.Poodla	6462658	6462635				Cu-pit
Major(wt%)								
SiO2	62.7	64.1	63.56	62.77	63.28		68.11	65.69
TiO2	1.07	0.95	0.97	1.03	1.01		0.74	0.79
Al2O3	13.9	14.2	14.3	14.27	14.17		13.01	12.95
Fe2O3T	7.2	7.25	7.07	7.31	7.21		7.38	11.2
MnO	0.05	0.02	0.05	0.06	0.05		0.02	0.02
MgO	1.43	1.9	1.52	1.85	1.68		0.59	0.46
CaO	1.83	0.61	1.44	1.53	1.35		1.68	0.31
Na2O	3.82	4.32	3.58	3.05	3.69		7.42	6.99
K2O	5.3	4.72	5.87	6.3	5.55		0.17	0.11
P2O5	0.3	0.28	0.37	0.35	0.33		0.22	0.06
SO3			0.01	0.01	0.01		0	0
LOI	1.02	0.93	0.71	0.87	0.88		0.15	0.78
Total	98.62	99.28	99.45	99.40	99.19		99.49	99.36
trace(ppm)								
Pb	175	175	227	269.30	212		4.69	6.6
Ba	2150	1650	985	1417	1551		168	65
Th	16	16	16	14	15		11	7.5
U	6	4.5	5.5	4.8	5.2		3	5.9
Nb	30	30	21	21	25		19	18
K	43979	39166	48709	52277	46032		1411	913
La	50	35	35	36	39		35	25
Ce	115	90	74	93	93		75	50
Pb	7	7	2.9	2.9	4.95		4.5	3.3
Sr	130	50	80	75.61	84		29.32	30
P	1310	1223	1615	1528	1419		961	262
Nd	55	50	31	35.72	43		38.79	26
Zr	360	310	176	167	253		185	280
Sm	4.0	5.5		7.35	8.4		9.48	
Ti	6415	5695	5815	6175	6025		4436	4736
Y	45	45	39	45	43		61	75
Sc	15	10	16	15	14		15	19
Cr	30	30	11	16	22		0	3
V	50	70	50	57	57		28	17
Co	55	50	31	30	42		62	83
Ga	25	25	21	23	23		28	23
Cu	50	17	78	29	44		32	2319
Zn	20	30	27	33	28		8	19
Ni	30	25	8.0	10	18		0	16

Sample No.	1060-014	1060-015	1060-016	1060-018	1060-021	1060-034	1060-041	1060-042
Rock type	antro	Antro	Antro	mafic Antro	Antro	Antro	Antro	albitised Antro
Location E	Rainy day	NE Ameroo,	NE Ameroo	isolated o/c near	West of	414117	412511	as for -041
N		NE-most o/c	SW o/c	E. Doughboy	Ameroo Hill	6454685	6457150	
Major(wt%)								
SiO2	70.69	67.39	64.46	52.59	63.5	56.73	60.4	62.95
TiO2	0.54	0.85	0.87	2.27	1.12	1.6	2.09	2.08
Al2O3	13.31	13.64	13.36	12.12	13.33	13.39	13.84	16.77
Fe2O3T	5.61	6.82	9.51	15.89	9.42	12.45	6.43	1.6
MnO	0.01	0.08	0.04	0.09	0.06	0.04	0.04	0.01
MgO	0.25	0.78	1.12	3.09	1.24	3.7	2.97	1.8
CaO	0.7	2.62	2.35	6.58	2.68	4	5.12	3.68
Na2O	7.59	6.68	7.2	6.24	6.94	7.54	8.01	9.55
K2O	0.06	0.38	0.43	0.53	0.92	0.1	0.08	0.12
P2O5	0.28	0.24	0.33	0.39	0.41	0.18	0.78	0.87
SO3	0	0	0.01	0.01	0	0	0	0.01
LOI	0.32	0.34	0.26	0.28	0.06	0.24	0.25	0.45
Total	99.36	99.82	99.94	100.08	99.68	99.97	100.01	99.89
trace(ppm)								
Pb	0.8	10	8.9	12	18	1.8	1.7	3.1
Ba	92	243	149	263	170	56	53	73
Th	12	7.7	9.9		7.9	5.8	18	25
U	3.9	2.9	2.7	2.20	4	4.8	5.9	4.6
Nb	23	20	17	15	19	27	58	49
K	498	3153	3568	4398	7634	830	664	996
La	23	33	28	26	25	14	45	56
Ce	56	56	68	62	63	42	151	172
Pb	2.2	1.8	4.3	5	10.7	6.6	2.3	4.1
Sr	39	55	39	99	55	15	21	27
P	1223	1048	1441	1703	1790	786	3406	3799
Nd	25	37	46	38	33	25	92	109
Zr	302	221	230	236	250	199	423	407
Sm								
Ti	3237	5096	5216	13609	6714	9592	12530	12470
Y	90	83	88	61	74	52	123	128
Sc	7	25	21	30	27	22	17	7
Cr	4	0	2	0	0	1	0	0
V	28	2	3	275	7	236	130	46
Co	43	54	44	69	39	31	34	16
Ga	26	25	26	26	24	20	22	25
Cu	33	33	77	172	58	6	3	5
Zn	7	14	14	21	32	9	11	2
Ni	3	0	2	38	5	19	12	14

Sample No.	1060-043	1060-044	1060-056	ZA000018	ZA000020	ZA001201	ZA001226	AVERAGE
Rock type	Antro(epidote	Antro (actinolite	Interm. intr.	Antro	Antro	Antro	Antro	ANTRO
Location E	altered)	& albite veins)	West of Ameroo	North Ltd	North Ltd	North Ltd	North Ltd	(n=16)
N	as for -041	as for -041	Hill	Rainy Day	Rainy Day	Nth Ameroo	Willow Well	
Major(wt%)								
SiO2	57.53	60.05	65.89	63.2	64.7	65.6	50.8	62.37
TiO2	2.37	1.85	0.95	1.01	0.83	0.85	1.48	1.31
Al2O3	13.67	11.48	13.25	13.8	12.5	13.1	12	13.27
Fe2O3T	4.93	4.43	8.56	10.5	11.4	8.6	16.2	8.88
MnO	0.04	0.04	0.03	0.02	0.02	0.1	0.07	0.04
MgO	3.58	6.65	0.92	0.7	0.49	0.7	4.48	1.97
CaO	8.78	7.15	1.98	1.54	1.29	3.14	5.45	3.47
Na2O	6.57	6.81	7.03	8.2	7.25	6.7	6.6	7.25
K2O	1.04	0.15	0.81	0.13	0.14	0.55	0.17	0.35
P2O5	0.88	0.41	0.28	0.31	0.21	0.22	0.27	0.37
SO3	0	0	0	–	–	–	–	
LOI	0.38	0.6	0	0.37	0.1	0.28	0.55	0.32
Total	99.77	99.62	99.70	99.78	98.93	99.56	98.07	99.59
								0.55
trace(ppm)								
Pb	29	2.1	11	4.0	4.5	15	14	9
Ba	210	45	112	65	35	220	220	132
Th	13	14	9.1	7.5	6.0	8.5	7.0	10.0
U	7.3	3.8	4.7	4	1.5	3.5	1.75	3.9
Nb	58	47	26	20	20	25	19	28
K	8630	1245	6721	1079	1162	4564	1411	2875
La	67	37	20	60	32	25	24	34
Ce	197	127	59	110	56	75	50	86
Pb	4.5	0.7	3.8	4	<4	7	4.3	4.1
Sr	100	15	31	20	15	65	90	44
P	3842	1790	1223	1354	917	961	1179	1628
Nd	116	76	37	55	34	40	24	50
Zr	367	391	302	350	400	280	220	297
Sm				10	6.5	8.5	5.3	2.3
Ti	14208	11091	5695	6055	4976	5096	8873	7860
Y	142	104	92	80	55	70	42	83
Sc	16	20	27	20	20	25	30	20
Cr	0	1	1	<50	<50	<20	50	3.6
V	132	90	3	30	<20	<20	410	85
Co	29	37	54	10	20	55	26	42
Ga	20	18	25	22	20	30	17	23
Cu	8	5	69	68	105	18	5	177
Zn	8	7	18	2	<2	10	20	12
Ni	16	40	2	20	<10	25	16	13

Sample No.	1060-035b	1060-035c	1060-036b	1060-036c	1060-058	1060-059	AVERAGE	10 (Pet.Gr.1)	9
Rock type	lamprophyre	lamprophyre	lamprophyre	lamprophyre	lamprophyre	lamprophyre	MALDORKY	lamprophyre	lamprophyre
Location E	462640	462640	457758	457758	454702	454840	LAMPROPHYRE	Muller et al.,	Muller et al.,
N	6414156	6414156	6420452	6420452	6414564	6414196		1993	1993
Major(wt%)									
SiO2	54.92	54.60	49.98	50.17	52.73	51.74	52.36	56.50	63.10
TiO2	0.79	0.80	1.99	2.01	1.76	1.88	1.54	1.33	2.36
Al2O3	12.31	12.28	11.32	11.56	12.77	12.46	12.12	12.20	13.10
Fe2O3T	8.23	8.29	12.28	11.94	9.68	10.95	10.23	7.66	4.84
MnO	0.09	0.10	0.07	0.07	0.08	0.11	0.09	0.20	0.29
MgO	4.59	4.51	7.86	7.51	4.99	4.30	5.63	3.40	3.60
CaO	5.10	5.40	4.56	4.77	5.00	6.04	5.15	4.12	0.07
Na2O	1.72	1.66	1.53	1.91	1.69	1.33	1.64	1.91	0.28
K2O	4.48	4.47	4.10	3.75	5.72	4.26	4.46	7.52	9.68
P2O5	0.61	0.63	1.05	1.08	0.94	0.99	0.88	1.39	0.20
SO3	0.09	0.07	0.24	0.23	0.04	0.04	0.12		
LOI	7.13	7.22	4.08	4.16	4.13	5.79	5.42	3.88	1.98
Total	100.06	100.03	99.06	99.16	99.53	99.89	99.62	100.11	99.50
K/Na+K(at%)	74.4	75.1	75.0	68.7	79.1	78.2	75.3	81.5	97.5
trace(ppm)									
Pb	237	238	303	287	402	277	291	655	652
Ba	735	761	1096	1070	1828	926	1069.3	2994.0	2720.0
Th	24.5	24.9	67.8	66.5	71.6	78.7	55.7		
U	5.7	6.2	15.9	16.9	15.2	13.1	12.2		
Nb	17	18	50	50	49	42	38	20	22
K	37174	37091	34021	31117	47464	35349	37036	62400	80323
La	40	36	207	216	216	222	156	147	129
Ce	85	80	350	358	359	361	266	287	252
Pb	0	0.9	6	6.3	6.1	2.7	3.7	36.0	41.0
Sr	49	47	247	276	275	81	163	448	462
P	2663	2751	4585	4715	4104	4323	3857	6069	873
Nd	40	36	207	216	114	106	119.8	106.0	88.0
Zr	221	219	556	567	634	602	466	1135	1101
Sm							0.0	17.6	13.9
Ti	4736	4796	11930	12050	10551	11271	9222.3	7973.3	14148.2
Y	30	29	34	32	38	36	33	21	78
Sc	21	20	29	29	26	28	26	14	19
Cr	200	216	412	363	153	166	252	95	95
V	150	157	313	318	277	290	251	415	542
Co	31	31	31	28	36	30	31	50	130
Ga	17	17	16	16	18	17	17		
Cu	5	11	10	16	31	6	13	150	185
Zn	11	11	45	44	26	27	27	65	210
Ni	55	57	118	105	37	35	68	140	240

AMPHIBOLITES	Sample No.	AMPH-UC1	AMPH-UC3	AMPH-UC9	AMPH-UC13	AMPH-UC14	AMPH-UC12	AMPH-232	AMPH-256
CATHEDRAL	Rock type	Amphibolite	Amphibolite	Amphibolite	Amphibolite	Amphibolite	Amphibolite	Amphibolite	Amphibolite
ROCK	Location E	Pierini,1994	Pierini,1994	Pierini,1994	Pierini,1994	Pierini,1994	Pierini,1994	Pierini,1994	Pierini,1994
	N	Cathedral Rock	Cathedral Rock	Cathedral Rock	Cathedral Rock	Cathedral Rock	Cathedral Rock	Cathedral Rock	Cathedral Rock
	Major(wt%)								
	SiO2	48.79	50.13	50.44	49.67	52.05	49.37	50.62	46.53
	TiO2	2.92	2.77	2.89	2.87	3.06	2.82	2.85	0.71
	Al2O3	11.61	11.66	11.92	11.66	12.27	11.45	11.89	13.02
	Fe2O3T	19.28	17.99	16.71	19.47	16.31	19.42	19.01	15.57
	MnO	0.19	0.27	0.23	0.29	0.24	0.29	0.26	0.24
	MgO	4.19	4.20	4.23	3.56	4.38	3.84	3.78	9.94
	CaO	6.29	7.77	7.31	7.00	5.61	7.72	6.77	9.44
	Na2O	4.33	3.40	3.71	3.69	3.89	2.95	3.10	2.79
	K2O	0.11	0.39	0.32	0.24	0.47	0.44	0.33	0.28
	P2O5	0.31	0.35	0.33	0.37	0.39	0.34	0.36	0.02
	SO3	395ppm	198ppm	588ppm	190ppm	2760ppm	471ppm	758ppm	332ppm
	LOI	1.47	1.23	0.29	0.91	0.74	0.28	0.39	1.26
	Total	99.67	100.44	98.68	99.99	99.83	99.27	99.84	100.11
	Mg#	0.23	0.24	0.26	0.20	0.27	0.22	0.22	0.47
	trace(ppm)								
	Rb	7	9	10	10	29	12	13	11
	Ba	43	80	96	58	121	226	321	430
	Th	0	4	1	4	0	0	0	1
	U	2	1	0	0	2	0	0	
	Nb	17	17	23	20	48	16	19	6
	K	913	3236	2655	1991	3900	3651	2738	2323
	La	20	16	25	20	18	14	24	8
	Ce	62	60	70	90	69	47	71	30
	Pb	97	5	1	5	5	6	6	4
	Sr	138	149	187	152	132	159	169	73
	P	1354	1528	1441	1615	1703	1485	1572	87
	Nd	28	36	33	30	29	24	45	2
	Zr	162	171	171	187	185	173	192	19
	Sm	7.71	7.73	9.97	8.29	10.92	7.53	9.95	2.38
	Ti	17505	16606	17326	17206	18345	16906	17086	4256
	Y	55	54	78	51	121	48	57	18
	Sc	49	43	44	43	49	47	42	64
	Cr	0	5	12	3	0	2	2	295
	V	420	385	401	348	328	378	351	427
	Co	51	55	43	60	65	57	55	59
	Ga	23	20	23	22	25	22	24	17
	Cu	24	34	26	29	16	29	31	22
	Zn	84	338	169	160	94	141	211	101
	Ni	9	11	6	5	1	7	9	142

APPENDIX D:

NORMALISED REE DATA

RAINY	Sample No.	ZA000019	LPT	ZA001241	ZA001242	ZA001230	ZA001208	ZA001209	ZA001239
DAY	Rock type	Dolerite		amphibolite	amphibolite	Qtz Gabbro	Gabbro	Dolerite	Gabbro
	Location E	North Ltd		North Ltd	North Ltd	North Ltd	North Ltd	North Ltd	North Ltd
	N	Rainy Day		Mutooroo	Mutooroo	Double Dam	Feldspar Mine	Feldspar Mine	Baxter's Bore
	La	16.01		4.08	5.39	8.01	5.82	5.82	7.13
	Ce	9.12		3.42	4.27	5.36	3.99	5.13	4.56
	Pr	10.81		5.68	7.57	6.76	5.41	5.41	7.57
	Nd	8.12		3.55	4.80	4.06	4.43	6.65	4.06
	Sm	5.63		3.27	3.94	3.56	3.70		3.15
	Eu	5.95		4.64	5.00	5.12	2.98	5.95	3.81
	Gd	5.03		3.27	4.36	3.27	3.36	5.03	3.10
	Tb	4.63		3.33	4.44	2.78	3.71	4.63	3.33
	Dy	4.75		3.12	3.93	3.12	4.07	4.07	2.85
	Ho	3.05		3.54	4.45	2.56	3.05	3.05	3.41
	Er			3.54	4.38	2.44	2.08	4.17	3.33
	Tm			3.38	4.05	2.43	2.06		3.38
	Yb	4.06		2.84	3.65	2.39	2.03	4.06	2.84
HPT	Sample No.	ZA001204	ZA001238	ZA001228	ZA001207	ZA001210	ZA001227	ZA001231	ZA001225
DOLERITES	Rock type	Gabbro	Gabbro	Dolerite	Gabbro	Gabbro	Dolerite	Gabbro	Qtz dolerite
	Location E	North Ltd	North Ltd	North Ltd	North Ltd	North Ltd	North Ltd	North Ltd	North Ltd
	N	Baxter's Bore	Baxter's Bore	Doughboy	Willow Well	Willow Well	Willow Well	Willow Well	Pimponda Mine
	La	20.38	23.29	33.48	29.11	13.10	34.93	30.57	26.20
	Ce	19.94	21.65	26.55	19.94	10.26	24.50	22.79	19.37
	Pr	16.22	27.03	29.73	21.62	10.81	34.05	32.43	21.62
	Nd	12.56	15.51	16.25	18.46	14.77	19.94	19.94	13.29
	Sm	6.76	10.36	10.14	7.88	6.76	13.29	14.19	9.23
	Eu	5.95	9.52	8.87	5.95	8.93	10.89	13.69	9.35
	Gd	6.71	9.23	6.88	10.07	11.74	10.57	11.24	7.55
	Tb	4.63	8.80	6.48	9.26	4.63	9.63	11.11	6.85
	Dy	8.82		5.83		10.18	8.68	10.04	6.51
	Ho	3.05	7.93	4.82	6.10	6.10	7.80	8.17	5.73
	Er	4.17	7.29	4.79	8.33	6.25	7.08	7.71	5.21
	Tm		6.76	4.59		6.76	5.95	7.70	5.27
	Yb	4.06	5.88	4.67	6.09	6.09	6.90	7.51	5.68

APPENDIX E:

ISOTOPE DATA & ISOCHRON PLOTS

sample no.	1060-007	1060-008	1060-010	1060-012	1060-050	1060-005	1060-054
rock	HPT	HPT	Poodla	Antro	LPT	Rainy Day	Outalpa
Nd ppm	18.8552	40.0320	35.7230	38.7895	5.9022	10.2361	10.5848
Sm ppm	4.6554	9.2393	7.3530	9.4754	1.6657	3.0768	3.1648
143/144 Nd	0.511928	0.511983	0.511608	0.512017	0.512310	0.512553	0.512595
2 sigma	0.000067	0.000030	0.000067	0.000045	0.000049	0.000069	0.000024
Sm/Nd	0.246904	0.230796	0.205834	0.244278	0.282217	0.300582	0.298992
147Sm/144Nd	0.149352	0.139609	0.124509	0.147764	0.170713	0.181822	0.180860
143/144Nd ch	0.512638	0.512638	0.512638	0.512638	0.512638	0.512638	0.512638
143/144Nd dep	0.513108	0.513108	0.513108	0.513108	0.513108	0.513108	0.513108
T mod:chur	2.28	1.74	2.17	1.93	1.92	0.87	0.42
T mod:dep	2.70	2.24	2.49	2.44	2.69	2.48	2.24
eps Nd (0)	-13.849929	-12.780949	-20.092151	-12.106625	-6.3982771	-1.6580901	-0.8450053
age (T)	1.5	1.5	1.63	1.65	1.5	1.5	1.7
143/144(T)	0.51045564	0.5106065	0.51027361	0.51041422	0.51062706	0.51076055	0.51057266
143/144ch T	0.51069888	0.51069888	0.51052992	0.51050392	0.51069888	0.51069888	0.51043889
eps Nd chT	-4.76	-1.81	-5.02	-1.76	-1.41	1.21	2.62
Sr87/86	0.740057	0.721881	0.84343	0.723396	0.7701	0.713845	0.716092
2 sigma	0.000116	0.000142	0.000047	0.00007	0.000086	0.000035	0.000139
Sr ppm	192.3951	325.4369	75.6078	29.31577	153.7771	138.924	139.129
Rb ppm	57.8196	2.13548	269.298	4.68572	19.50718	14.31279	5.75166
Rb/Sr	0.300525	0.006562	3.561775	0.159836	0.126854	0.103026	0.041340
frac 87	1.214519	1.212349	1.226862	1.212530	1.218106	1.211389	1.211658
at wtSr	87.614602	87.615866	87.607502	87.615760	87.612524	87.616426	87.616269
87Rb/86Sr	0.872248	0.019012	10.441953	0.463157	0.369260	0.298260	0.119707
87/86(T)	0.721279	0.721471	0.598922	0.712416	0.762151	0.707424	0.713167
87/86/300	0.736334	0.721799	0.798852	0.721419	0.768524	0.712572	0.715581
87/86/400	0.735089	0.721772	0.783951	0.720758	0.767997	0.712146	0.715410
87/86/500	0.733842	0.721745	0.769028	0.720096	0.767469	0.711720	0.715239
87/86/800	0.730092	0.721663	0.724133	0.718105	0.765881	0.710438	0.714724

Isotope data for the Olary Block mafic rocks.

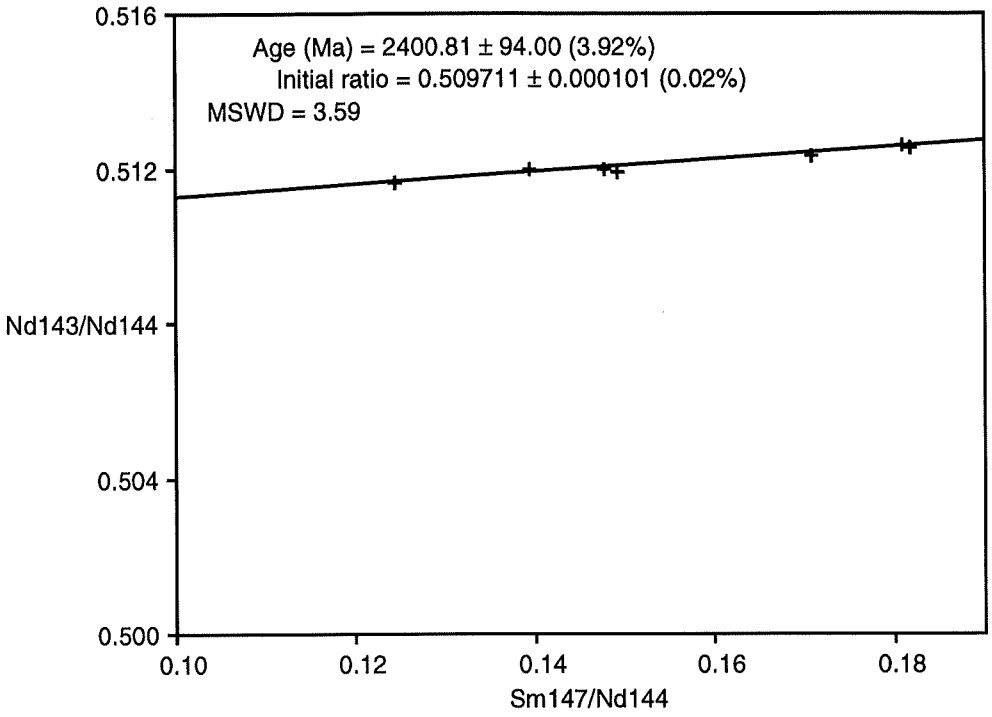

Sm-Nd isochron for all of the Olary Block mafic and intermediate rocks.

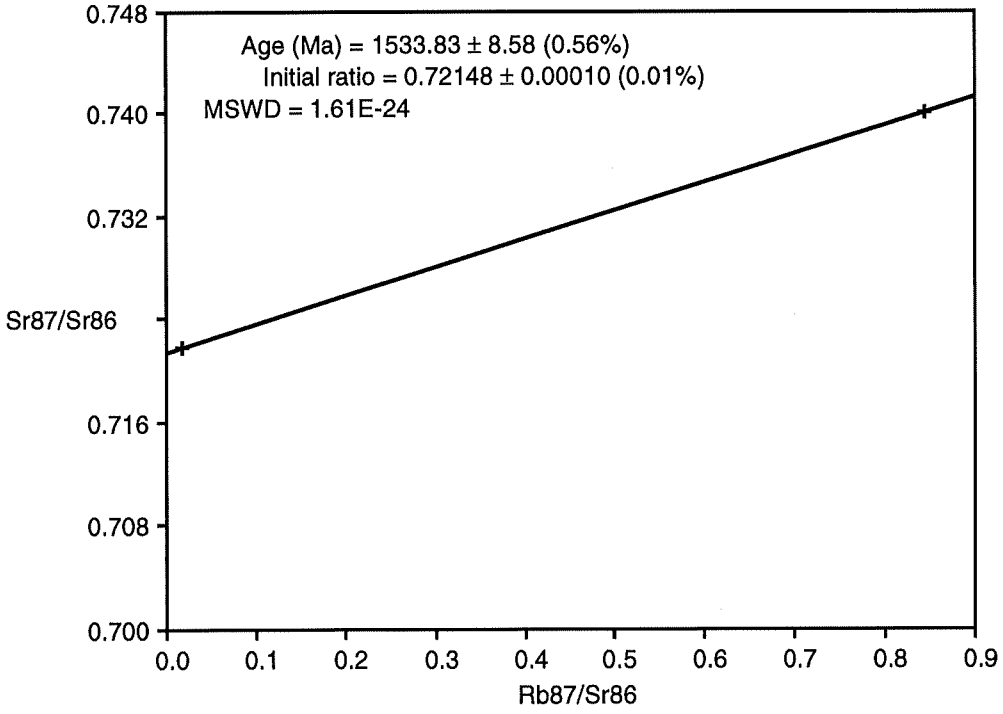

Two point Rb-Sr isochron for the HPT dolerites.

APPENDIX F:

RESULTS FROM THREE Pb/Pb ZIRCON EVAPORATION ANALYSES ON THE ANTRO GRANITOID AT 'RAINY DAY'

RUN SUMMARIES: **Sample A1060-012**

ZIRCON	AGE (Ma)	2 SIGMA
Antro Z1 RIM	1652.4	±17.2
Antro Z1 CORE	1680.7	±5.0
Antro Z5	1689.7	±15.1
Antro Z6	1675.1	±10.3
Total Population	**1679.5**	**±12.9**

See histogram on next page.

APPENDIX G:

ALTERATION OF THE INTERMEDIATE GRANITOIDS: A DISCUSSION

Post-magmatic Alteration of the Poodla and Antro Granitoids

The marked contrast in alkali abundances of the Poodla and Antro granitoids is a direct result of K_2O-Na_2O exchange during potassic alteration and albitisation (e.g.Fig 4.3.6). Albitisation on a local scale (a few metres) can be described thus;

$$CaAl_2Si_2O_{8(an)} + SiO_2 + Na^+ + 4H^+ \Longleftrightarrow NaAlSi_3O_{8(ab)} + Ca^{2+} + Al^{3+} + 2H_2O$$

(Merino 1995).

A major consequence of the above reaction is that SiO_2 is consumed and therefore albitisation of plagioclase is enhanced in quartz+plagioclase-rich rocks. Furthermore, it requires the mobiltiy of aqueous Al. Inspection of the major element data set for the granitoids reveals that the *all* Poodla samples contain greater Al_2O_3(wt%) than *any* of the Antro samples. Albitisation of the Antro granite has undoubtedly contributed to Al loss. However, this phenomenon is difficult to explain on a scale of hundeds of metres due to the low solubility of Al at low temperatures. One explanation may involve generation of stress between adjacent grains during pseudomorph replacement (Merino *et al.*,1993; Merino *et al.*, 1994). This stress could vastly increase Al solubility.

Figure G1 is a representation of the extreme temperature control on feldspar composition in the alkali feldspar-chloride solution system. For a given fluid composition X (K/(K+Na)<0.25), and at 500°C, the fluid is in equilibrium with albite. K-feldspar forms at the expense of albite only if (i) the fluid has K/K+Na>0.25 or (ii) if the temperature drops to ~400°C (Williams and Blake, 1993). Such a scenario may explain the fundamental discrepancy between the feldspar (and whole rock) compositions of the Antro and Poodla granites.

Moreover, this type of fluid interaction obviously has implications for metallogenesis. An analogy can be drawn here from the study of Dilles and Einaudi (1992) on the Ann-Mason porphyry Cu deposit in Nevada. These authors proposed several fluid phases including a main stage sodic-calcic phase that did not deposit sulphide and caused addition of Na along with leaching of K-Fe-Cu. This was follwed by an ore forming potassic fluid that formed biotite+K-feldspar-rich assembleges and deposited Cu. A simplified representation is given in Fig G2. (Note the similarity between the mineral assembleges that charactarise the fluid phases and the mineralogy of the Olary Block intermediates).

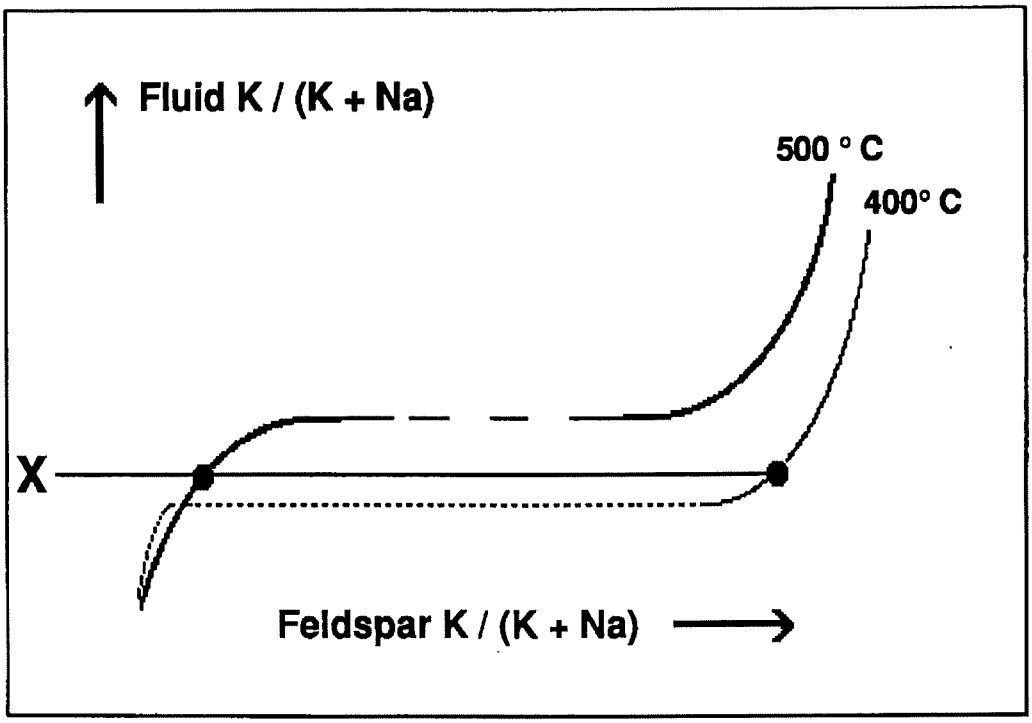

Fig G1 Representation of the high temperature dependence of feldspar composition for a given fluid composition, X. (after Williams and Blake, 1993). See text for discussion.

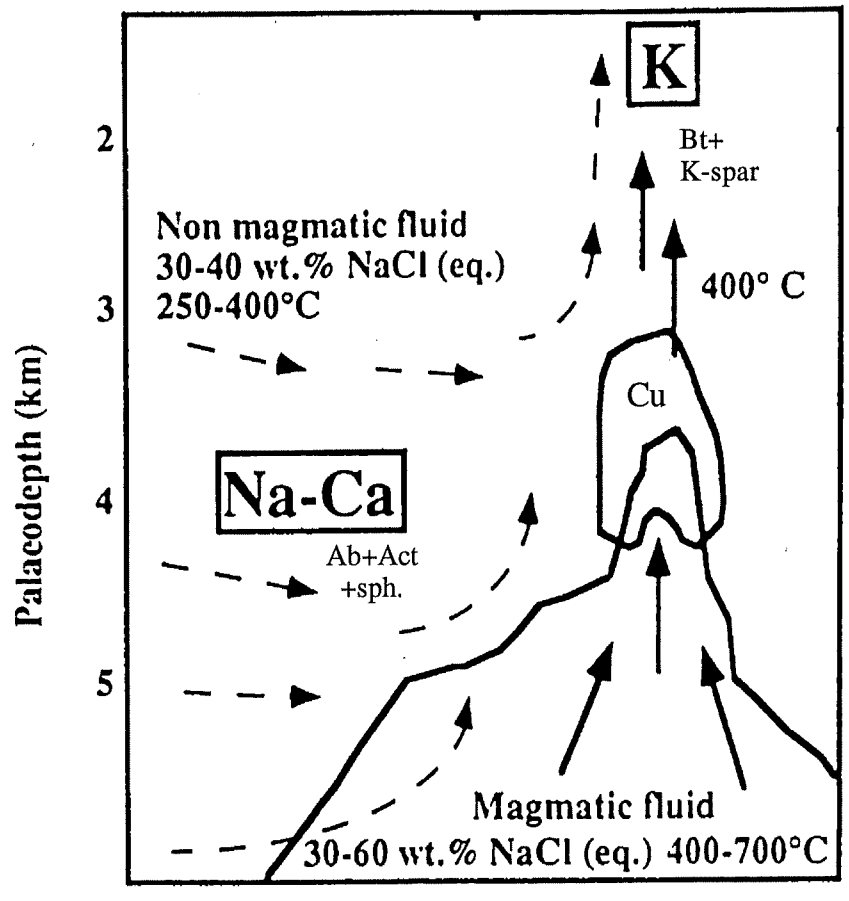

Fig G.2 Model for alteration styles observed in the Ann-Mason Porpyry system, Nevada (Dilles and Einaudi, 1992). Influx of Na-Ca-rich fluids causes sodic metasomatism at high temperatures. Migration away and cooling of these fluids results in precipitation of K-feldspar at the expense of albite. From Williams & Blake (Alteration in the Cloncurry district; lecture notes, 1995).

APPENDIX H:

TECTONIC DISCRIMINATION DIAGRAMS

1A; calc-akaline basalts
1B; calc-alkaline & volcanic arc basalts
1C; volcanic arc tholeiites
2A; continental tholeiites
2B; back-arc basin basalts
3A; calc-alkaline continental basalts
3B; E-type MORB
3C; weakly enriched MORB
3D; N-type MORB

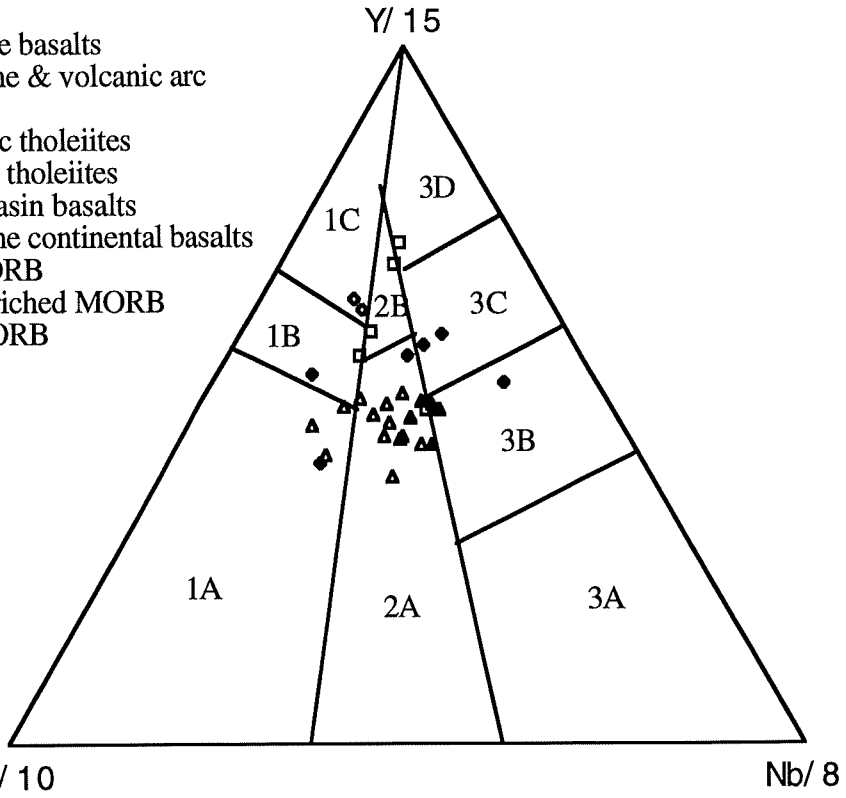

Fig. . Y/15-La/10-Nb/8 tectonic discrimination diagram after Cabanis & Lecolle (1989). Symbols as for above diagram; filled triangles are Cathedral Rock amphibolites (data from Pierini, 1994).

AI; within plate alkali basalts,
AII; within-plate alkalic and tholeiitic basalts,
B; E-type MORB,
C; within-plate tholeiitic and volcanic arc basalts,
D; N-type MORB.

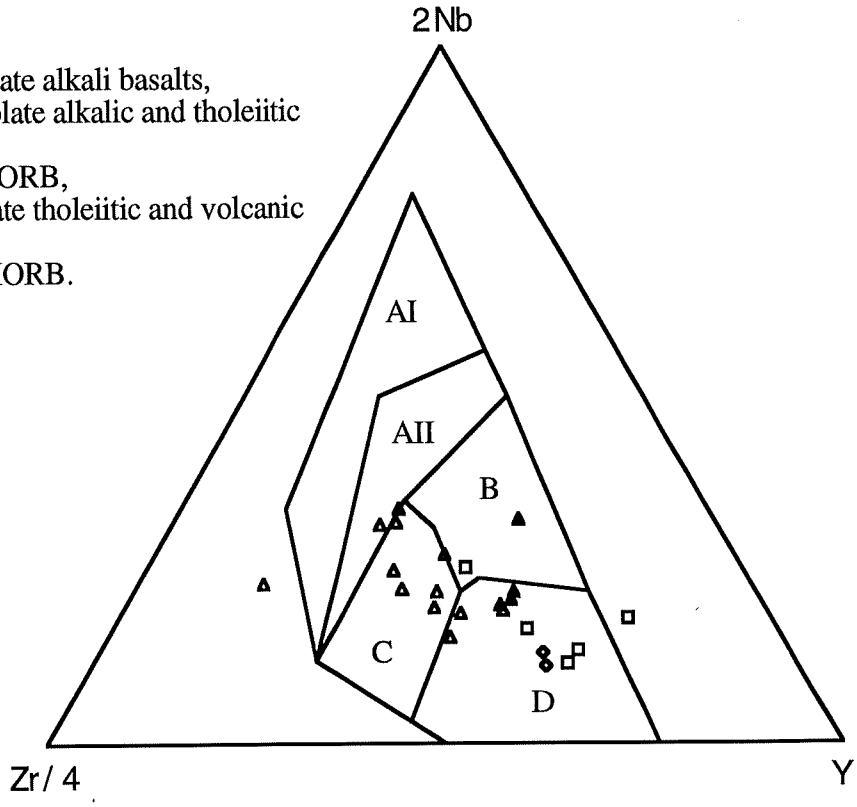

2Nb-Zr/4-Y tectonic discrimination diagram after Meschede (1986).
HPT; open triangles,Outalpa amphibolites; filled trianges
LPT; open squares, Rainy Day; open diamonds.

THE GEOLOGY OF THE AREA WEST OF AMEROO HILL, OLARY BLOCK, S.A. (1:5000).

LEGEND

Cx	soil, sand, gravel, clay, vegetation
p	pegmatite; qtz-feldspar-muscovite-tourmaline
Ga	Regional 'Bimbowrie' S-type granitoid; qtz-plagioclase-K spar-biotite
Gd	'Antro' grantoid; qtz-Na-plagioclase-actinolite-clinopyroxene; accessory sphene-magnetite-K- spar-biotite, I-type GRANODIORITE - TONALITE
Eb	Pelite; bedding indistinct; biotite-quartz-rich rock
fe	gossan; 'Bimba Suite'; qtz-plagioclase-magnetite-haematite-goethite
S	Psammite; massive, medium grained; quartz-rich, minor feldspar, biotite and garnet
cax	Calcalbitite; massive to crudely bedded; qtz-albite-K spar-calcsilicates (eg epidote, actinolite); clearly brecciated locally.
a	'Outalpa' amphibolite; massive to foliated; plagioclase-hornblende -epidote-CPX(?)-magnetite+/-haematite
Plm	Fine to medium grained pelite and psammopelite; well bedded and laminated; qtz-feldspar-biotite-muscovite-andalusite-magnetite-haematite

THE GEOLOGY OF THE AREA 2km NE OF ANTRO WOOLSHED, OLARY BLOCK, S.A. (1:2500). *('Rainy Day Grid').*

THE GEOLOGY OF THE AREA 5km EAST OF ANTRO WOOLSHED, OLARY BLOCK, S.A. (1:2500).

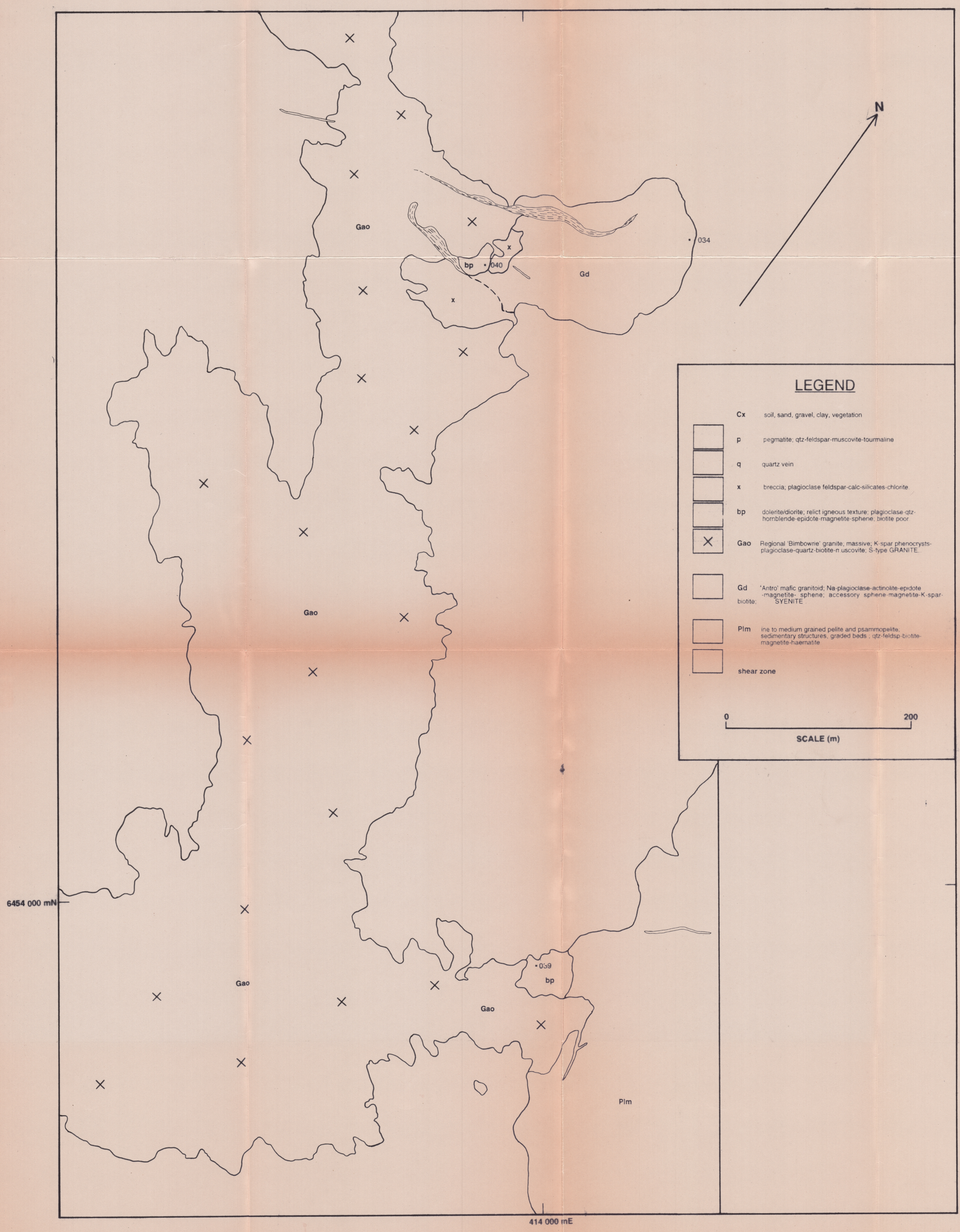

LEGEND

- Cx — soil, sand, gravel, clay, vegetation
- p — pegmatite; qtz-feldspar-muscovite-tourmaline
- q — quartz vein
- x — breccia; plagioclase feldspar-calc-silicates-chlorite
- bp — dolerite/diorite; relict igneous texture; plagioclase-qtz-hornblende-epidote-magnetite-sphene, biotite poor
- Gao — Regional 'Bimbowrie' granite; massive; K-spar phenocrysts-plagioclase-quartz-biotite-n uscovite; S-type GRANITE.
- Gd — 'Antro' mafic granitoid; Na-plagioclase-actinolite-epidote -magnetite- sphene; accessory sphene-magnetite-K-spar-biotite; SYENITE.
- Plm — ine to medium grained pelite and psammopelite; sedimentary structures, graded beds ; qtz-feldsp-biotite-magnetite-haematite
- shear zone

0 — 200

SCALE (m)